68605

A FIBER-OPTIC LOOP MEMORY STRUCTURE BASED ON OPTICAL CODE DIVISION MULTIPLE ACCESS

A THESIS SUBMITTED TO
THE GRADUATE SCHOOL OF NATURAL AND APPLIED SCIENCES
OF
MIDDLE EAST TECHNICAL UNIVERSITY

BY

ERTAN ZENCIR

IN PARTIAL FULLFILLMENT OF THE REQUIREMENTS FOR
THE DEGREE OF MASTER OF SCIENCE
IN
THE DEPARTMENT OF ELECTRICAL AND ELECTRONICS ENGINEERING

JULY 1997

Approval of the Graduate School of Natural and Applied Sciences.

Prof. Dr. Tayfur Öztürk
Director

I certify that this thesis satisfies all the requirements as a thesis for the degree of Master of Science.

Prof. Dr. Fatih Canatan
Head of the Department

We certify that we have read this thesis and that in our opinion it is fully adequate, in scope and quality, as a thesis for the degree of Master of Science.

Prof. Dr. Rüyal Ergül
Supervisor

Examining Committee in Charge:

Prof. Dr. Yalçın Tanık (Chairman)
Prof. Dr. Rüyal Ergül
Assoc. Prof. Dr. Mete Bulut
Prof. Dr. Murat Aşkar
Yük. Müh. Cenk Argon (Siemens A.Ş.)

ABSTRACT

A FIBER-OPTIC LOOP MEMORY STRUCTURE BASED ON OPTICAL CODE DIVISION MULTIPLE ACCESS

Zencir, Ertan
M.S., Department of Electrical and Electonics Engineering
Supervisor: Prof. Dr. Rüyal Ergül

July 1997, 96 pages

In this study, a new fiber-optic loop memory configuration which uses optical code division multiple access technique for data storage is investigated. Code division multiple access technique and its performance in optical medium is reviewed. Some of the previously developed optical data storage systems and related concepts are summerized. The fiber-optic loop memory structure using optical CDMA is proposed. A simulation program is developed for the investigation of memory read, write and clear operations. In order to improve the performance, use of double optical hard-limiters in the decoding part of the memory is proposed . The bit-error probability performance and its performance analysis is done.

Keywords: Optical code division multiple access, fiber-optic loop memory.

ÖZ

OPTİK KOD BÖLMELİ ÇOKLU ERİŞİME DAYALI BİR FİBER-OPTİK DÖNEL HAFIZA YAPISI

Zencir, Ertan
Yüksek Lisans, Elektrik ve Elektronik Mühendisliği Bölümü
Tez Yöneticisi: Prof. Dr. Rüyal Ergül

Temmuz 1997, 96 sayfa

Bu çalışmada, veri depolama için kod bölmeli çoklu erişim tekniğini kullanan yeni bir fiber-optik dönel memory konfigürasyonu araştırılmıştır. Kod bölmeli çoklu erişim tekniği ve performansı incelenmiştir. Daha önce geliştirilmiş bazı optik veri depolama sistemleri ve ilgili kavramlar sunulmuştur. Optik kod bölmeli çoklu erisimi kullanan fiber-optik dönel hafıza yapısı tanıtılmıştır. Hafıza yazma, okuma ve silme işlemlerini örneklerle gösteren bir program gelistirilmiştir. Bit-hata ihtimali performansını geliştirmek amacıyla hafıza yapısının veri çözümleme kısmında çift optik sınırlayıcı kullanılması önerilmiş ve performans analizi yapılmıştır.

Anahtar Kelimeler: Optik kod bölmeli çoklu erişim, fiber-optik dönel hafıza.

ACKNOWLEDGEMENTS

The author would like to thank to his supervisor Prof. Dr. Rüyal Ergül for his help, supervision and encouragement during the development of of this thesis.

The author also wishes to express his deep gratitude to his sincere friends for their support during his studies.

TABLE OF CONTENTS

ABSTRACT iii

ÖZ iv

ACKNOWLEDGEMENTS v

TABLE OF CONTENTS vi

LIST OF ABBREVIATIONS viii

CHAPTER

1 INTRODUCTION 1

2 OPTICAL CDMA AND OPTICAL ORTHOGONAL CODES 4

2.1 Introduction 4

2.2 System Description 4

2.3 Optical Orthogonal Codes 11

2.4 Fundamental Properties and Upperbounds 12

2.5 (n,6,1,1) OOC's 14

2.6 Performance Analyis of (n,w,1,1) Optical Orthogonal Codes 16

3 VARIOUS IMPLEMENTATIONS OF FIBER OPTIC LOOP MEMORY 19

3.1 Intrdouction 19

3.2 Optical Data Storage Using Multistable Oscillations 19

3.3 Fiber-optic Loop Memory for Optoelectronic Computer 25

3.4 A Fiber-optic Memory Device with All-optical Regeneration 28

3.5 Fiber-optic Loop Memory Used in ATM Packet Buffering 31

3.6 Bit-error Rate (BER) Measurements in Random Access Fiber Loop 33

4 A FIBER-OPTIC LOOP MEMORY STRUCTURE BASED ON OPTICAL CODE DIVISION MULTIPLE ACCESS 38
4.1 Introduction....38
4.2 Basic Properties....39
4.3 Loss in the Fiber Loop....40
4.4 Memory Structure Based on Optical CDMA....43
4.5 Examples of Data Storage and Usage of Codewords....47
4.6 Performance Analysis of FOMD with Double Optical Hard-limiters....59
5 CONCLUSION....75
REFERENCES....78
APPENDIX....82

LIST OF ABBREVIATIONS

FOMD	Fiber-optic memory device
CDMA	Code division multiple access
PN	Pseudo-noise
OOC	Optical orthogonal code
OOK	On-off keying
EO	Electrical-to-optical
LD	Laser diode
RZ	Return-to-zero
PD	Photo-detector
WDM	Wavelength division multiplexing
OC	Optical Correlator
HL	Hard-limiter

CHAPTER I
INTRODUCTION

The discovery of electromagnetic waves was followed by a development in the use of unguided waves, from the low frequencies of the first broadcast to the high frequencies of optical network communications. The guidance of the high-frequency electromagnetic waves used in optical communications nowadays is provided by glass fibers. Just as in the case of communication with metallic conductors, this is a form of guided transmission of information. Communications with metallic conductors is adequate for the frequency range from 0 Hz to a few gigahertz, but when the light is used to carry information in glassfiber communication systems, it has a much higher frequency. The frequency range used for glassfiber communication extends from about $2x10^{14}$ Hz to about $10x10^{14}$ Hz, this corresponds to a wavelength range from 750 to 1500 nm, or a frequency band in a single glassfiber of $2x10^{14}$ Hz. In such a wide frequency band, an unbelievably large amount of information can be transmitted at least in theory.

The rapid developments in optical signal processing and the advantages of fiber-optic cables over their metallic counterparts lead to the replacement of electronic communication systems with optical ones. Spread spectrum communication systems [1] which use very large bandwidths if compared to other systems, are important in today's communication applications. Although in spread spectrum communications a large amount of excess bandwidth is needed, there are many advantages, especially if the number of users in the communication networks is considered. Due to the large bandwidth available in optical fibers and due to the fast optical signal processing methods, the idea arose to use spread spectrum in fiber-optic communication systems.

Possibility of high speed signal processing and huge bandwidth brought a new research area, 'fiber-optic memories'. The use of fiber loops as recirculating delay lines or 'optical memories' have been discussed for several years. The introduction of new broadband services will yield significant traffic growth that could lead the existing electronic switching nodes to insufficiency. All optical networks using optical switches will be realizable in future and especially high-speed ATM networks will be based on such high capacity networks. The asynchronous operation of ATM requires buffering and hence very high-speed memories. The operating speed of these memories will be such that all optical construction would be needed. This is why we propose a fiber-optic loop memory structure.

Increasing of the information capacity of a fiber-optic memory device (FOMD) is normally achieved either by increasing the length of fiber circulation loop accompanied by added complexity of the synchronization circuit or by using conventional channel multiplication methods, i.e. spectral, polarization, and temporal methods. The nature of circulator memory systems makes it also possible to form additional information channels that can be employed for attaining both reliable addressing, synchronization, noise-immune encoding and increased information capacity of the FOMD [2] but at the expense of complicated hardware.

This study is concerned with the method of increasing the information capacity in a circulator fiber-optic memory by creating virtual channels using code division multiple access technique which can be realized by using hardware of reasonable complexity.

A possible implementation of optical code division multiple access technique in recirculating fiber-optic loop memory will be fully described.

Following the outline presented in chapter I, the general concepts of optical code division multiple access (CDMA) systems and their descriptions are discussed in chapter II. Optical orthogonal codewords which are used in intensity-modulation-direct detection fiber-optic communication systems are also reviewed.

Chapter III gives a brief discussion on various fiber-optic memory implementations in literature.

Chapter IV covers the theory and design of the proposed fiber-optic loop memory structure based on optical code division multiple access technique. The bit-

error probability performance improvement technique which uses double optical hard-limiters in the memory structure is introduced.

In chapter V, conclusions and future work on how to improve the proposed structure to obtain higher bit storage capacities are presented.

In the appendix computer source codes for the simulation of the FOMD with single and double optical hard-limiters are given.

CHAPTER II
OPTICAL CDMA AND OPTICAL ORTHOGONAL CODES

2.1 Introduction

In this chapter optical CDMA systems and optical orthogonal codes will be discussed since the memory structure studied in this work is based on optical CDMA and it uses the optical orthogonal codes. In references [1],[2],[3],[4],[5],[6], optical CDMA systems are examined. The main advantage of using fiber cables instead of their metallic counterparts for transporting information in telecommunications systems is because of the reason that fibers have much larger bandwidth than metallic cables. This large bandwidth permits high-speed signal processing and a large number of users. The ability to perform high-speed optical signal processing helps to reduce the growing electronics and software complexity that is present in communications systems.

Optical CDMA takes the advantage of excess bandwidth available in fibers to convert low-rate electrical signals into high-rate optical signals to achieve asynchronous or synchronous communication access. The only limitation in the use of large optical bandwidth is due to the electrical-to-optical and optical-to-electrical conversion for signal processing. However, optical components will offer much higher speeds for optical signal processing, if they are fully developed and integrated.

2.2 System Description

A typical optical telecommunications system is shown below in Figure 2.1 [1,3] .

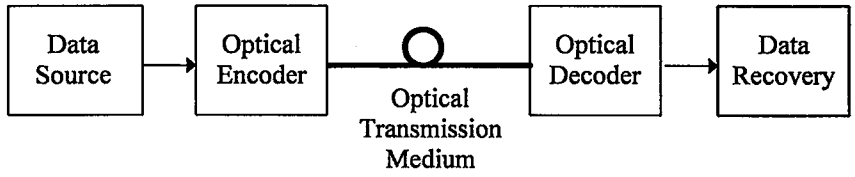

Figure 2.1. A fiber-optic communication system

The information data source is followed by a laser and an optical encoder combination that converts each bit of the information sequence into a high-rate optical sequence (PN), which is afterwards coupled into the fiber channel. At the receiver side, the optical sequence is compared to a stored replica of itself (optical correlator). Afterwards, it is passed through a threshold device in order to recover the data.

In an optical CDMA system there are N users with optical transmitters and receivers as described above in Figure 2. 1. . A possible system configuration would be a star fiber-optic network as in Figure 2.2. [1].

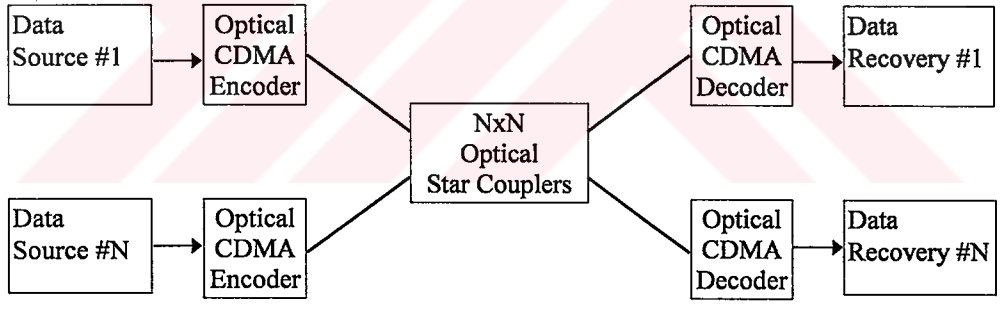

Figure 2.2. Optical CDMA communications systems

In the system in Figure 2.1., the light sources are LASER sources. The optical-to-electrical conversion in the receivers is done by means of suitable photodetectors through which the electrical current flowing is directly proportional to the incident light intensity.

To each user a specific optical address code or signature sequence is assigned. If user i sends data to user j, it impresses the address code for receiver j upon the data of the encoder i. As stated earlier, the purpose in a CDMA system is to extract the

data with the intended optical sequence in the presence of all other optical sequences by optical processing.

Optical CDMA systems can be grouped into coherent and incoherent CDMA. One is employing coherent, the other incoherent detection of the optical sequences. This chapter considers only incoherent optical CDMA. Coherent CDMA systems are examined in [5] and [6].

In incoherent optical CDMA the phases of the light are of no importance since they are summed on the basis of power, rather than electric field. The optical CDMA system can be modeled as a positive system [1], since optical signal processing is based on power measurement. A positive system is a system that is not able to manipulate its signals to add up to zero.

An important element of an optical CDMA system is the design of high-rate optical sequences upon which the information bits of the users are mapped. The main criteria in the design of these sequences named Optical Orthogonal Codes (OOC) will be investigated briefly in this chapter.

For the time being, it is enough to know that the signature sequences (or codewords) satisfy the following two properties:

1. each sequence can be distinguished from a time-shifted version of itself.

2. each sequence can be distinguished from a possibly time-shifted version of another sequence.

Two codewords of an optical orthogonal code of chiplength n=32 and weight $\omega = 4$ are as follows[1]:

a=(0,9,12,27)
b=(0,4,11,30)

where the numbers in the parentheses denote the chip positions which are equal to one. All other chip positions are set to zero. The two codewords are shown in Figure 2.3

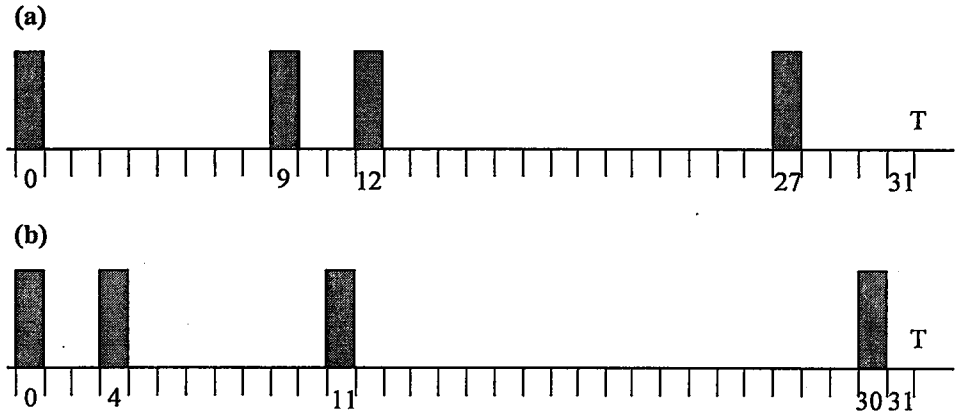

Figure 2.3. Two optical signature (PN) sequences a and b

The optical sequences are (0,1) sequences, i.e., they have the 0 and 1 level instead of the ±1 levels which are the possible levels in electrical communication systems. Various implementations of the optical encoders and decoders are presented in [1] , [2] , [5] ,[6], [7] , [8] . One application is to multiply the optical pulse by the stored signal by using a fast optical modulator, or a switch, and the detected result is integrated by electronic means.

Some problems arise while using this implementation, since perfect synchronization of the sequences at the encoders and decoders is required for proper operation. Even if perfect synchronization is achieved, this scheme would be more effective in time division multiple access, or in a switching network. The other application is using more optical signal processing .

Most of the common structures are the optical encoders and decoders based on power splitting and combining by means of 1 x ω and ω x 1 splitters and combiners and fiber delay lines, where ω is the weight of the codewords. The encoders and decoders using this approach are shown in Figure 2.4.

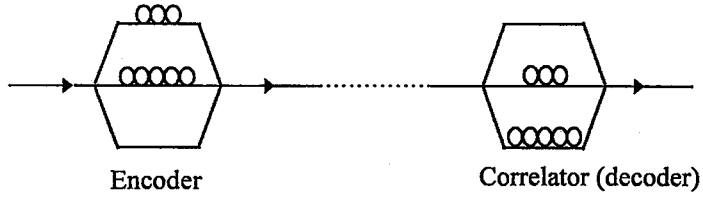

Figure 2.4 Optical CDMA encoder and decoder based on power splitting and combining

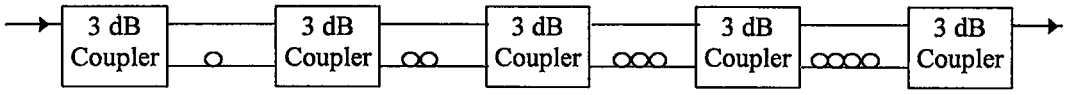

Figure 2.5. Optical CDMA encoder based on ladder network

The lengths of the delay lines of the encoder are adjusted such that a pulse of one chip duration at the input is mapped to the chip positions of value " 1 " of the specified PN sequence. The number of the delay lines required is equal to ω, the weight of the code used in the optical CDMA system. The lengths of the delay lines of the receiver correlator are such that the characteristics is exactly the replica of the PN sequence. Obviously, the number of delay lines of the correlator is also equal to ω.

There is no need for storing the replica of the PN sequences in optical CDMA applications. Also, there is no need for synchronization of the PN sequence generators as it is needed in the DS spread spectrum systems.

At this point, it should be pointed out that the optical CDMA system employed in the memory device does not implement binary coding on the information bits, i.e., the encoder sends the PN sequence when its data is "l" and sends no light when the data is "0". This is equivalent to on-off keying (OOK). In optical transmission systems this type of modulation is named as intensity modulation (IM).

In the configuration in Figure 2.4., it is observed that as the weight of the code increases, the number of delay lines used also increases.

Also, the light power in each delay line is equal to (1/ω) of the light power at the encoder input. Therefore, as ω increases, the power in the delay lines is decreasing.

To overcome the problem of power splitting and to avoid the increasing complexity of the system to be realized, the ladder network shown in Figure 2.5. can be used [6]. These ladder networks are made from cascaded 2 x 2 couplers. An n-stage network consists of (n+1) fixed 3-dB couplers connected in cascade by n

double fiber links. When such a network is used, the encoder total bit energy reduction is only a factor of 2.

However, one limitation exists for the choice of ω which has to be a power of 2, i.e.,

$$\omega = 2^{n} \qquad (2.2.1)$$

when an n-stage ladder network is employed.

Another solution to compensate the power reduction due to splitting would be to place an optical amplifier with gain ω after the encoder as shown in Figure 3.6. .

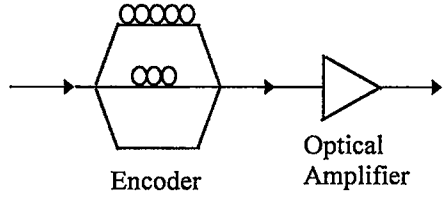

Figure 2.6. Optical CDMA encoder with optical amplifier

With this configuration, the peaks of the optical pulses at the output of the optical amplifier are equal to the pulse peak at the input of the optical encoder.

There is a source of error at the receiver side. Let a codeword A of an optical orthogonal code of weight 4 be as follows:

$$A = \{\ 1011000100000\ \} \qquad (2.2.2)$$

The output of the correlator for this codeword has a maximum value "4" as well as the interference of the form

$$I = \{\ 1000000300000\ \} \qquad (2.2.3)$$

Therefore, a false detection would occur. To eliminate this problem, an optical limiter could be employed in front of the decoder as shown in Figure 2.7. Hence, all received pulses will be of constant power.

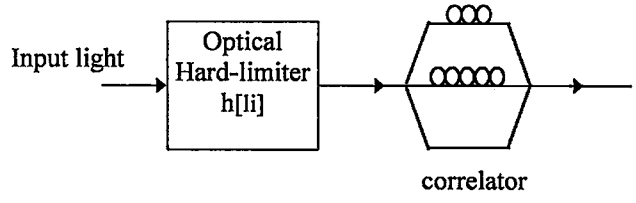

Figure 2.7. Optical decoder with optical hard-limiter

The characteristics of the optical hard-limiter is as follows:

$$h[li] = \begin{cases} 1 \text{ for } & li \geq 1 \\ 0 \text{ for } & li < 1 \end{cases} \qquad (2.2.4)$$

where li is the input light intensity at the limiter input.

The interference pattern given in (2.2.3) when passed through the limiter would be converted to I' where

$$I' = \{\ 1000000100000\ \} \qquad (2.2.5)$$

and would produce a maximum value of "2" at the correlator output of the codeword A. This value would not cause an error when the threshold of the decision device which is placed after the correlator is set to a value greater than 2.

As mentioned in the encoder case, again there is the problem of power loss due to the power splitting at the decoder. To overcome this problem, the structure of an optical CDMA decoder, where the power loss is compensated by using an optical amplifier, is shown in Figure 2.8.

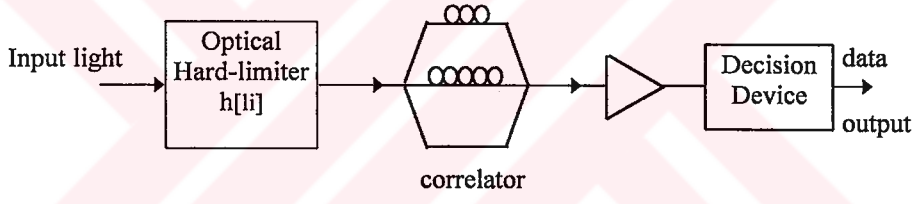

Figure 2.8. Optical CDMA decoder

Another phenomena, worth to be mentioned is the attenuation of the optical pulses propagating in the optical fiber. In fact, attenuation of optical signals during transmission through the optical fiber cable does not cause serious problems, since the attenuation in fibers is very low [9,10,11]. Attenuation in silica-based optical fiber materials can be as low as 0.2 dB/km when the operating wavelength is 1.55 μm.

Another problem which appears in optical CDMA systems is the need for a very short pulse at the input of the optical encoder as shown in Figure 2.9.

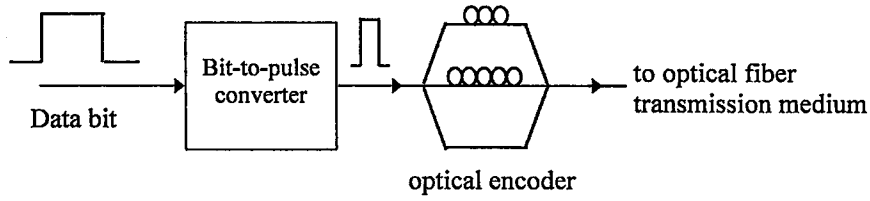

Figure 2.9. Optical encoder with bit-to-pulse converter

This bit-to-pulse converter is necessary to convert the low-rate information bit to a high-rate optical sequence. The input information (or data) bit is mapped to a short pulse which then passes through the optical fiber delay lines. The resulting optical orthogonal codeword (or PN sequence) is then coupled to the optical transmission medium.

As it can be seen, the implementation of an optical CDMA system is very attractive if compared to the electronic systems. Both encoder and decoder structures are very simple to implement and synchronization of PN sequences is not necessary due to the optical correlators used.

2. 3 Optical Orthogonal Codes

Various design methods for PN sequences for CDMA-employing communication systems have been explained in detail in [12] , [13] , [14] and [15]. Among these, sets of orthogonal code sequences such as the maximal length or m-sequences have received considerable attention. M-sequences are shift register sequences of length

$$N=2^n-1 \qquad (2.3.1)$$

which is the longest sequence length which can be generated using an n-stage binary linear feedback shift register. The important characteristic of an m-sequence is that it has a two-valued discrete autocorrelation function [13], which is equal to N at the end of the bit interval and -1 at the other time instants. Moreover, a lower bound exists for the crosscorrelation function between any two m-sequences. This lower bound is equal to

$-1+2^{(n+1)/2}$.

Another class of codes is derived using m-sequences by choosing those exhibiting the minimum possible crosscorrelation peak (equal to $-1+2^{(n+1)/2}$). These are referred to as preferred maximal length sequences.

In addition to the preferred m-sequences, Gold sequences [14] are also proposed for CDMA transmission systems. A Gold code is a set of N+2 code sequences given by

$$G = \{ a, b, a \oplus b, a \oplus Tb, ..., a \oplus T^{N-1} b \} \qquad (2.3.2)$$

where {a,b} is a preferred maximal length sequence pair, and T^i denotes an operator that shifts a sequence cyclically i chips to the left. The operator $\oplus$ denotes mod 2 addition.

The above mentioned sequences exhibit good autocorrelation and crosscorrelation properties in electrical communication systems where the ±1 levels are used. However, these sequences are not appropriate in non-coherent optical CDMA systems where only the 0 and 1 levels are available. That means, the signals cannot add up to zero to yield good correlation properties.

Although, in [16] an optical code-multiplex transmission system employing Gold sequences is reported, this system does not yield satisfactory results, since Gold sequences are not constant-weight codes and the correlation properties are not good enough in an optical environment. Therefore, the code design for non-coherent optical systems differs from the classical coding problems for electrical communication systems.

2.4 Fundamental Properties and Upperbounds

An $\{n, \omega, \lambda_a, \lambda_c\}$ optical orthogonal code (OOC) is a family of (0,1) sequences of length n (number of chips) and weight ω (number of ones in the codeword) which satisfy the following two properties:

1. Autocorrelation property

$$\Theta_{xx}(m) = \sum_{i=0}^{n-1} c_x[i] c_x[(i+m) \bmod n] \le \lambda_a \qquad (2.4.1)$$

for any codeword $C_x = (c_x[0], c_x[1], ..., c_x[n-1])$ and any integer m, $0<m<n$. $c_x(i)$ denotes the value of the i^{th} chipposition; $c_x[i] \in (0,1)$.

2. Crosscorrelation property

$$\Theta_{xy}(m) = \sum_{i=0}^{n-1} c_x[i]c_y[(i+m) \bmod n] \le \lambda_c \qquad (2.4.2)$$

for any codewords $C_x \neq C_y$ and any integer m.

$\Theta_{xx}(m)$ and $\Theta_{xy}(m)$ are the discrete periodic autocorrelation and discrete periodic crosscorrelation functions, respectively.

$$\Theta_{xx}(0) = \omega \qquad (2.4.3)$$

because each sequence C_x has weight equal to ω.

The numbers λ_a and λ_c ($0 < \lambda_a, \lambda_c \le \omega$) are the autocorrelation and crosscorrelation properties, which must be satisfied for a given code. The (0,1) sequences of an optical orthogonal code are called its codewords. The size of an OOC C, denoted by $|C|$, is the number of codewords in it.

The largest possible size of an $(n,\omega,\lambda_a,\lambda_c)$ OOC is denoted by $F(n,\omega,\lambda)$ where

$$\lambda = \max\{\lambda_a, \lambda_c\} \qquad (2.4.4)$$

An OOC having the maximum size is said to be optimal.

Upperbounds on $F(n,\omega,\lambda)$ can be obtained from results in algebraic coding theory [17]. Let $A(n,d,\omega)$ denote the maximum size of an errorcorrecting code of length n, constant codeword-weight ω, and minimum Hamming distance d. The Hamming distance between two n-tuples is the number of bit positions in which they differ. Then, the Johnson bound [17] states that

$$A(n,2\delta,\omega) \le \frac{n(n-1)\cdots(n-\omega+\delta)}{\omega(\omega-1)\cdots\delta} \qquad (2.4.5)$$

The Johnson bound will be used to derive the upperbound for $F(n,\omega,\lambda)$. For any $(n,\omega,\lambda_a,\lambda_c)$ OOC C, let C' be the error-correcting code consisting of all cyclic shifts of codewords of C. For every codeword in C there exists n possible cyclic shifts. In general, the sizes of the two codes are related by

$$|C'| = n|C| \qquad (2.4.6)$$

Every n tupple in C' has Hamming weight ω. In addition, for any two members of C', there are at most λ bit positions where they have both a one. Thus, C' has minimum distance of at least 2ω-2λ, and therefore,

$$|C'| \le A(n,2\omega-2\lambda,\omega) \qquad (2.4.7)$$

In OOC's, no distinction is made between cyclic shifts of a codeword, i.e., a codeword and a cyclic shifted version of itself are equivalent. Using (2.4.6)

$$|C| \le \frac{1}{n} A(n, 2\omega - 2\lambda, \omega) \tag{2.4.8}$$

Substituting $\delta = \omega - \lambda$ in (2.4.5) and combining with (2.4.8), the upperbound for the OOC is found to be

$$F(n,\omega,\lambda) \le \frac{(n-1)(n-2)\cdots(n-\lambda)}{\omega(\omega-1)\cdots(\omega-\lambda)} \tag{2.4.9}$$

While designing OOC's, the aim is to design a set of (0,1) sequences with constant weight and minimum overlap.

2.5 (n,6,l,l) OOC's

Design of (n,6,1,1) optical orthogonal codes based on extended sets are explained in detail in [25]. In the design of FOMD (500,6,1,1) optical orthogonal codes are used. Six positions of the chip of length 500 are filled with ones while the other positions are all zero. The (500,6,1,1) codewords are obtained in [25] as in Table 2.1.

Table 2.1. (n,6,1,1) OOC codewords based on Extended sets

USER	CODEWORD
C1	(0,2,14,42,92,177)
C2	(0,3,16,46,99,188)
C3	(0,4,19,52,107,200)
C4	(0,5,22,56,113,208)
C5	(0,6,24,60,121,222)
C6	(0,7,27,65,129,233)
C7	(0,8,29,70,138,243)
C8	(0,9,32,76,149,255)
C9	(0,10,35,82,161,271)
C10	(0,11,37,86,170,281)

In Figures 2.10 and 2.11 the autocorrelation function of codeword C1 and the crosscorrelation function of C1-C4 are given. As it is observed, the properties are satisfied for both codewords.

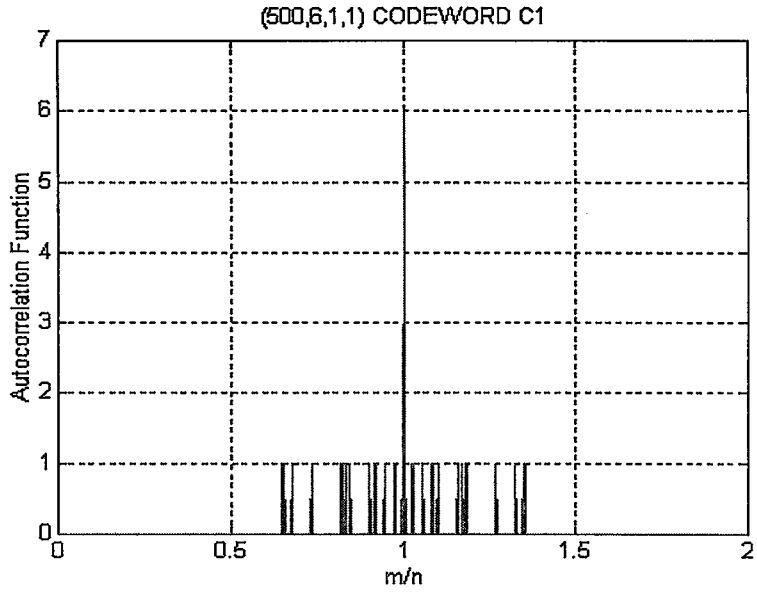

Figure 2.10. Autocorrelation of (500,6,1,1) codeword C1

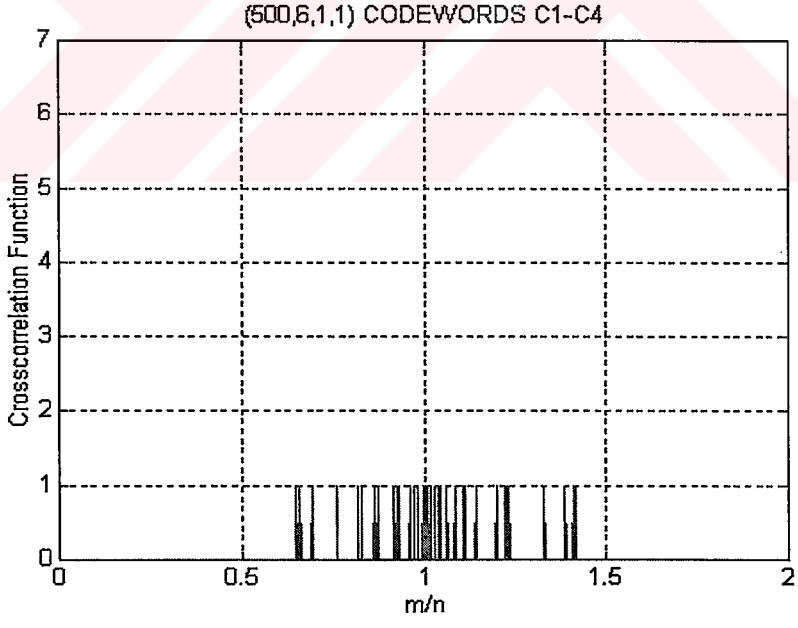

Figure 2.11. Crosscorrelation of (500,6,1,1) codewords C1-C4.

2.6 Performance Analysis of (n, ω,l,l) Optical Orthogonal Codes

Performance analysis for CDMA systems are discussed in detail in [12,18,19,20]. However, the analysis are based on ±1 levels which are not available in intensity modulated optical CDMA systems where true (0, 1) sequences are employed. The analysis for OOC's are presented in [21,22,23,24]. In this section, the analysis refers to [21] where the effects of attenuation, dispersion and scattering [9,10,11] of the optical pulses propagating in the fiber cable are ignored. In addition, the effect of various noises such as the shot noise and dark current present in photo detectors are not taken into consideration. Therefore, the main source of noise to be considered is the interference due to the simultaneous users transmitting information through the optical transmission medium using the same spectrum.

If Z_i denotes the optical signal after the correlator of user I, then

$$Z_1 = d_1\omega + I_1 \tag{2.6.1}$$

where $d_1 \in \{0,1\}$ is the data sent to user I, ω=weight of the code employed and I_1 denotes the interference due to the other N-1 users. Then, the probability density function for I_1 assuming chip synchronous transmission can be written [21] as

$$p_{I_1}(I_1) = \sum_{I=0}^{N-1} \binom{N-1}{i} q^i (1-q)^{N-1-i} \delta(I_1 - i) \tag{2.6.2}$$

where

$$q = \frac{\omega^2}{2n} \tag{2.6.3}$$

It is quite obvious that chip synchronous transmission is the worst possible case since it yields the largest possible output at the correlator.

In (n,ω,1,1) OOC's, two codewords overlap at most at one chip position and there are ω^2 ways of passing the ω pulses of two users. Hence, q represents the probability that a pulse belonging to a particular user overlaps with one of the pulses of the desired user and n denotes the number of chips. The 1/2 factor in q accounts for the probability that the interferor is transmitting a one. If the threshold of the decision device which is placed after the correlator is set to Th ($0<Th\leq\omega$), then the probability of error is

$$P_e = \Pr\{Z_1 \geq Th | d_1 = 0\}\Pr\{d_1 = 0\} + \Pr\{Z_1 < Th | d_1 = 1\}\Pr\{d_1 = 1\} \quad (2.6.4)$$

However, if $d_1=1$, then $Z_1 = \omega+I_1$ and $I_1>0$ since optical power is measured; therefore, $Z_1>\omega$. This results in $\Pr\{Z_1<Th | d_1=1\}=0$ and if equally likely signaling is assumed, i.e., $\Pr\{d_1=0\}=\Pr\{d_1=1\}=1/2$, (2.6.4) reduces to

$$P_e = \frac{1}{2}\Pr\{Z_1 \geq Th | d_1 = 0\} \quad (2.6.5)$$

Using the probability density function given in (2.6.2), the probability of error may be expressed as

$$P_e = \frac{1}{2}\int_{T_h}^{\infty} p_{I_1}(I_1)dI_1 = \frac{1}{2}\sum_{i=Th}^{N-1}\binom{N-1}{i}q^i(1-q)^{N-1-i} \quad (2.6.6)$$

It should be pointed out, that the probability of error, as expressed in (2.6.6) is derived for the case when no optical limiter is employed at the receiver side. However, using an optical limiter at the front of the correlator improves the performance of the system considerably. Hence, for the power limited case, the probability of error is equal [21] to

$$P_e = \frac{1}{2}\binom{\omega}{Th}\prod_{m=1}^{Th}\left(1-\nu^{N-m}\right) \quad (2.6.7)$$

where

$$\nu = 1-\frac{\omega}{2n} \quad (2.6.8)$$

denotes the probability of no coincidence of ones of two different codewords. The probability of error expression in (2.6.7) can be derived as follows.

There are $\binom{\omega}{Th}$ ways of reproducing a pattern with ω pulses up to the threshold level Th. A coincidence of a particular chip position of a desired sequence occurs for the first time with probability $(1-\nu^{N-1})$. Then, the next chip position of the intended pattern-n overlaps with one less effective number of the total interference signal, i.e., $(1-\nu^{N-2})$. Hence, assuming the presence of N-1 interferors,

$$\Pr\{Z_1 \geq Th | d_1 = 0\} = \binom{\omega}{Th}\prod_{m=1}^{Th}\left(1-\nu^{N-m}\right) \quad (2.6.9)$$

is obtained. Substituting this result in (2.6.5) yields (2.6.7).

In Figure 2.12., the probability of error versus the number of interfering users is plotted for the (500,6,1,1) OOC for the threshold levels 5 and 6 are given. It is observed that even if all ten users are sending information, the probability of error is less than 10^{-6} for Th=5 and slightly greater than 10^{-9} for the Th=6 case. Hence, the performance of the (500,6,1,1) OOC is satisfactory for a reliable communications system.

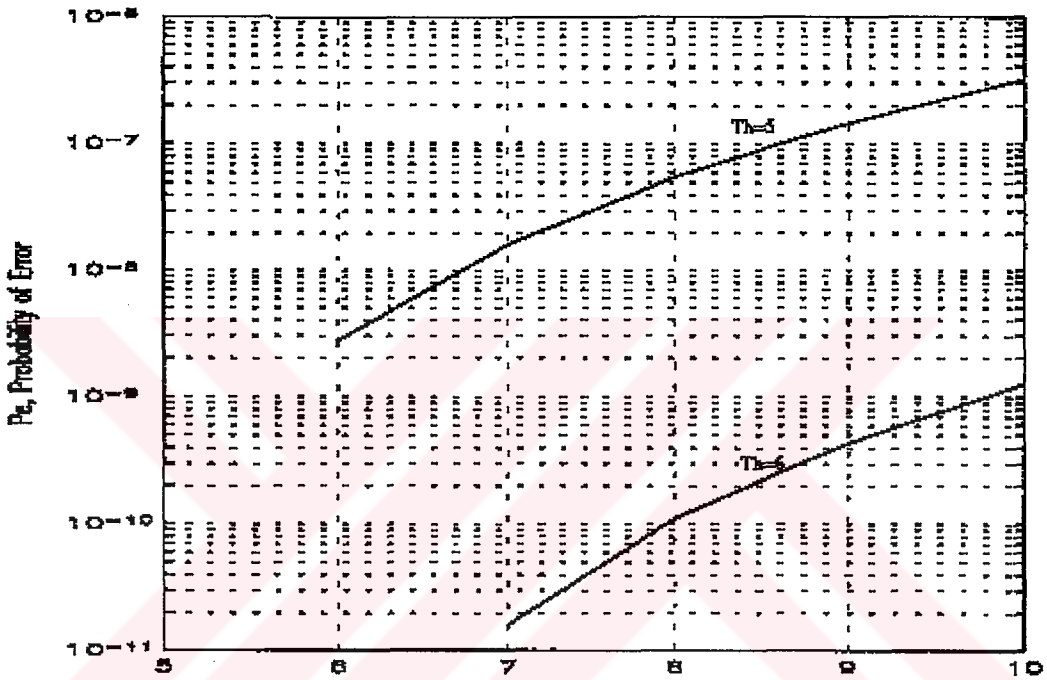

Figure 2.12. P_e for (500,6,1,1) OOC

CHAPTER III
VARIOUS IMPLEMENTATIONS OF FIBER-OPTIC LOOP MEMORY

3.1 Introduction

Using fiber-optic medium for information storage attracted researchers and scientists for many years. There has been several implementations cited in references which implement the fiber-optic loop memory by circulating the information carrying pulses in a closed loop delay line made of a fiber-optic material.

In order to see the developments and compare already published fiber optic loop memory implementations with the proposed structure, four previously reported work will be summarised in this chapter. The techniques used in these relatively recent references indicate that the proposed structure has advantages in overcoming losses as well as regeneration and read-write problems in fiber-optic loop memory systems..

In the following sections of this chapter, four different loop memory structures, which are reported in references [40], [28], [30], [42] will be shortly reviewed and some related concepts will be explained.

3.2. Optical Data Storage Using Multistable Oscillations

The proposed configuration of the loop memory for data storage given in reference [40] is shown in figure 3.1. The nonlinear ring oscillator is formed by an optical fiber loop of round-trip time T_r, including an active nonlinear element with response time T_m. Couplers dedicated to write, erase, read and locking ports are employed to inject or to detect signals. The delayed feedback of the read output to write is used for the erase operation. The active nonlinear element is assumed to have a sinusoidal type relationship between input intensity and output intensity. In a hybrid electro-optical implementation, the nonlinear element could be a laser with an EO intensity modulator [26].

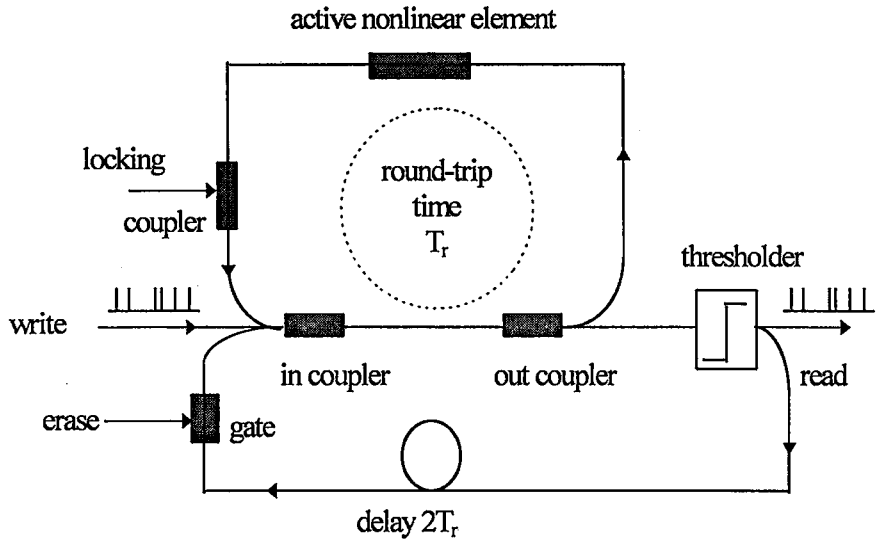

Figure 3.1. Loop memory configuration

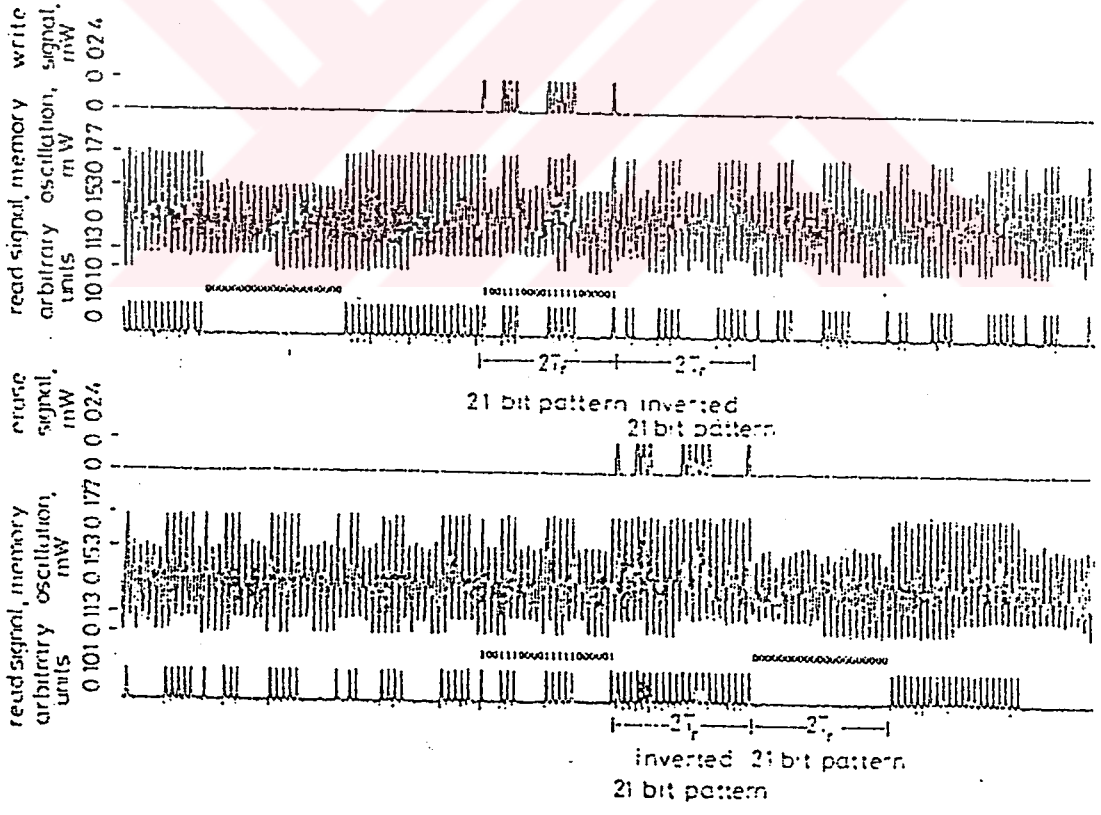

Figure 3.2. Example of write and erase of 21 bit sequence of '100111000011111000001'

Effective delay is defined as the ratio of round-trip time T_r to response time T_m. With large effective delay, (i.e. $T_r / T_m >> 1$), many different modes can oscillate stably in the ring. The modes can be classified into classes, each class labeled by (n,m) where n is an odd harmonic and m is a bifurcation order [27]. Examples of (21,2) modes are shown in figure 3.2.

The relationship between the modes and the data stored in the waveform is as follows. A mode in the (n,2) class can be considered as a carrier oscillation of period $2T_r/n$, whose peaks (and also valleys) are modulated in two levels, 1-level (high) and 0-level (low). The peak modulation pattern corresponds to a cyclic 2n-bit pattern. Data stored in the modulation peak pattern can be read by thresholding the peak levels. The resulting read signal is a periodic RZ binary optical pulse train, corresponding to a sequence of n bits of information in a time interval of length $2T_r$ followed by the inverted n-bit sequence. With phase identification, there is an (n,2) oscillation for every n-bit sequence, and the capacity of the memory using the (n,2) oscillations is n bits.

The important feature of this memory configuration is that write and erase of data can be executed using the same sort of RZ binary pulse train which is obtained as a read signal. The write is executed by injecting an n-bit RZ binary optical pulse train into the loop through the in coupler. Input pulses should have both width and separation of about T_r / n. An n-bit input pulse train has total length $2T_r$. The erase operation can be executed by injecting a read signal of length $2T_r$ back into the loop after a delay of $2T_r$, which corresponds to superposed write of the inverse bit pattern to cancel the n-bit pattern stored in the oscillation waveform. Phase identification is achieved by locking the oscillation through the locking port. All timings of the memory operations can be identified with locking to the external reference oscillation.

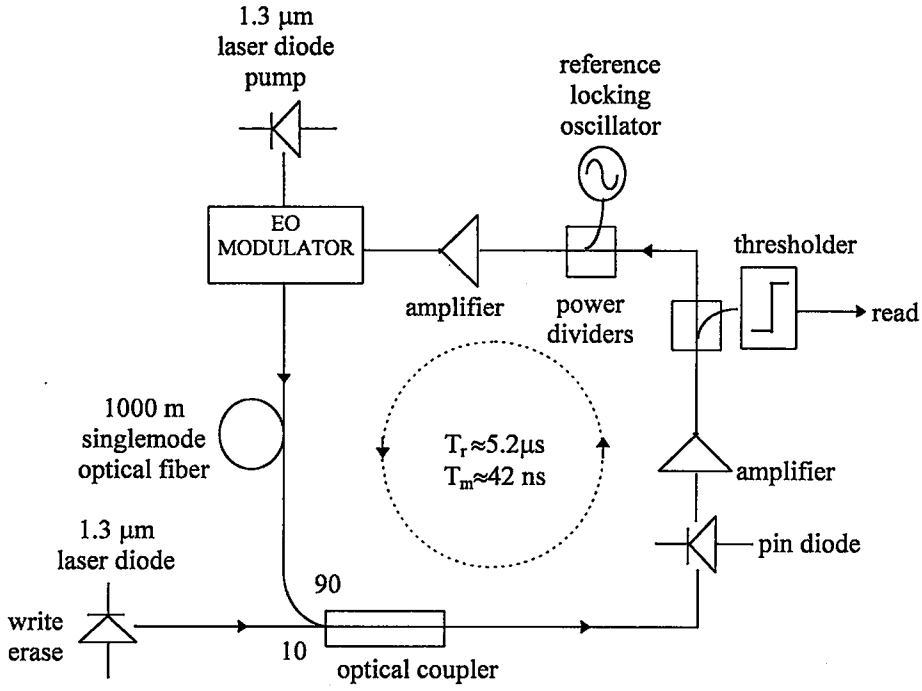

Figure 3.3. Experimental setup

The experimental setup used to confirm the feasibility of the proposed memory structure in reference [40] is shown in figure 3.3. The ring generating the multistable oscillations is a hybrid electro-optical ring resonator, essentially consisting of a Fabry-Perot (FP) laser diode (LD), an EO intensity modulator with waveguide Mach-Zehnder structure, a 100 m singlemode optical fiber delay line, pin photodiode for 1.3 μm optical communication and high-speed video amplifiers with 3 dB bandwidth from DC to 150 MHz [26]. The active nonlinear element is the combination of LD and EO modulator. The EO modulator has a sinusoidal EO modulation characteristics. In this experiment effective delay is set as $T_r / T_m \cong 124$ ($T_r \cong 5.2$ μs and $T_m \cong 42$ ns) by introducing a lowpass filter at the output port of the first stage video amplifier. For the in coupler, an optical coupler with a splitting ratio of 90:10 is used. The other couplers in figure 3.1 are substituted with electrical power dividers in figure 3.3.

The ring resonator is pumped by the LD with constant optical power. The class of (n,2) modes could be selected and phase-locked to an external reference oscillation by injecting a small amplitude sinusoidal signal at a frequency near the

carrier frequency, $n/(2T_r)$ into the loop. For the (21,2) modes shown in figure 3.2, the LD pump power is 0.76 mW. The frequency and amplitude of the external reference oscillation is set to be 1.99566 MHz and 0.5 % of the amplitude of the oscillation in the loop, respectively. The locking range under the above mentioned condition is about 0.0023% of the free-running frequency of the (21,2) mode. The range increases in proportion to the amplitude of the injected reference signal. Different modes in the (21,2) mode class are found to have almost identical locking ranges. With this locking technique phase stability and identification of the cyclic 42-bit memory pattern can be obtained.

Figure 3.2 [40] shows an example of write, read and erase of 21 bit binary data. One of the memory states, the one corresponding to all 0 is used as an initial state for write operation. This state can be reached from any other memory state with the erase operation described below.

Another 1.3 μm FP LD, directly driven by a an arbitrary function generator, is used to generate the write signal, a 21 bit RZ binary optical pulse train of length $2T_r$. The write signal is injected through the optical coupler. The optical power of the light pulses injected into the loop is 0.024 mW. When injected with the correct timing, the write pulses are superposed on the low 0 peaks of the initial state oscillation in the loop as shown in figure 3.2.a.

In the read operation, the peak levels of the electrical oscillation signal output from the electrical stage of the ring are thresholded midway between the 1 and 0 levels to obtain a cyclic 42 bit RZ pulse sequence of period $4T_r$ (21 bit RZ pulse sequence of length $2T_r$, followed by the inverted 21 bit RZ pulse sequence of length $2T_r$), as indicated in the lower waveforms of figure 3.2. In the test of erase operation, shown in figure 3.2.b., the same write signal as in figure 3.2.a is injected with a delay of $2T_r$ with respect to the first bit of the 42 bit cyclic memory pattern so that it is added onto the inverted peak pattern to cancel the data in memory. In the write and erase operations shown in figure 3.2, the RZ pulse height and width of write (or erase) signal injected into the loop is about 0.024 mW of optical power and 50% of duty ratio, respectively, which roughly corresponded to the difference between high and low peaks of the (21,2) oscillation waveform in the loop. With the optimum pulse height and width, the waveform quickly settles to the destination memory state

with little transient as shown in figure 3.2. However, some variation of the pulse height and width could be tolerated, due to the dynamical stability of the oscillation mode.

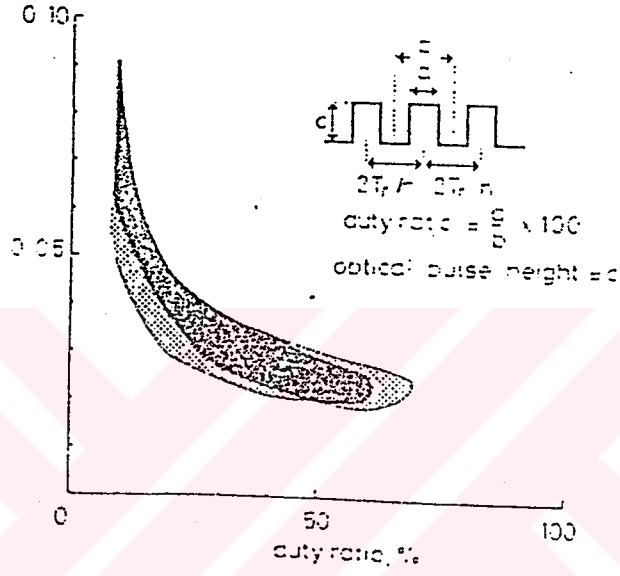

Figure 3.4. Regions of pulse height-pulse width space for reliable write and erase of 21 bit sequence of '100111000011111000001'

Figure 3.4 [40] shows a typical example of the region of the pulse height-pulse width space in which the write operation for a 21 bit pattern could be reliably executed. The shape of the region shows that the narrower the pulse width the larger the pulse height. Although there are small differences in the region for write and erase of the same bit pattern and there is a small dependence on bit pattern, it is found that for all the bit patterns examined the area around 0.024 mW pulse height and 50% pulse width is suited to reliable write and erase operation.

3.3. Fiber-optic Loop Memory for Optoelectronic Computer

This section is concerned with the method of increasing the information capacity and reliability of information storage in a circulator fiber-optic memory by forming an additional built-in channel with contrary-directed signal circulation [28].

In the structure proposed in [28], two contrary-directed circulation channels (main and additional ones) are organized in a single fiber-optic memory device (FOMD) loop. The FOMD is shown in figure 3.5.

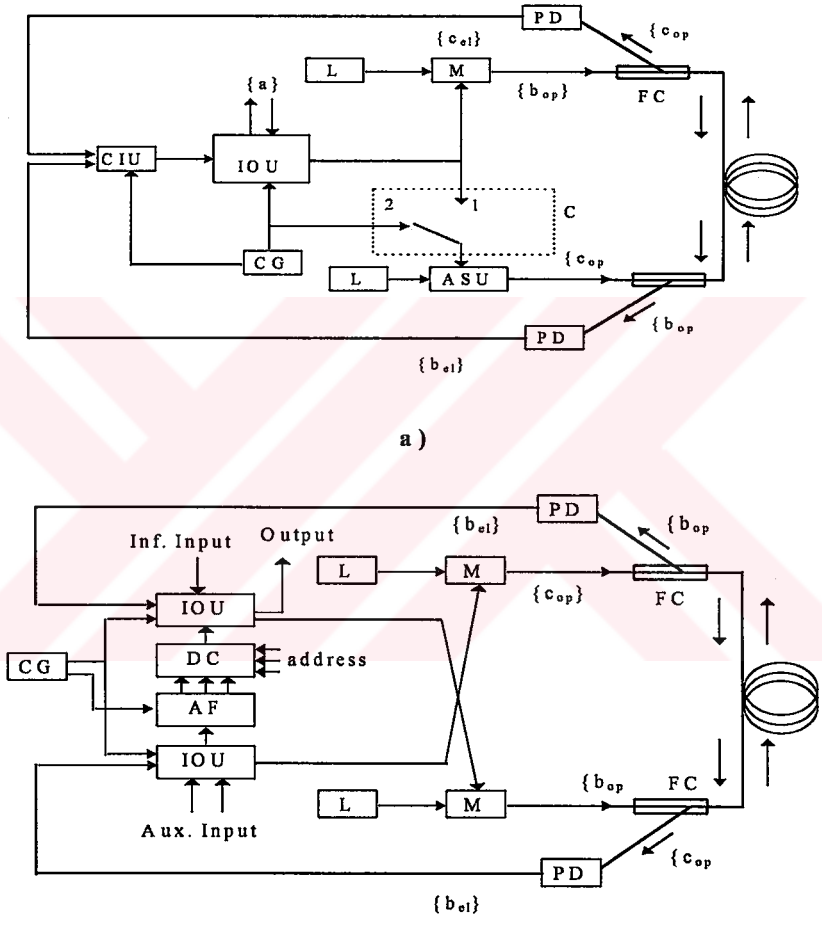

Fig.3.5. Structural diagram of the fiber-optic memory loop with contrary directed circulation of the signals.

In the structure shown in figure 3.5., PD is photodetector, M is modulator, ASU is unit for formation of auxiliary signals, C is commutator, CIU is unit for correction of information, L is laser, IOU is information input/output unit, FC is

fiber-optical coupler, CG is generator of the clock pulses, AF is address former, DC is digital comparator.

Information signal sequence circulates in the main channel, while the additional channel is used to transmit both part of the information sequence and auxiliary signals (verifying, synchronizing, and addressing words) formed by the auxiliary signal unit (ASU). In the latter case, optical signals circulating in both channels can be transmitted at both the same and different carrier frequencies. In the case shown in figure 3.5.a., the additional channel serves to transmit a verifying correcting sequence and ensures enhanced reliability of storage of the main information sequence. The input information sequence {a} is subjected to convolutional symmetrical coding and is converted to the corresponding sequences of information $\{b_{op}\}$ and test optical signals $\{c_{op}\}$. In this case the commutator is switched to position 1 (figure 3.5.a.), and the ASU acts as a convolutional encoder consisting of two series-connected phase modulators whose control voltage is set equal to zero or half-wave value depending on the value of the information signal.

Separated information and test signal flows arrive simultaneously in the fiber-optic circulation loop through couplers placed on its opposite ends. The contrary directed flows $\{b_{op}\}$ and $\{c_{op}\}$ also emerge simultaneously at the loop outputs and being converted to the corresponding sequences of electrical signals $\{b_{el}\}$ and $\{c_{el}\}$, are used for decoding information and correcting errors with out any demultiplexing required. The corrected information sequence is again subjected to encoding.

The use of the contrary-directed channel in the fiber-optic circulator makes it possible to increase error-free storage probability owing to a two-fold reduction of the character repetition rate in the optical tract or to achieve a two-fold increase in the stored information volume at the same clock frequency.

To ensure a reliable access to any segment of circulating information sequences and to improve its storage security, the additional channel can be used as an addressing channel. In this case (Figure 3.5.b.), writing of the informations sequence and the auxiliary (addressing) sequence into the loop is achieved by feeding them synchronously to the information (Inf. input) and auxiliary (aux. input) input terminals of the input/output unit (IOU), respectively, and further to control input terminals of the corresponding electrooptical modulators. As the addressing

sequence circulates in closed loop, its segments (address words) are also synchronously written into an n-bit address former (AF) thereby forming the address of a coming information sequence. Synchronous circulation of signal flows along identical channels allows simultaneous feeding of the IOU input terminals independent of any external influences.

Access to the required information signal (rewriting, retrieval) is realized through setting appropriate address on the address inputs of a digital comparator. When the contents of AF coincides with the set address during the next passage of the address sequence along the circulation loop, the DC generates a control signal used to strobe information signals.

In order to reduce error probability in forming address words, it is advantageous to use a pseudo-random sequence (PRS) as address sequence. The PRS length is $M=2^N-1$, where N is the PRS generator bit capacity; the address former represents an n-bit shift register, where n is not less than N. In case a redundant length of the PRS address words is used, i.e. for $n>N$, addressing is free of errors even if the received address word has several incorrect (spoilt) bits.

The additional channel can also be used for transmission of a sequence of clock signals whose time parameters are matched with those of the information signal. In this case, the information and synchronizing sequences circulate in synchronism in opposite directions along the same loop, which excludes their mistiming caused by the influence of external temperature and mechanical factors on the fiber-optic tract thus improving reliability of the information signal synchronization. In this case, the ASU represents a modulator that is identical to the main channel modulator controlled by the clock pulse generator (commutator in figure 3.5.a. is switched to position 2). The clock signals at the output end of the additional channel are used for synchronous detection of the output information sequence. The repeated input of the restored information signals into the circulation loop is performed synchronously with pulses of a quartz clock.

The contrary-directed channel in the fiber-optic circulator can be employed for amplification and compensation of attenuated information signals propagating in the light guide, making an electrooptical regenerator superfluous. Moreover, by

closing the loop with the couplers, an all-optical FOMD with multiple propagation of signals in the loop is obtained. Even if the electrooptical regenerator is employed, optical amplification allows formation of a considerably longer loop and, hence, obtaining of a higher FOMD capacity.

Optical amplification in a fiber can be accomplished by using various nonlinear optical effects, for example, stimulated Raman scattering (SRS).[29]

The bi-directional circulation regime discussed in this section makes it possible to find an effective solution to the problems of increasing the information capacity and attaining reliable storage of information in the FOMD circulation loop. Moreover, it allows optical amplification of information signals to be achieved. Amplification of information signals can be effected by using both continuous wave pumping and synchronizing signals of appropriate power. Thus, the contrary-directed channel can be simultaneously used for both synchronization and amplification of information pulses. The required optical power of the pump wave is of the order of some hundreds of miliwatts. [30]

3.4. A Fiber-optic Memory Device with All-optical Regeneration

The optical recirculating loop used for the all-optical regeneration is shown in figure 3.6. It includes an SRS (Stimulated Raman Scattering) amplifier, a filter that suppresses radiation at the Stokes wavelength, an SRS generator, and a fiber delay line. A singlemode polarization-preserving fiber with a core diameter of 6 μm is used. The fiber length in the SRS amplifier is 22 m. The SRS generator and fiber delay line are made of an 840 m long fiber. The first 30-50 m of the fiber participated effectively in the SRS generation. Attenuation of the Stokes and pump radiation by the filter is 30 and 2 dB, respectively.

An Nd YAG mode-locked laser with wavelength 1.064 μm, a pulse repetition frequency of 100 MHz, and pulse duration of 70-100 ps is used as a pump source. The average power of the laser pump radiation launched into the SRS amplifier in the setup is 2-2.5 W. This value is somewhat lower than the SRS threshold power in the 22 m long optical fiber. The average pump power launched into the SRS generator is about 1.5 W, which is somewhat higher than the SRS threshold power in a 50 m long fiber.

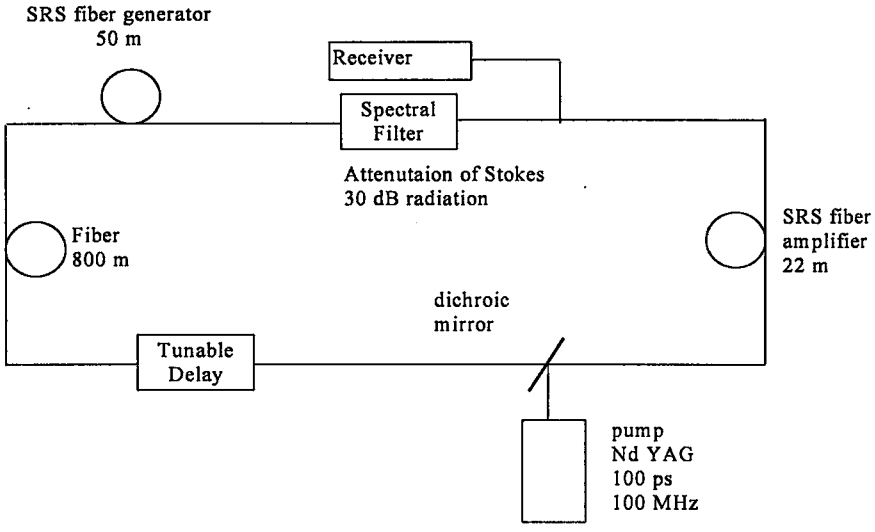

Figure 3.6. Fiber-optic memory device with all-optical regeneration

The SRS amplifier, SRS generator, and the filter form an SRS inverter. The Stokes signal of a sufficiently high intensity (logic one) fed into the SRS amplifier simultaneously with the pump pulse is amplified and causes its depletion. The resulting high Stokes signal is suppressed by the filter, and the depleted pump pulse is unable to generate a sufficiently intense Stokes signal in the SRS generator. As a result, a logic zero (a low intensity Stokes pulse) is formed at the output of the SRS generator. If there is no input Stokes pulse, the pump radiation travels to the SRS generator almost unattenuated and gives rise to a high intensity Stokes pulse corresponding to a logic one at the output of the SRS generator.

The dependence of the output Stokes pulse intensity on the input intensity can be rather sharp, and the ratio between a logic one and logic zero at the output can be higher than at the input. The Stokes pulses recirculating through the loop with the inverter are transformed from logic one to logic zero after every passage through the inverter. After several round trips the intensities of logic ones and logic zeros reach a high and low stable level, respectively. As a result, once launched into the loop, the information in the form of a pulse sequence with low and high intensities will be preserved, and occasional deviations of amplitudes from the stable levels will vanish.

After the pump radiation is launched into the fiber loop, a sequence of logic ones is formed at the output of the inverter. When this sequence passes through the

loop and reaches the input of the inverter, the sequence of logic zeros begins to be formed at the output and so on. As a result, the simplest signal sequence of logic zeros and ones that change from one into the other at each round trip arises in the loop. Figure 3.7.a. depicts the envelope of the pulse train at the Stokes wavelength at the output of the SRS amplifier just after switching on the pump radiation for the case when the information is conserved during circulations. Circulations of the sequence for more than 10 min are observed. The situation when the sequence is destroyed is presented in figure 3.6.a. In this case the amplitudes of logic ones and zeros tend to one level and after several circulations become indistinguishable. The type of operation that will be achieved depend on the intensity of pump pulses, the delay in the loop, and the parameters of the spectral filter.

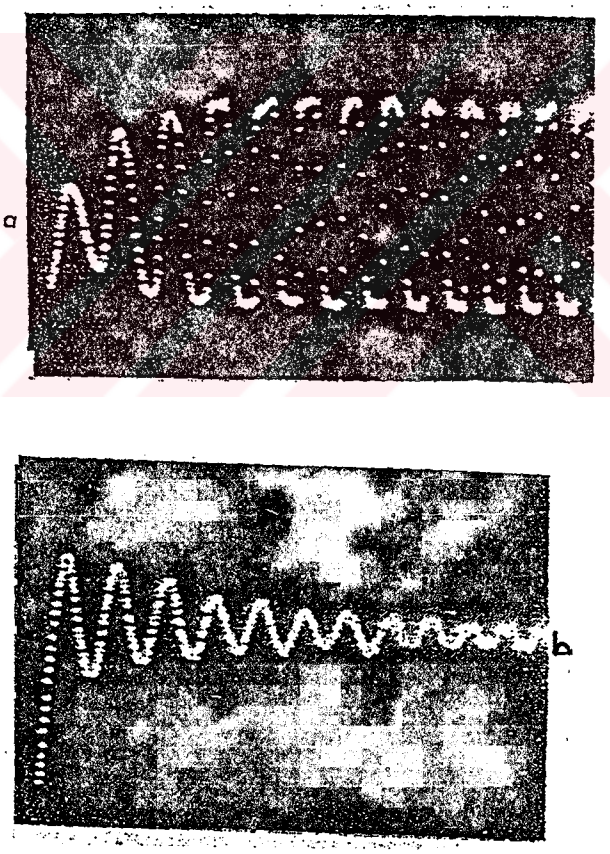

Figure 3.7. Oscilloscope traces of envelopes of Stokes pulse train at output of SRS amplifier (a: information conserved in loop, b: information destroyed)

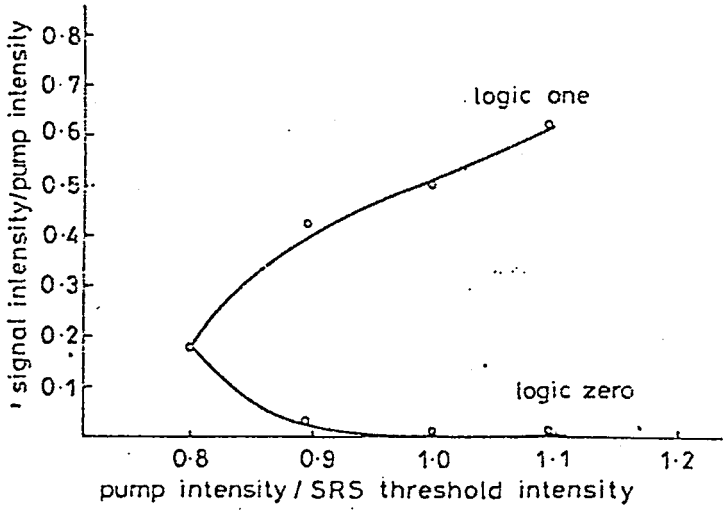

Figure 3.8. Intensities of logic ones and logic zeros against pump intensities launched into SRS amplifier

The effect of the pump power is demonstrated in figure 3.8. It shows the average intensities of logic zeros and ones in the loop as a function of the pump power launched into the SRS generator. It is seen that for the pump power in the SRS generator below 0.8 of the threshold, ones and zeros do not differ from each other. As the pump intensity grows, the intensity of ones reaches a level of 0.5 of the pump intensity. The ratio between the intensities of the trains of ones and zeros can be higher than 50.

3.5. Fiber-optic Loop Memory Used in ATM Packet Buffering

In this section, a photonic high bit-rate switching fabric, capable of routing ATM cells and solving cell contention given in reference [42]is introduced [31,32]. One of its key functions is the optical buffering of ATM cells, based on fiber-loop memories: to reduce the amount of optical hardware, the exploitation of the wavelength domain is proposed. The operation of a multiwavelength fiber-loop

memory is described. The simultaneous and independent storage of 622 Mbits/s ATM cells in the same fiber-loop by using two different wavelengths is explained.

As shown in figure 3.9 [42] the fiber loop is split into two branches, each assigned to a fixed optical wavelength (λ_1 and λ_2, spaced by ~0.3 nm) and providing gating and filtering. Semiconductor optical amplifiers (SOA) are used for gating: one packet is stored (i.e. keeps circulating) as long as the SOA dedicated to its wavelength is switched on, whereas the memory position is erased if the SOA is switched off for one round-trip time. Filtering is provided by fiber Fabry-Perot filters (FFPF'S, bandwidth ≈10 GHz). Two FFPF'S, one preceding and one following the SOA gate have been used in each branch to reduce the level variations caused by multipath interference (due to leakage through the transmission tails of the FFPF'S). The path common to all wavelengths includes a fiber span and an erbium-doped fiber amplifier (EDFA). The loop delay is adjusted to the packet duration plus a guard band.

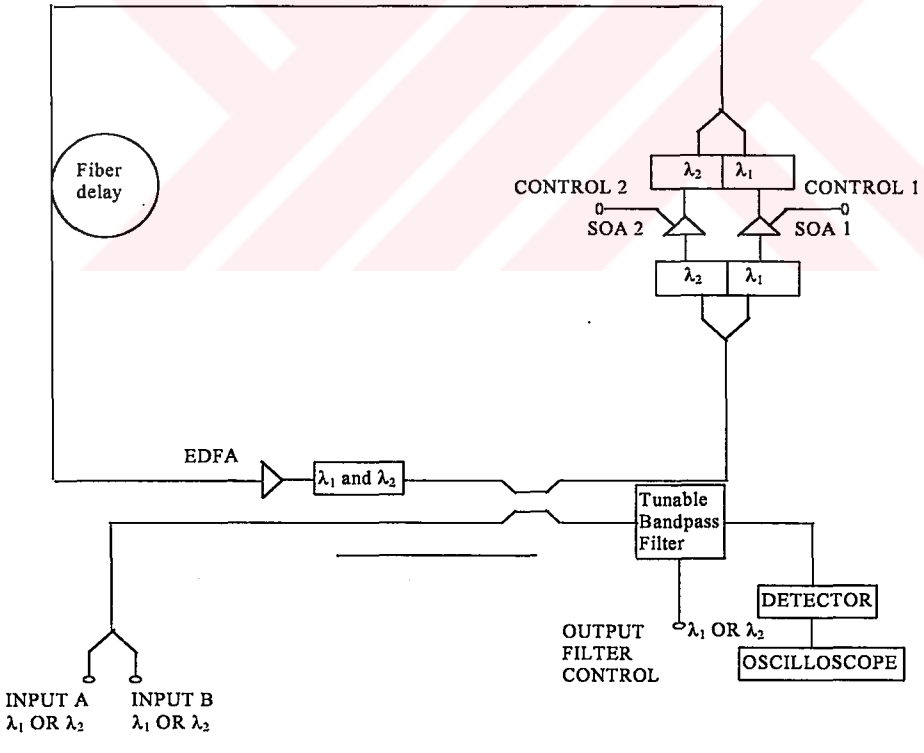

Figure 3.9. Diagram of the two-wavelength fiber-loop memory structure

The input signals to the fiber-loop memory are provided by externally modulated distributed-Bragg-reflector lasers, emitting at either λ_1 or λ_2. Data packets (424 bits long) at 622 Mbits/s for the input signals are produced by a programmable generator, which also drives the loop gates.

To avoid the effect of interferometric noise at the fiber loop output due to the nonideal extinction ratio of the input signals, the sources emit at λ_1 or λ_2 just during the packets' transmission and are detuned to a trash wavelength λ_1 for the rest of time; λ_1 is chosen to keep the beat (λ_1-λ_2) or (λ_2-λ_1) outside the receiver bandwidth. This solution has been successfully tested, sending to the fiber-loop data coming from a wavelength converter based on gain-saturated SOA [33,34] which typically features a reduced extinction ratio.

At the output a narrow band (≈3 GHz) tunable filter selects the desired channel. More than 10 circulations have been observed, with a signal quality comparable to that obtained in the single-wavelength case [35].

3.6. Bit-error Rate (BER) Measurements in Random Access Fiber Loop Optical Memory

In this section, a fiber loop optical memory with active swtiching and amplifying elements and capable of random access presented in [41] is discussed. Transmission of 1.7 Gbits/s, 512 bit ATM-cell is achieved at BER=10^{-9} for up to seven fiber loop round trips.

The optical amplifiers are required in the fiber loop but ring laser operation has to be avoided. Two solutions are examined experimentally. In [33], an optical frequency translator was inserted into the loop. A disadvantage of this method is the difficulty in applying it to high data rates (≥ 1 Gbits/s). This is a serious argument because operation at high data rates was considered to be a main advantage of the delay line memories. Another way to avoid ring-laser operation is the periodic gating of the loop. First experiments enabled 160 Mbits/s transmission at BER=10^{-9} for one round-trip and at BER=10^{-4} for two round trips [34]. In this Letter transmission of a 1.7 Gbits/s signal (cell length 512 bit) is measured for constant signal power (-20 dBm) at the input of the memory (point a in figure 3.10.) with a constant BER=10^{-9}

for up to seven round-trips in the loop. The number of round trips has only been restricted by experimental constraints before.

Figure 3.10 [42] depicts the setup. It consists of four parts: the transmitter, the memory, the receiver, and the control unit. The optical paths are indicated by the thick lines and the electrical paths by thin lines. The optical and electrical signals at points A, B, and D are depicted in figure 3.11 [42] .

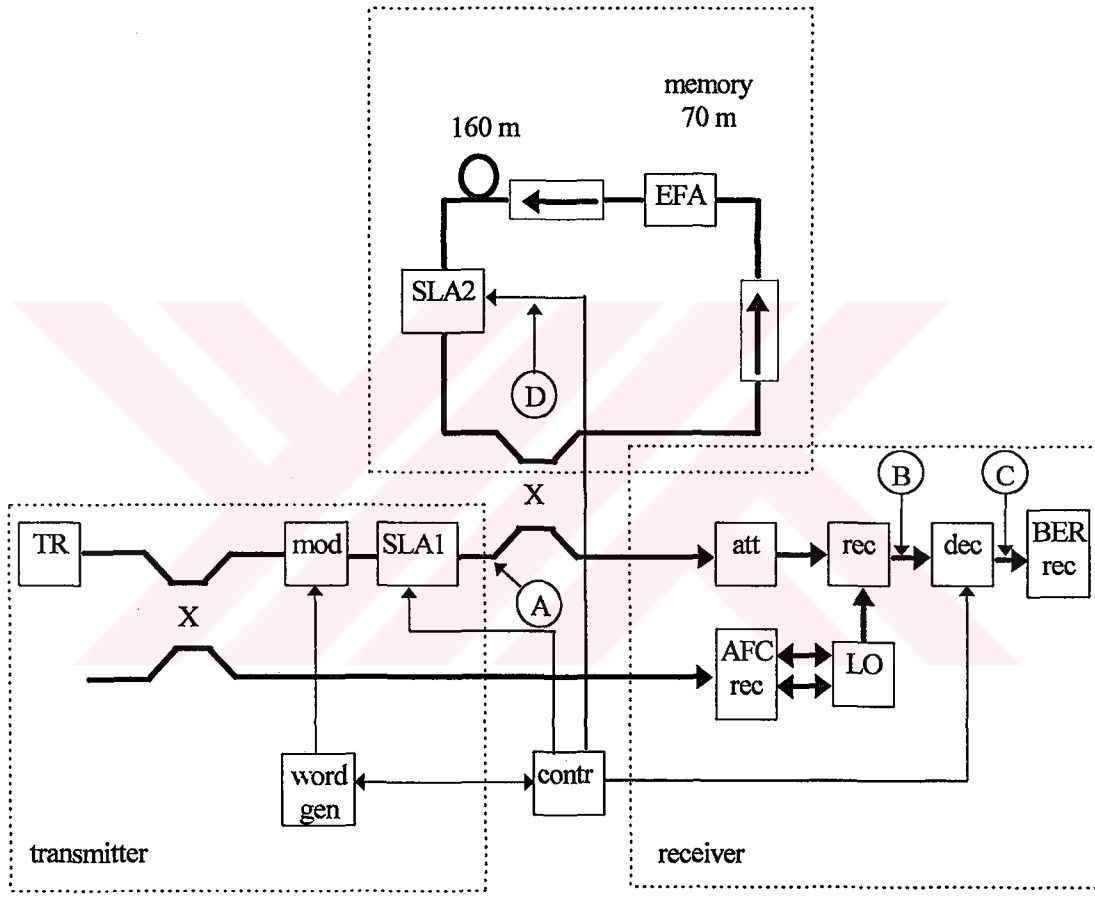

Figure 3.10. Setup consisting of transmitter, fiber loop memory, receiver, and control unit

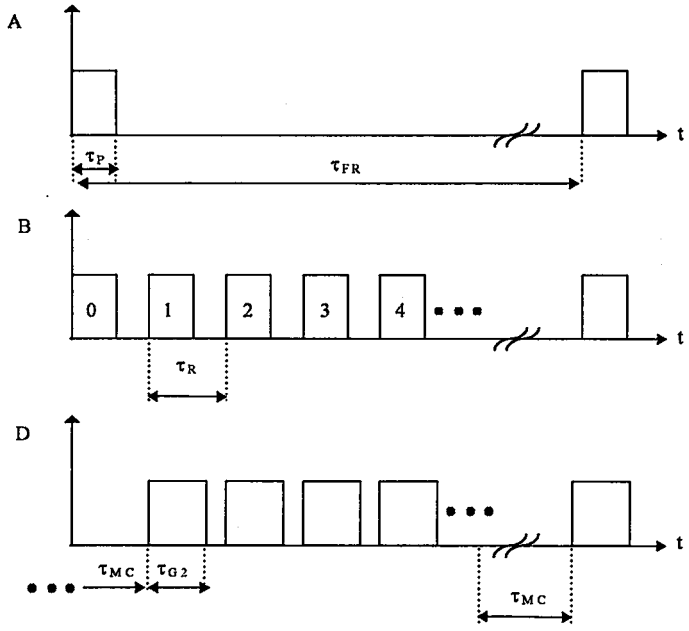

Figure 3.11. Schematic diagram of optical and electrical signals at points A, B, and D indicated in figure 3.9.

The transmitter outputs signal (A in figure 3.11) has two characteristic times, the packet length τ_p and the frame length τ_{PR}. In the experiments τ_p=0.6 μs and τ_{PR}=9.64 μs are used. The ATM-cell is a fraction of the packet with cell length $\tau_C<\tau_p$ (τ_C=512). $(B_T)^{-1}$=0.301 μs where the bit rate B_T=1.7 Gbits/s. The packet is generated by the gate SLA_1, which is a semiconductor laser amplifier operating as optical switch and the ATM-cell is generated by the transmitter laser TR, the modulator 'mod' and the word generator 'word gen'. Th timing of both the packet and the ATM-cell is controlled by the control unit 'contr'. Signal B in figure 3.12 represents a train of packets seen by the receiver. The numbers n=0,1,2,.... indicate the number of round trips in the loop. The number 0 designates the directly transmitted packet. In the 'dec' (decision circuit and gating unit) the signal B is gated such that only the packet with the desired number n is received by the BER receiver. The gate is controlled by the control unit 'contr'. In a more realistic system this gating operation is part of the memory and is performed in optical domain. In the transmitter and receiver parts, components of a coherent optical transmission system is used [36]. In the transmitter part, TR is an external cavity and mod is a $LiNbO_3$ phase modulator. Physically the ATM-cell is a phase-modulated (DPSK) carrier wave. In the receiver

part, 'rec' is a balanced phase and polarization diversity receiver, which converts the optical packet train into an electrical packet train. Contrary to a more realistic direct detection system, the coherent system needs additional components: the gate SLA1, the local oscillator LO and the additional AFC path for the control of the intermediate frequency. The memory consists of a fiber coil (length 160 m), a 3 dB fiber coupler, an erbium doped fiber amplifier (EFA, length 70 m) with optical isolators, and a semiconductor laser amplifier (SLA2) operating as optical switch. The SLA2 is switched periodically by the gating signal D as indicated in figure 3.11. The memory has three characteristics times, the round trip τ_R, which a packet needs for one circulation in the loop, the gating time $\tau_{G2}<\tau_R$ during which the SLA2 is in the transmission state and the memory clear time $\tau_{MC}>\tau_R$. In the experiment we used τ_R=1.1 μs, τ_{G2}=0.7 μs and the τ_{MC}=1.4 μs. The loop requires an automatic gain control. This operation is simply obtained by gain saturation in the EFA and the SLA. The control unit contr is an essential part of the present experimental setup, but in a more realistic system it is replaced by a control unit which controls the memory part.

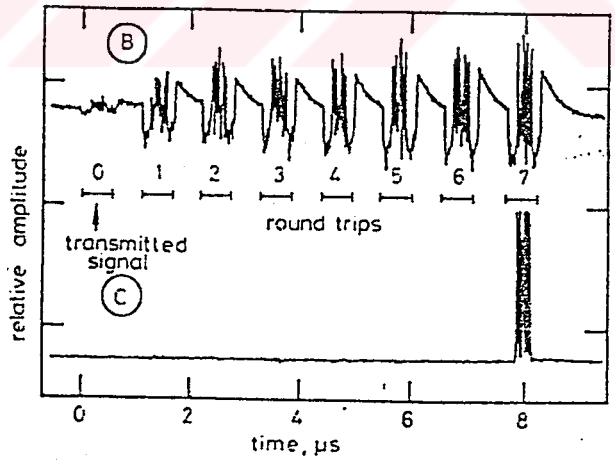

Figure 3.12. Packet train before (point B in Fig.3.9) and behind (point C in Fig.3.9) decision circuit and gating unit DEC.

Figure 3.12 [42] shows in the upper part of an oscilloscope trace of the received packet train (signal point B in figure 3.10). Indicated is the number n of round trips in the fiber loop of each received packet. Note that the directly transmitted (n=0) has much less signal power than the packets that have circulated in the loop,, because the loop has an effective gain of approximately 10 dB. In the lower part of figure 3.12, the signal behind the decision circuit (point C in figure 3.10) is depicted with the gate dec transmitting only the packet with the round trip number n=7. The oscilloscope trace shown in figure 3.12 does not correctly display the structure of the signal, because the data rate is comparable with the sampling rate of the oscilloscope. BER measurements are performed with constant signal power at the input of the memory (point A in figure 3.10). The attenuate (att) at the receiver input is necessary to attenuate (10 dB) the packets with n=1 to n=7 relative to the directly transmitted packet (n=0), when measuring the BER. The result is that BER=10^{-9} was obtained independently of the round trip numbers n=1 to n=7 for fixed input power and fixed attenuate.

Having reviewed the previous works on fiber-optic loop memory, we are now ready to start the discussion of the FOMD based on optical code division multiple access.

CHAPTER IV
A FIBER-OPTIC LOOP MEMORY STRUCTURE BASED ON OPTICAL CODE DIVISION MULTIPLE ACCESS

4.1. Introduction

In the previous chapter various fiber-optic loop memory structures are discussed. This chapter introduces the application of optical CDMA to the general fiber loop structure accompanied with hardware modifications and complexity.

In multiple-access communication systems in which a number of users share a common channel bandwidth, some of the users may send data simultaneously over the common channel. If, to each user, a different pseudo-random pattern, (also called code) is assigned, the transmitted signals in the common spectrum may be distinguished. The intended receiver can recover the transmitted data by knowing the pseudo-random pattern. Therefore, this communication technique allows multiple users to share simultaneously a common channel for transmission of information. In addition optical CDMA systems can be realized using the relatively simple, off-the shelf laser sources without controlling wavelengths needed for wavelength-division multiplexing (WDM). Thus optical CDMA systems are expected for future ultra-high speed and real-time computer communications where the bit rate more than 100 Gbps is expected. Optical memory concept comes into the picture as an important part of the optical CDMA networks to be used in the cross-connect buffering structures. In this study, forming additional channels is realized by using different optical orthogonal codes of same chiplength. There are 10 virtual channels to store information packets. Using 10 encoders, 10 decoders, peripheral processing devices and transducers brings more complexity on the hardware of the structure as compared

to the memory devices introduced in chapter III but easy timing and increased data storage capacity makes the structure attractive. It could be thought that using codewords of length 500 brings a drawback to the data storage capacity but it can be overcome by increasing the rate.

4.2. Basic Properties

Number of bits that a fiber loop of length L, and refractive index n can hold is given by

$$N = \frac{Ln}{c} R \qquad (4.2.1)$$

where L is fiber length, n is refractive index, c is speed of light, R is data rate
For example if L=1 km, n=1.5 fiber is used at R=1000 Mbps then

$N = 5\,\text{Kbits/km}$ is obtained.

This means 5000 bits can be stored in a fiber loop of length 1 km. Hence, either R or L should be large in order to have significant storage. To increase the information storage capacity of a FOMD, CDMA or WDM (wavelength division multiplexing) or both can be used. If WDM and CDMA are used together, N increases by the relation

$$N' = N * n_c * n_\lambda \qquad (4.2.2)$$

where n_λ is number of wavelengths and n_c is number of codewords used.
The storage capacity of the previous example when 10 wavelengths and 10 optical codes (n_λ=10, n_c=10) are used for the fiber becomes

$N' = 5000 * n_c * n_\lambda = 5000*10*10 = 5 \cdot 10^5$ bits/km = 500 Kbits/km at R=10 Gbps.

For compactness, dimensions and the volume of the fiber delay line are important. A fiber pack of 10 km length with a diameter of 250 μm can be wound into a toroid with the dimensions given in figure 4.1. The storage capacity can be as high as 5 Mbits with a density of 5.3 Kbit/cm^3.

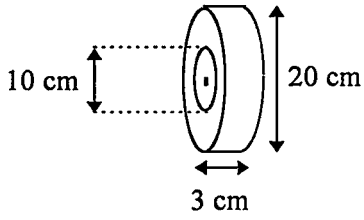

Figure 4.1. Dimensions of a fiber pack of length 10 km

It is possible to design special fibers with smaller outside diameter for higher storage densities. Care should be taken to avoid overwriting using the same code or wavelength. This means length of data should be limited and physical length should be less than the length of fiber-loop. If the core refract index is 1.5 and propagation 5 μsec per kilometer. The maximum length of a data segment can be calculated as:

$L_{segment}$=5 Kbits/Km

If write operation at 1Gbits/s and read operation at 10 Mbits/s (average) are realized, a buffering duration is defined as

T_{buffer}=1 Gbps/10 Mbps * 5 μsec/Km

= 0.5 msec/km

If n_c codes, n_λ wavelengths are used:

T_{buffer}=0.5* n_c*n_λ msec/km is obtained.

For example if n_λ=10, n_c=10 then T_{buffer} becomes 50 msec for a 10 km long optical fiber memory.

4.3. Loss in the Fiber Loop

Fiber channel loss is a measure of optical signal attenuation through the fiber. This loss is a function of laser emission wavelength, fiber length and fiber splice or connector losses. The optical fiber loss for the fiber delay lines and other interconnecting optical lines used in the design of FOMD is α=0.2 dB/km at 1550 nm wavelength. Attenuation of light power is to be compensated in order to obtain an infinite circulation of information carrying light pulses around a closed-loop fiber-optic medium. Therefore it is necessary to know the attenuation factor by which the initially pumped power decreases at the end of each round-trip. We start with the fundamental structure shown in figure 4.2.

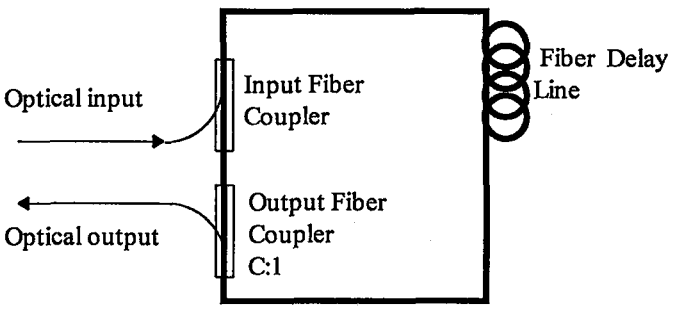

Figure 4.2. Fundamental Optical Memory Structure

If the loss per kilometer (α) is assumed to be the same over the whole delay line and the coupling ratio for the output fiber coupler is C:1, power available at the input of the coupler at the end of the n'th round-trip , P(n) is given by

$$P(n) = P(0)\left[\frac{C-1}{C}\right]^n \left[10^{-\frac{\alpha D}{10}}\right]^n \qquad (4.3.1)$$

where α is loss per kilometer for the fiber, C is coupling coefficient of the output fiber coupler, n is number of round-trips, D is length of the fiber loop, P(0) is initial light power (mWatts), L is optical attenuation factor.

If the initial light power is taken to be P(0)=1 mW , changes in the power of the light pulses are obtained as in figure 4.3 for different number of round-trips. Length of the fiber is varied between l=100m and l=5 km.

There must be a limit to the attenuation which can be tolerated in a loop. It depends very strongly on detector sensitivity and many other factors but it is possible to take it as 95%. If 95 % attenuation is assumed for a fiber loop of length D, maximum number of round trips that can be traveled by the optical pulses shows a variation as in figure 4.5. For example, for a fiber loop of length 2 km, an optical pulse which has an initial power of 1 mW can travel slightly less than 16 round-trips around the loop until its power drops below 50 μW.

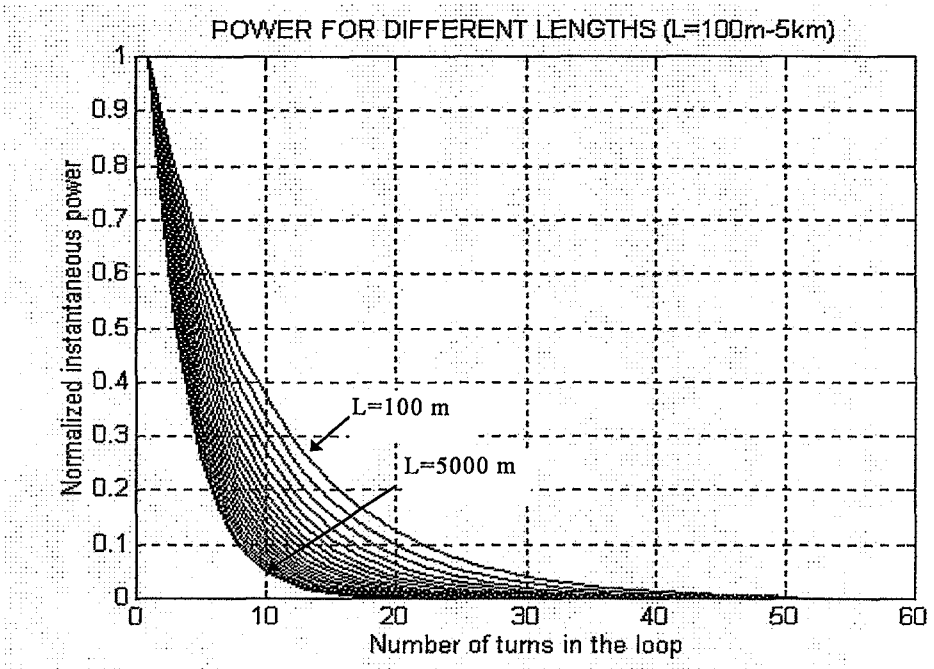

Figure 4.4. Change in the light power versus number of round-trips

Figure 4.4. Maximum number of round-trips for 95 % attenuation

4.4. A Memory Structure Based on Optical CDMA

The method used in this design is optical code division multiple access. The (500,6,1,1) optical orthogonal codes whose properties are given in chapter II are used for encoding the incoming data streams. Here N is 10 for this OOC group therefore the information carrying capacity of the fiber-optic loop structure is increased by a factor of 10 at a fixed wavelength of the electrical-to-optical converter (a laser diode). Hence the fiber delay line can carry at most 10 distinct optically encoded data groups.

The optical sequences are (0, 1) sequences, i.e. they have 0 and 1 level instead of ±1 levels which are the possible levels in electrical communication systems. The optical CDMA system of the FOMD investigated in this work implements binary coding on the information bits, i.e. the user sends the PN sequence when its data is '1' and sends no light when the data is '0'. In optical transmission systems this type of modulation is named as intensity modulation.

Fiber optic loop memory structure based on optical CDMA is shown in figure 4.5. The structure consists of a main loop with optical and electrical signal processing units . Thick lines show the optical medium and thin lines show the electrical medium. There is a control unit to handle the read, write, clear operations and clock control. This unit is communicating with the switching unit by which all the read and write operations are performed. Electrical part of the loop has optical-to-electrical and electrical-to-optical converters. Their detailed operation are explained in references [3], [4], [5], [6], [7].

In the memory , write and read rates are expected to be different. Normally data will be stored at a higher rate. This implies that it is convenient to refresh data not every cycle but 10 cycles, i.e. refresh the optical signals at the end of 10^{th}, 20^{th}, 30^{th}, ... , $n.10^{th}$ (n=1, 2, 3,...) round-trips. Since the buffering of the electrical signals to the electrical-optical converters are dependent on the clock cycles, we must know the time difference between write time and the time when the electrical signals reach the buffering unit. To calculate T, the refreshment period, we must know the response times of the memory components and the time elapsed in the loop during the 10 round-trips of one optical pulse. In the design fiber length is chosen as 2 km This means one pulse travels a distance of 20 km at the end of 10^{th} round trip.

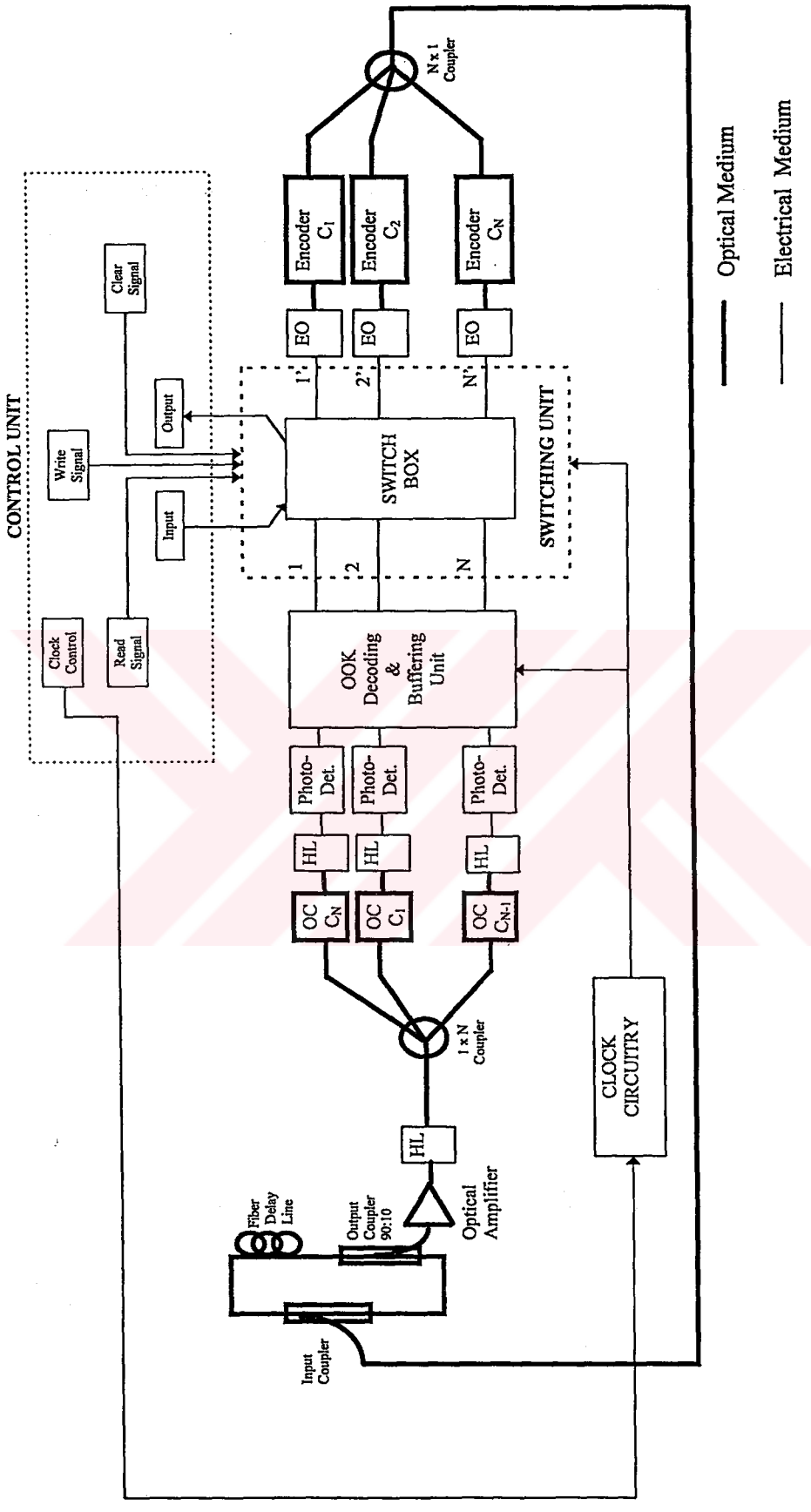

Figure 4.5. Fiber-optic loop memory structure based on optical code division multiple access

Assuming the refractive index of the core is 1.5, total elapsed time in the loop for 10 round-trips is found as τ_{loop}=100 μs (c= 3.10^8 m/s).

If response times of the electro-optical transducer is τ_{EO}, response time of the photodectector is τ_{PD}, process time of threshold device is τ_{TD}, process time of decision and buffering unit is τ_{DB} and the total propagation delay in the optical media except for the fiber delay loop is τ_d, the refreshment period is found as

$$T = \tau_{loop} + \tau_{EO} + \tau_{PD} + \tau_{TD} + \tau_{DB} + \tau_d \qquad (4.4.1)$$

The reason for changing the codewords used in encoding in each regeneration time is to allow the codes sequences stayed in the loop to die out .

Two modes of operation, i.e. synchronous and asynchronous, are possible in the loop memory. If synchronous operation is selected, perfect synchronization of the sequences at the encoders and decoders are required for the proper operation. Achieving synchronization is difficult and even if perfect synchronization is achieved, this scheme would probably be too complex. In this work, in order to simplify operation and reduce complexity asynchronous operation was selected.

The optical encoders and decoders are based on power splitting and combining by means of 1xω and ωx1 splitters and combiners and fiber delay lines where ω is the weight of the codewords. The lengths of the delay lines of the encoder are adjusted such that a pulse of one chip duration at the input is mapped to the chip positions of value '1' of the specified PN sequence. The number of the delay lines required is equal to ω, the weight of the code used in the optical CDMA system. The lengths of the delay lines of the receiver correlator are such that the characteristics is exactly the replica of the PN sequence. Obviously the number of delay lines of the correlator is also equal to ω. There is no need of storing the replica of the PN sequences in optical CDMA applications. Also, there is no need for synchronization of the PN sequence generators as it is needed in the DS spread spectrum systems.

One of the most important problems for CDMA systems is the channel interference when light pulses of many users are simultaneously multiplexed. It produces an asymptotic floor to the error probability and limits the number of simultaneous users. The channel interference is the ultimate limit in link performance with CDMA. One way to reduce the degradation due to channel interference is to use

an optical hard limiter (an optical threshold element [37]) which is placed before an optical correlator. Although an optical hard-limiter advantages when combating the channel interference only, it is attractive for optical CDMA systems where the channel interference is a prime noise factor. The performance of optical CDMA systems with an optical hard-limiter using optical orthogonal codes (OOC's) as signature codes was analyzed where the effects of the quantum noise and the thermal noise are neglected [21]; using the optical hard-limiter improves the system performance and make it possible for the system to accommodate more users. This means capacity of the optical memory can be increased by using more codewords.

Initially a write signal is sent through switching unit to the electrical-to-optical converter. Electrical-to-optical converter converts the information-carrying electrical pulses to optical pulses and these pulses are fed into the encoder which is designed according to the optical orthogonal code C_1. After encoding, power of the light pulses are attenuated by a factor of 6 which is the weight of the (500,6,1,1) optical orthogonal codes. Optically coded sequences are coupled into the fiber-optic loop by means of the input fiber coupler. The optical pulses circulate in the loop continuously with a certain attenuation in power. With the parameters of the fiber and coupling ratio of the output fiber coupler, the time when the power of the optical pulses drop to a predetermined level can be calculated and the switching unit can be controlled properly by a clock circuitry. Some of the optical power in the loop is continuously coupled to an external optical line. An optical hard-limiter before the correlators is employed to eliminate possible decoding problems but it is not preferred in this design since the data lengths examined are not too long. An optical switch which switches to optical correlators (OC) follows the optical hard-limiter. Power of the light pulses decreases by a factor of N, the number of decoders (N=10 in our case). These optical correlators are designed in such a way that their outputs are the uncoded sequences produced by using ω optical delay lines whose amounts of delay are determined according to the optical orthogonal codes chip positions. In decoding, light pulses are splitted by passing through the ω optical delay lines. placed at the appropriate chip positions corresponding to the codeword. The matched optical corrrelator can recognize the arrival of the desired sequence. When the desired optical pulse sequence travels through the OC, the output lights intensity traces out

the autocorrelation function of the input sequence. The sum of the received optical pulses' intensities located in the same mark positions of the OOC used for the desired channel is obtained at the last chip position. The output of the second optical hard limiter is converted to the electrical signal by the photodetector and the output electrical signals are sent to the on-off keying decoding and buffering unit. The OOK decoder compares the magnitude of the electrical signals with a threshold level θ. It decides that '1' is sent if the magnitude is greater than θ and '0' is sent otherwise.

The 'OOK Decoding & Buffering Unit' also controls the buffering of the decoded bits to the switching unit which will be used for refreshment, clear or read operations. If a clear signal is sent by the control unit the corresponding decoder output is not refreshed and that channel becomes free for writing a new data block. If a read signal is sent by the control unit, electrical pulses are sent to the output device and also refreshed by the following encoder. If the previous OOC used for encoding the data block is C_i then the refreshment is made by the OOC $C_{(i+1) \bmod 10}$. Therefore the previous OOC C_i can be used for encoding a new data segment. If a new write operation is to be performed, a write signal is sent to the switching unit by the control unit.

4.5. Examples of Data Storage and Usage of Codewords

Writing data segments into optical loop using related optical orthogonal codes is realized at the integer multiples of the period T. Depending on whether a write signal is sent by the control unit or not, switching unit gets ready. If the write signal (1) is sent to the switching unit, this unit waits for the input electrical data pulses to be encoded by the corresponding encoder.

Control unit follows the circulations in the loop and stores the information that which channels will be occupied in the next round-trip. Table 4.1 shows the memory channel occupation and usage of codewords for 7 random write operations. At the reference time t=0, the first input data stream is encoded by C_1 which means the channel 1 is occupied by the optically encoded version of the input data sequence. Output of the second decoder (uses C_1 for decoding) in the decoder group carries light after 10 round-trips of the optical pulses are finished. Decoded sequence is encoded by the second encoder in the encoder group with codeword C_2. Channel 1 is

now free and ready for another write operation. Another write signal is sent to the switching unit from the control unit at a time between t=0 and t=T. The new sequence is encoded by the codeword C_1. Therefore channel 1 and 2 are occupied between time t=T and t=2T. At time instants 2T and 3T no write signal is sent. Therefore code sequences are shifted to the next channels by leaving the previous channels for writing the second oldest sequence. At times t=4T, 5T, 6T, 7T, 4 new data sequences are written. No data is written at t=8T and t=9T. At time t=10T, initially encoded sequence appears in the first channel and the new-comer sequence is encoded by C_5.

Table 4.1. Data Storage for seven random write operations

			CHANNELS									
Time	**Write Signal**	**Codeword for write**	**1**	**2**	**3**	**4**	**5**	**6**	**7**	**8**	**9**	**10**
0	1	C_1	X_1									
T	1	C_1	X_2	X_1								
2T	0	none		X_2	X_1							
3T	0	none			X_2	X_1						
4T	1	C_3			X_3	X_2	X_1					
5T	1	C_3			X_4	X_3	X_2	X_1				
6T	1	C_3			X_5	X_4	X_3	X_2	X_1			
7T	1	C_3			X_6	X_5	X_4	X_3	X_2	X_1		
8T	0	none				X_6	X_5	X_4	X_3	X_2	X_1	
9T	0	none					X_6	X_5	X_4	X_3	X_2	X_1
10T	1	C_5	X_1				X_7	X_6	X_5	X_4	X_3	X_2

In figures 4.6-4.26 you will find the time plots for the status of loop memory for the writing regime up to t=7T given in table 4.1. In these figures, data sequence to be stored, content of the loop memory after writing that sequence and the status of loop after each refreshment are shown. As it can be seen from these figures, enough attenuation is obtained for the code sequences in the loop and the power of each newly encoded optical sequence is much greater than that of the previously stored optical pulses.

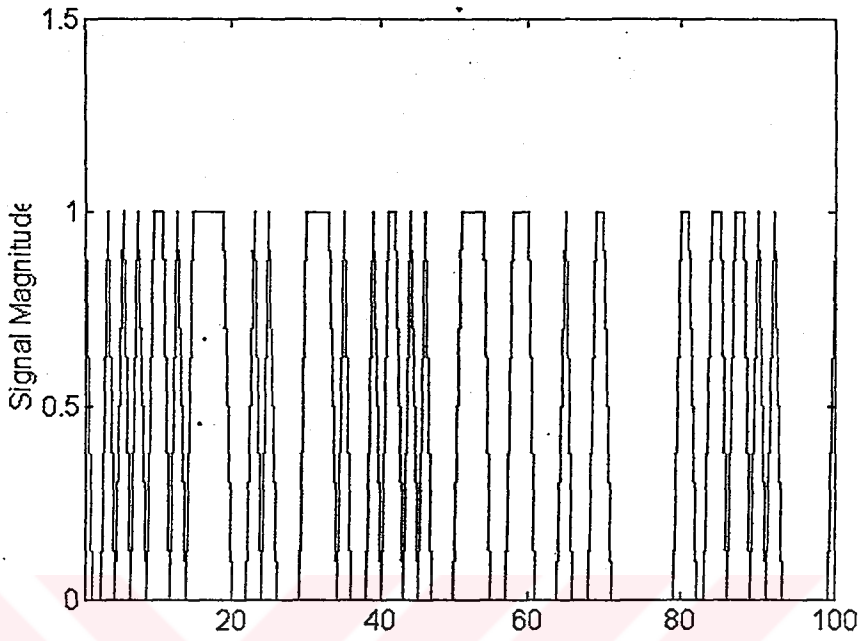

Figure 4.6. First data sequence written into the memory

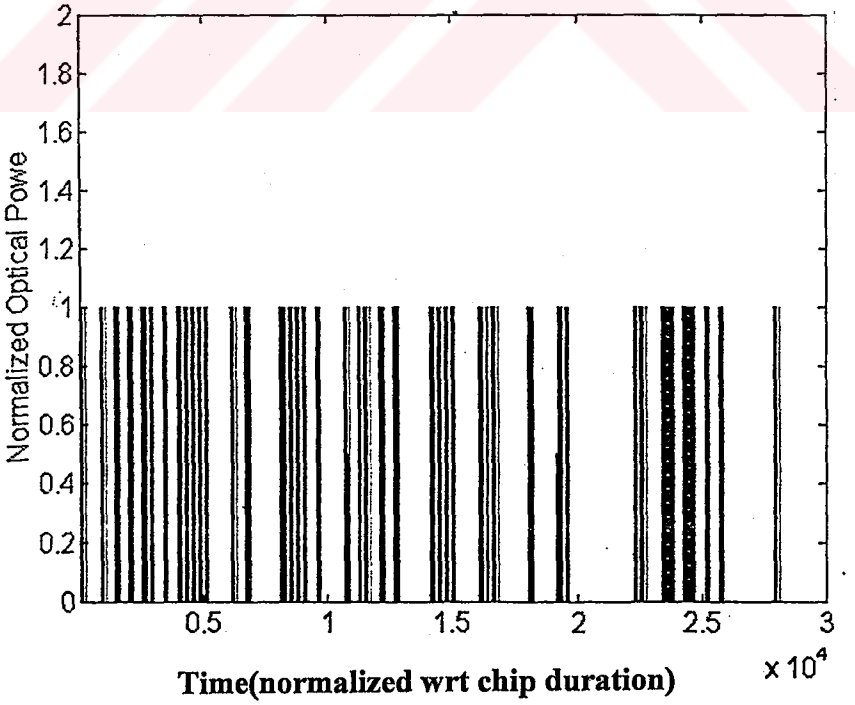

Figure 4.7. Content of the fiber loop after first write operation

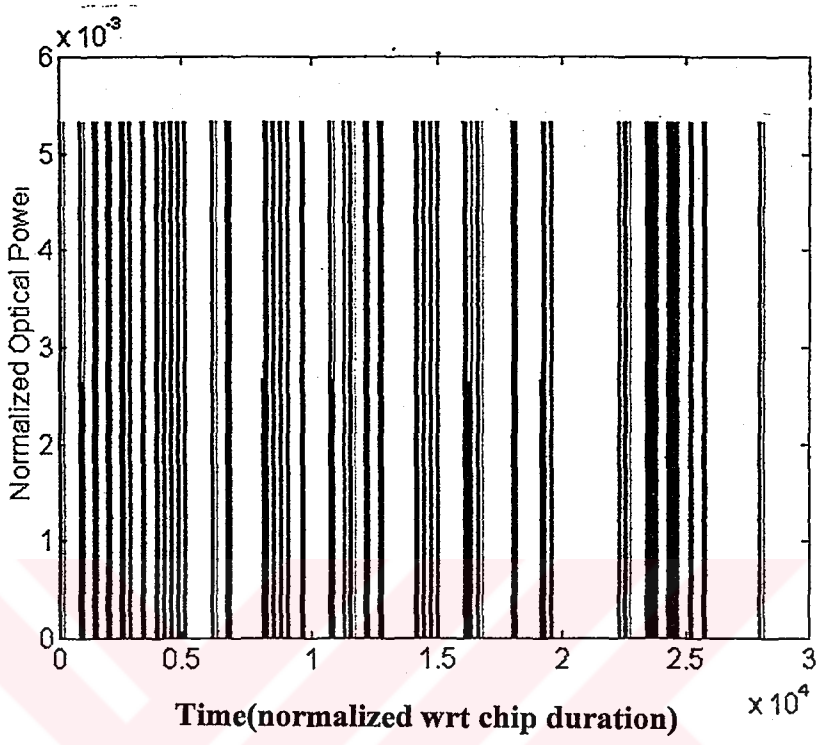

Figure 4.8. Fiber coupler output at t=T

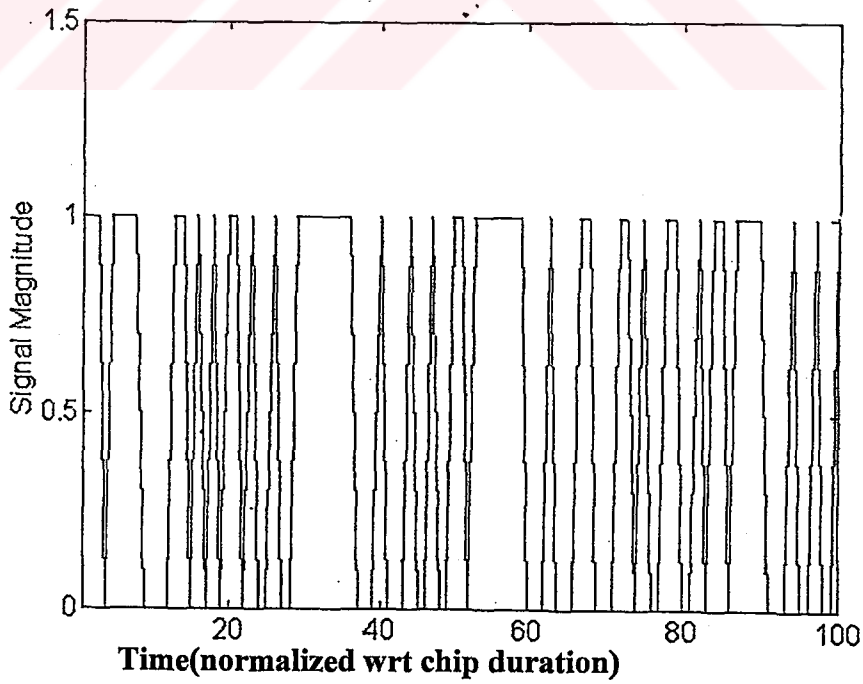

Figure 4.9. Second data sequence written into the memory

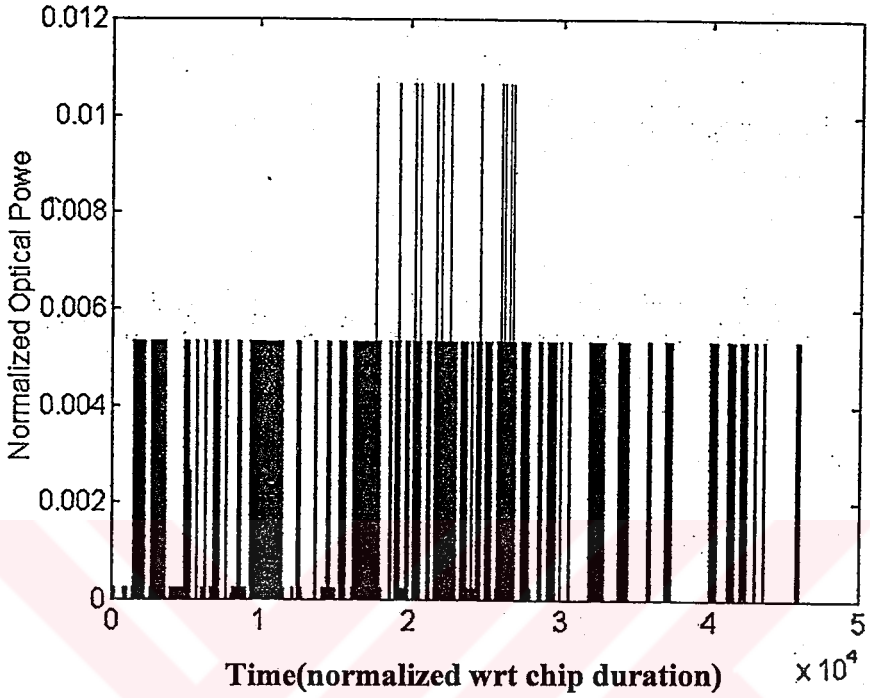

Figure 4.10. Fiber coupler output at t=2T

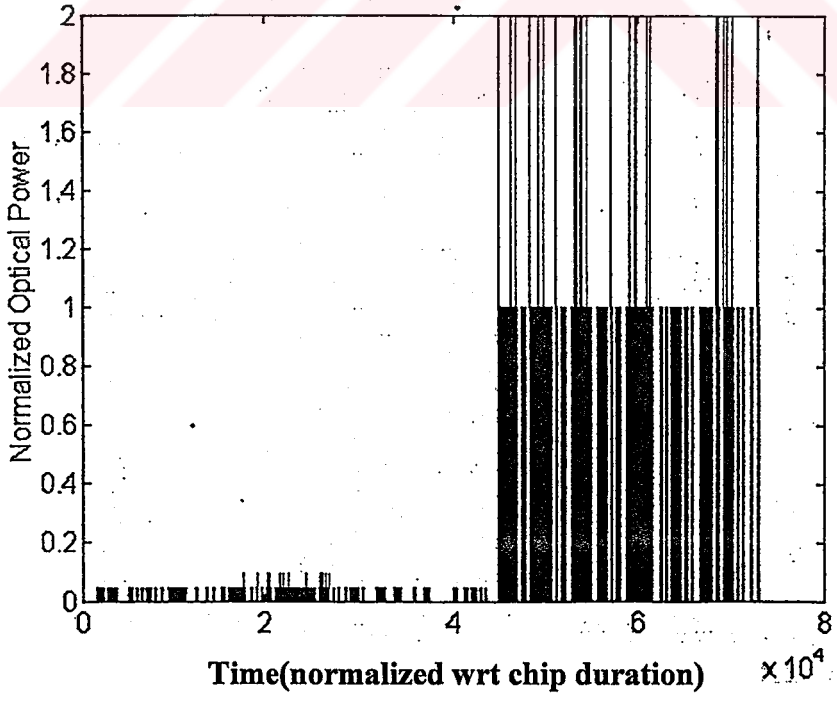

Figure 4.11. Fiber loop content just after refresh operation

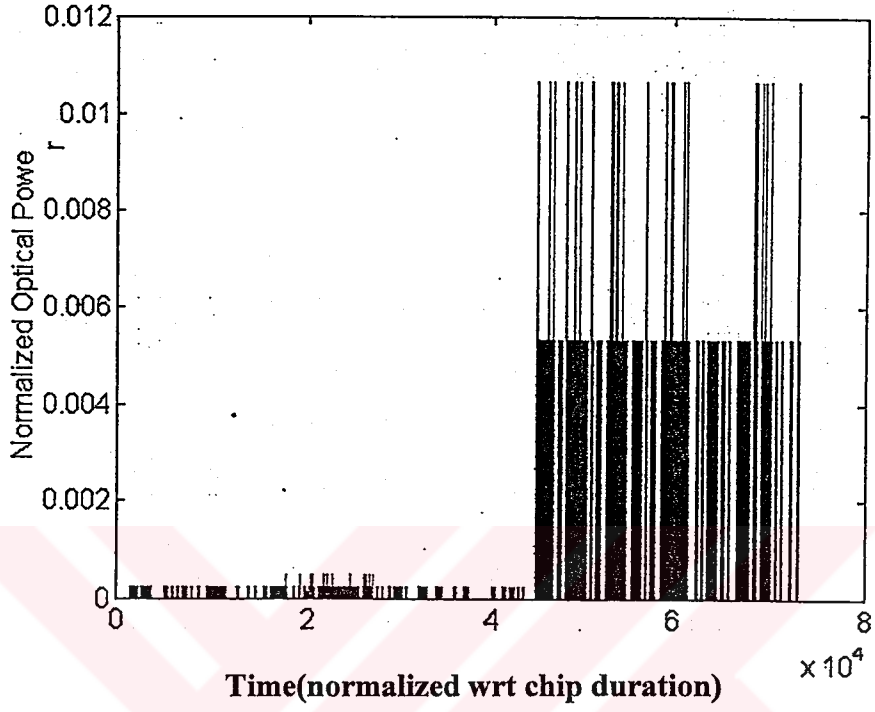

Figure 4.12. Fiber coupler output at t=3T

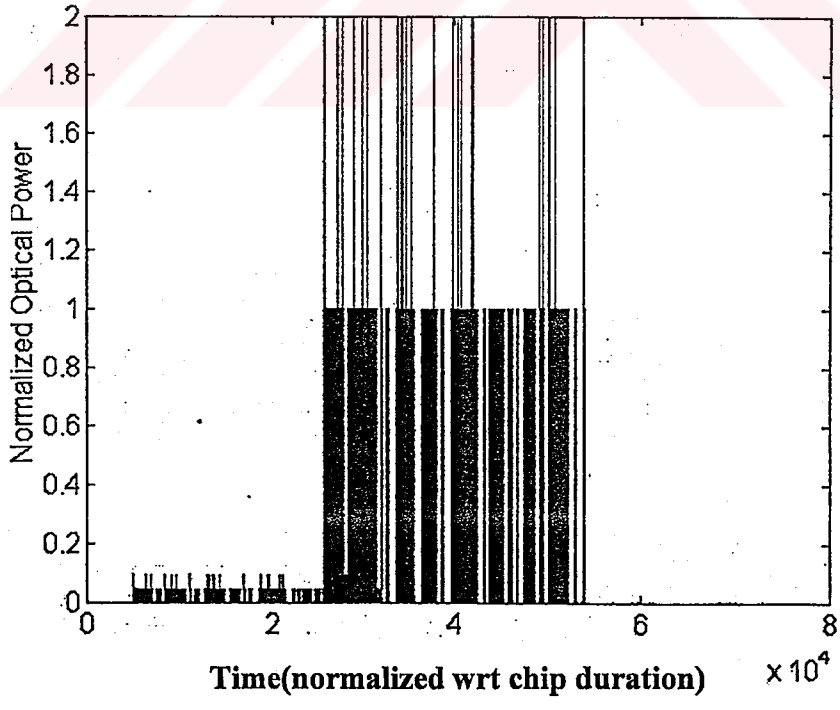

Figure 4.13. Fiber loop content just after refresh operation

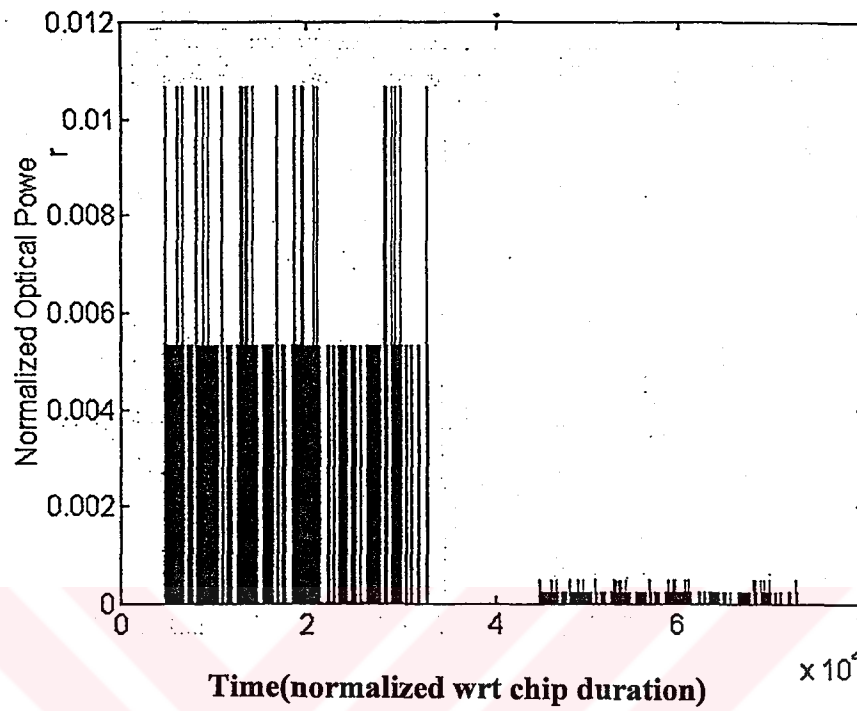

Figure 4.14. Fiber coupler output at t=4T

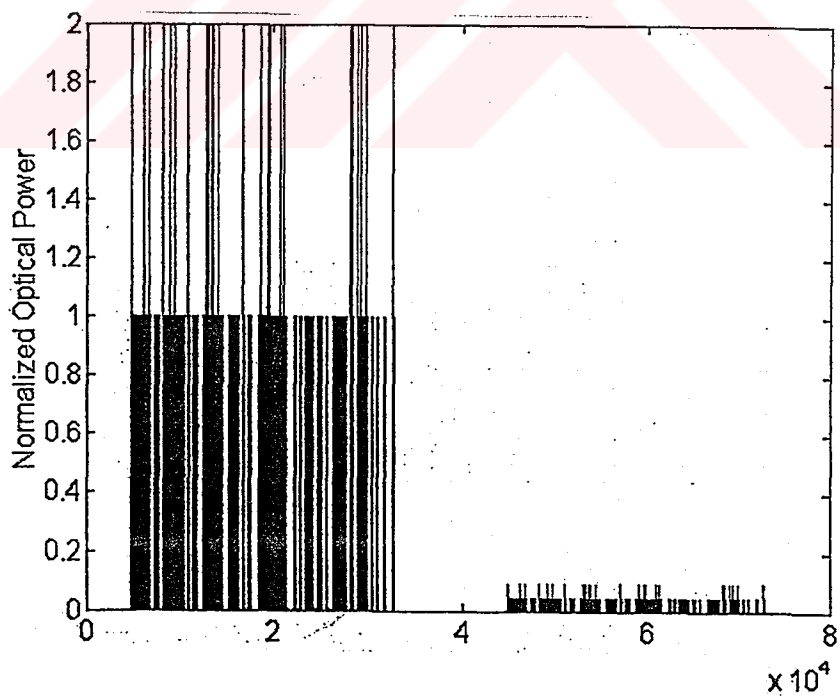

Figure 4.15. Fiber loop content just after refresh operation

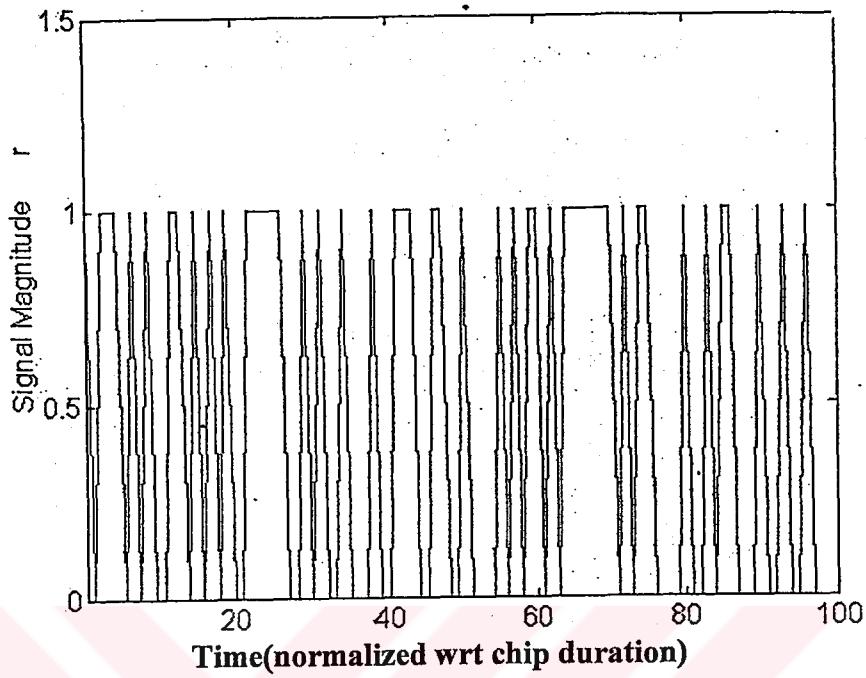

Figure 4.16. Third data sequence written into the memory

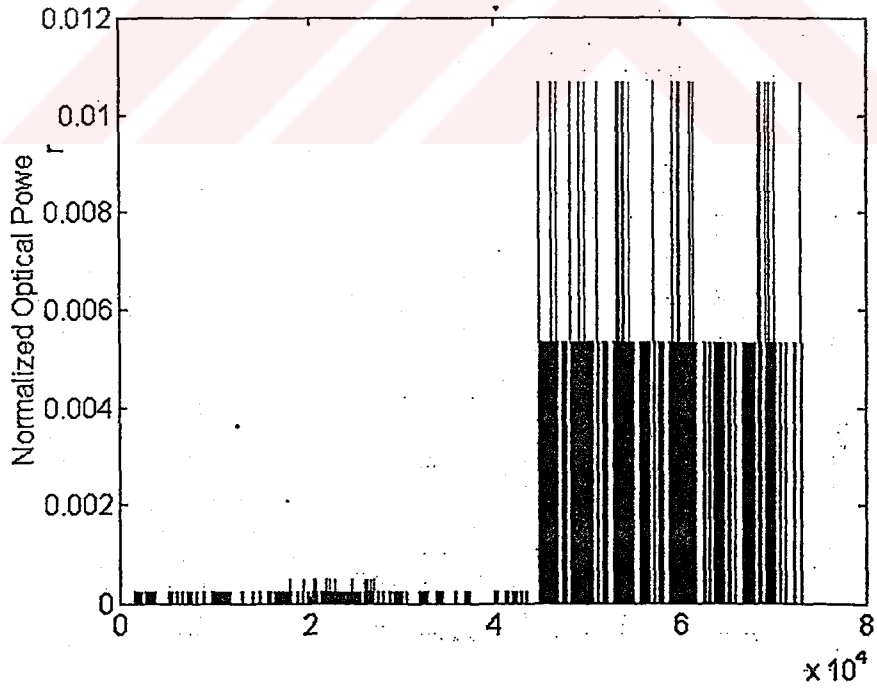

Figure 4.17. Fiber coupler output at t=5T

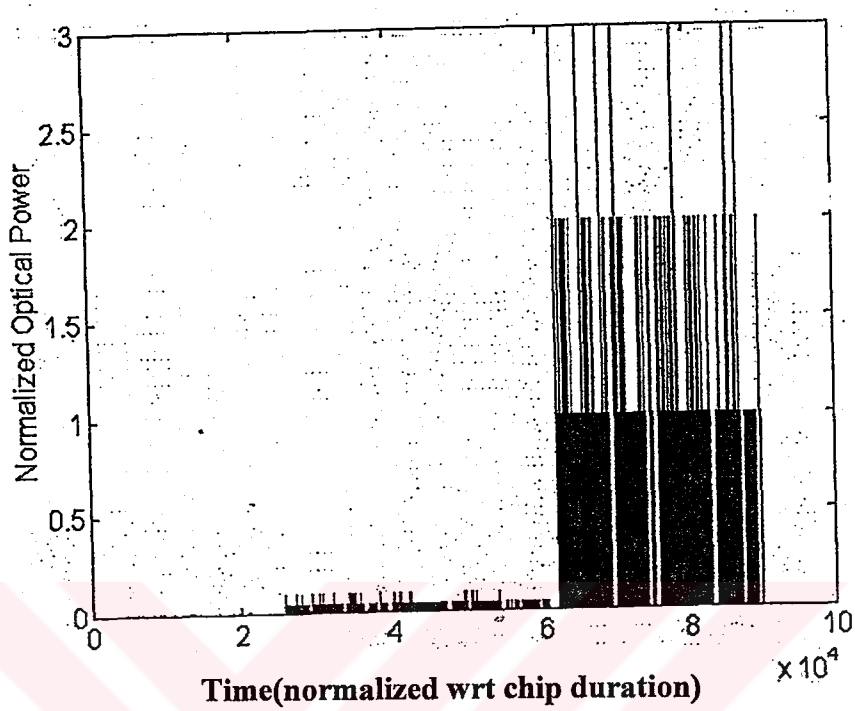

Figure 4.18. Fiber loop content just after refresh operation

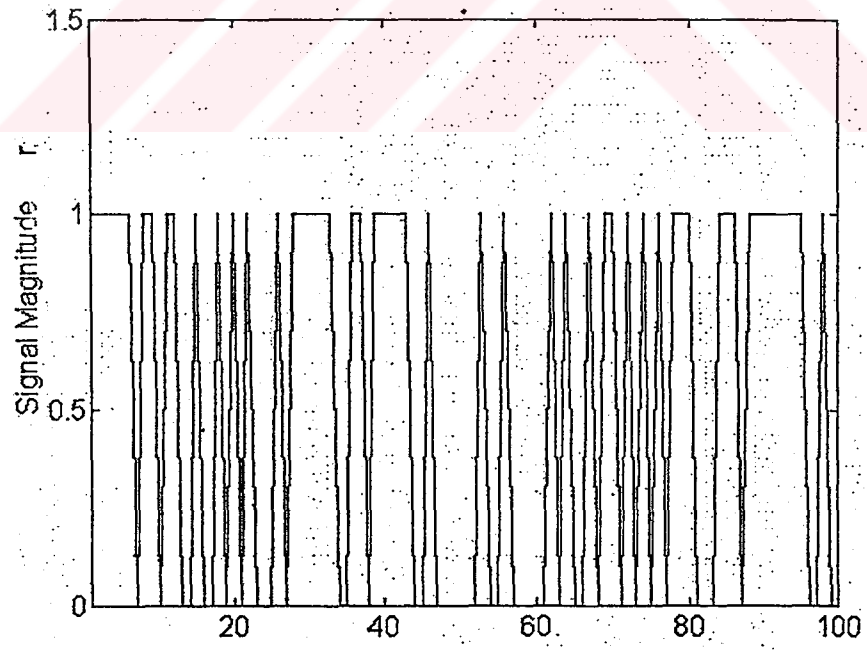

Figure 4.19. Fourth data sequence written into the memory

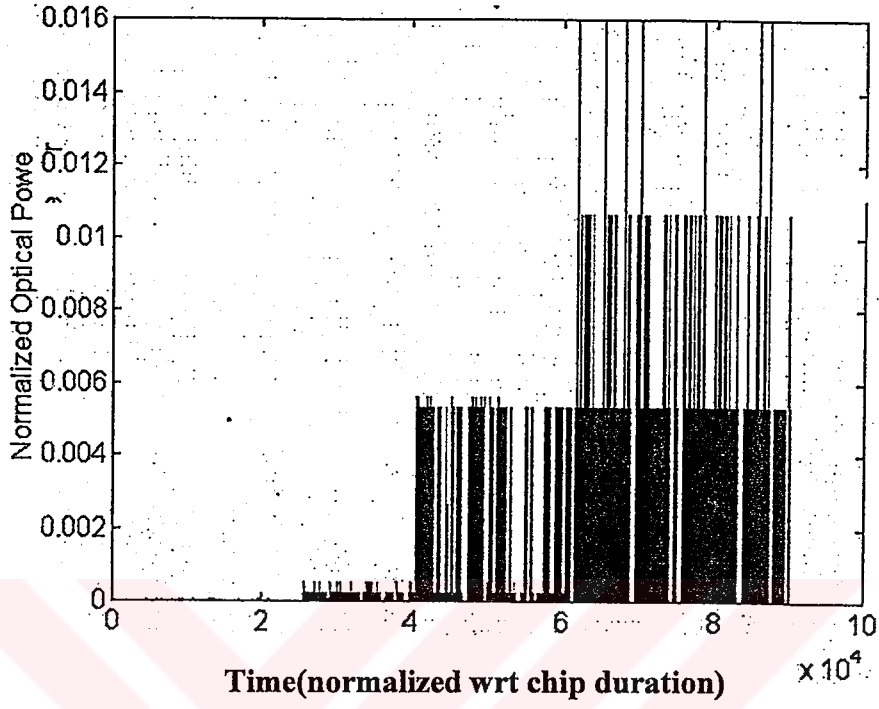

Figure 4.20. Fiber coupler output at t=6T

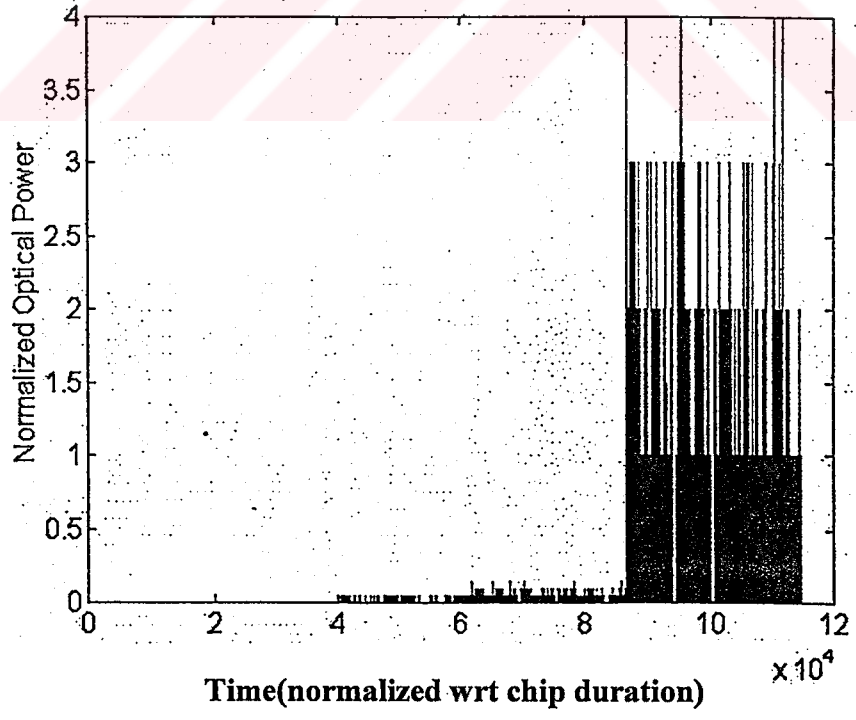

Figure 4.21. Fiber loop content just after refresh operation

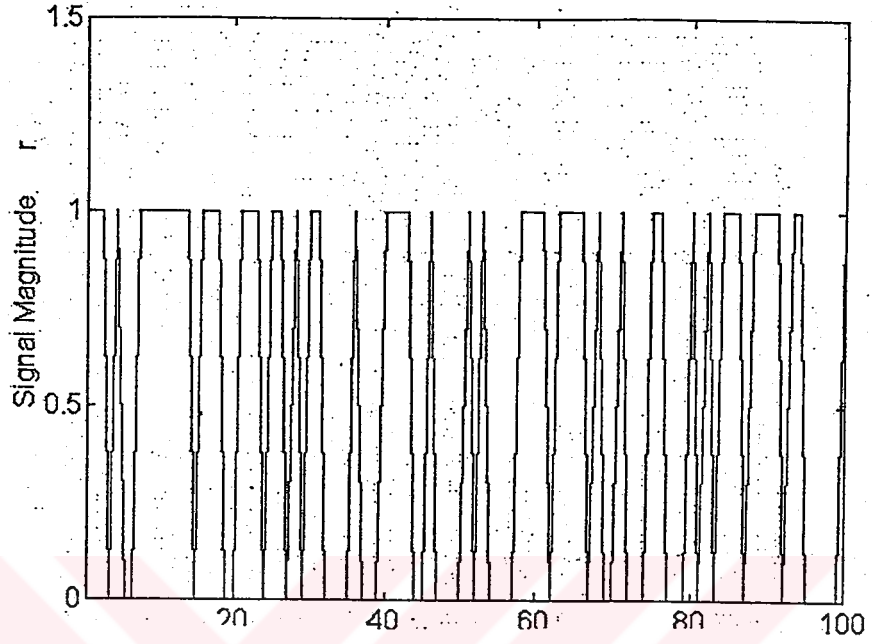

Figure 4.22. Fifth data sequence written into the memory

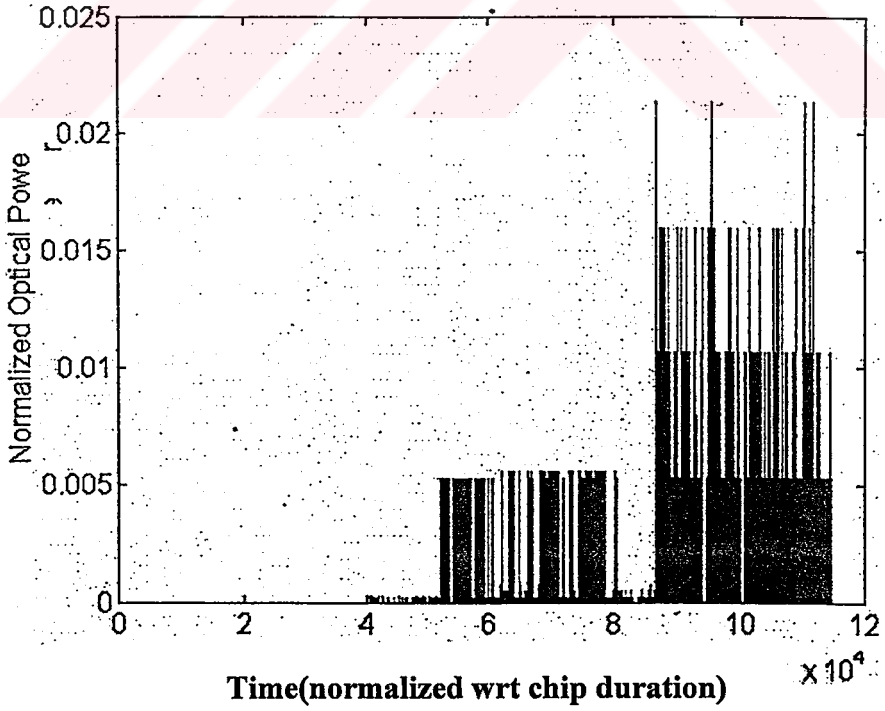

Figure 4.23. Fiber coupler output at t=7T

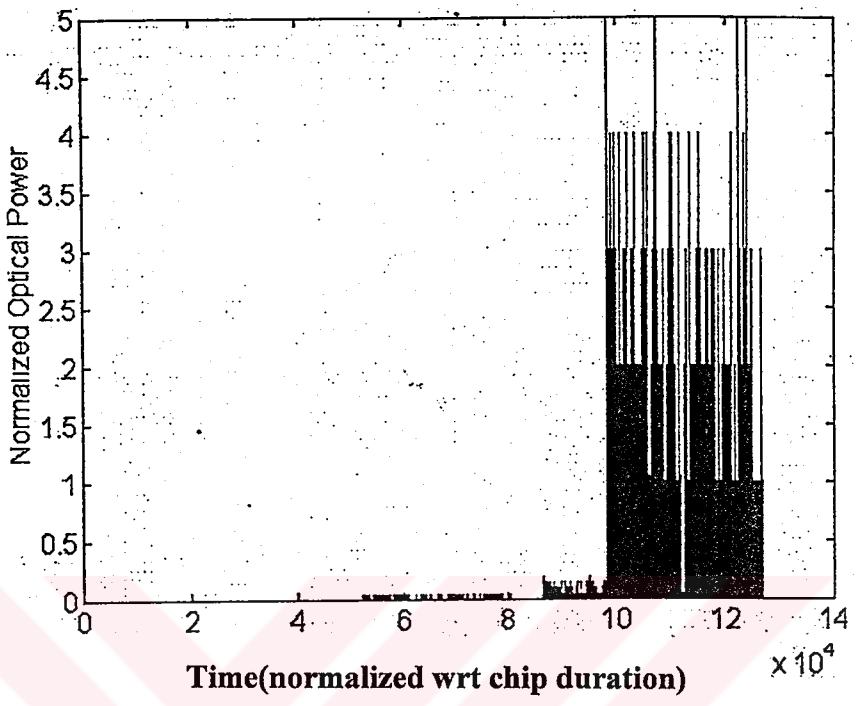

Figure 4.24. Fiber loop content just after refresh operation

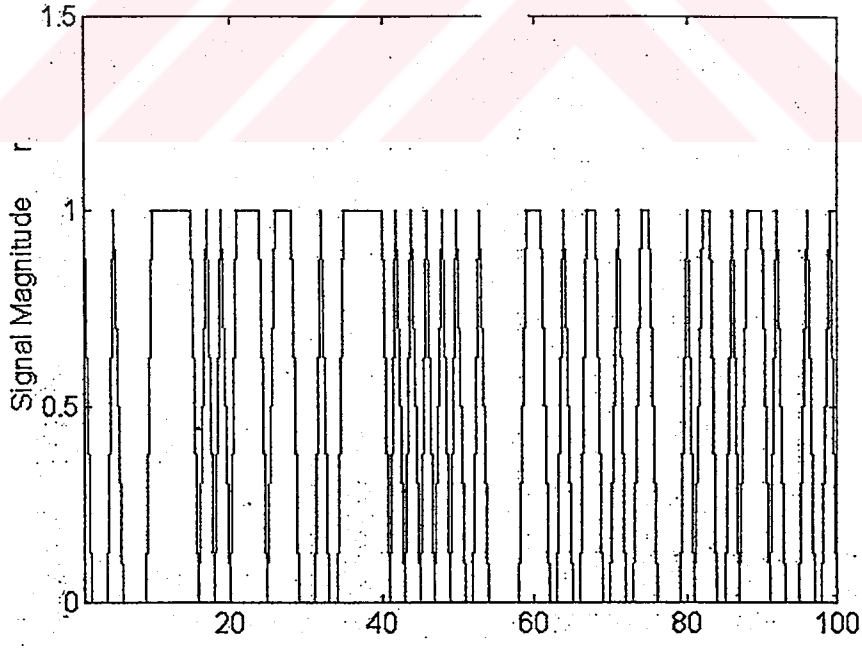

Figure 4.25. Sixth data sequence written into the memory

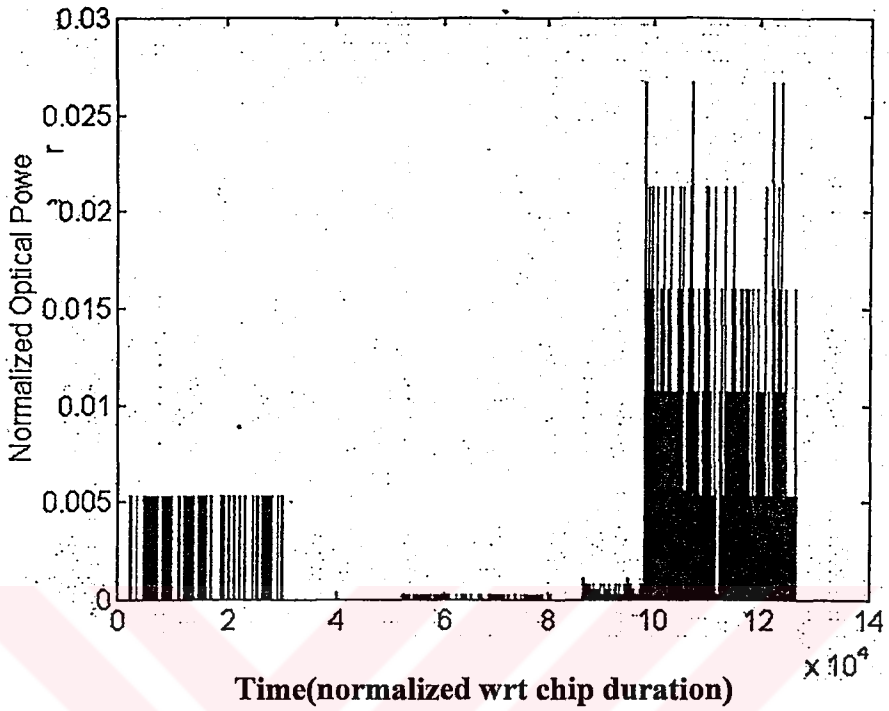

Figure 4.26. Fiber coupler output at t=8T

No errors were encountered when the decoded sequences are compared with the original data sequences. Since the number of users, N, is 10 and the bit-error probability is very low, no error occurs in decoding. If the number of users is increased to ,say, 15 errors start to be detected especially when the data sent is '0'. In order to prevent errors in decoding, we make a new proposal: use a decoder system with double optical hard-limiters so that some more interference patterns will also be excluded. In the following section theoretical basis of this new improvement proposal will be presented and the memory outputs will be shown for the structure using double optical hard-limiters.

4.6. Performance Analysis of FOMD with Double Optical Hard-limiters

Up to this point we have explained the operation of the proposed memory structure. In this section performance improvement supplied by our structure which uses double optical hard-limiters, one before the optical correlator and the second

after the correlator will be discussed. Equation 4.2.2. says that number of virtual channels can be increased either by using more than one wavelengths and/or increasing the number of code sequences. The former is beyond the scope of our research. The latter is dependent on the error probability performance of the system, i.e. you can not increase the number of codewords as much as you want since bit error rate increases for the structure with one optical hard-limiter. Therefore increasing the number of code sequences calls the need of reducing the accompanying error probability. Using double optical hard-limiters performs this task. Theoretical basis of this idea is in the following paragraphs.

To improve the bit error probability performance, double optical hard-limiters can be used [39]. The optical hard-limiters are placed before and after the correlator, respectively.

For the optical CDMA system with the single-optical hard limiter, there are some interference patterns which are not completely removed with the single optical hard-limiter placed before the optical correlator. In order to improve the system performance by excluding some combinations of interference which cause incorrect bit decisions for '0' bit transmission, optical CDMA system with double-optical hard limiter is proposed. Figure 4.27 shows the receiver block diagram of the optical CDMA system with two optical hard-limiters.

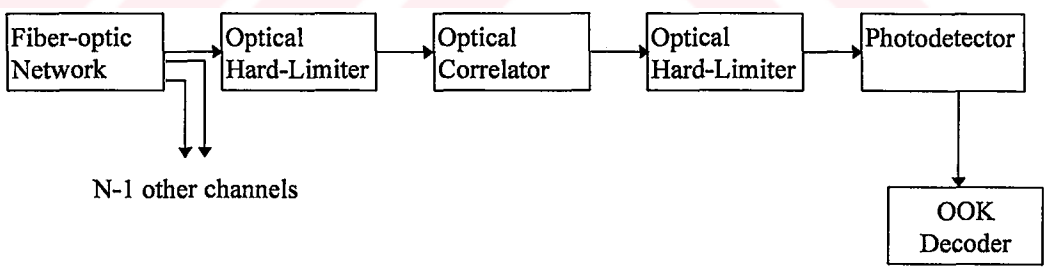

Figure 4.27. Receiver block diagram of optical CDMA system with double optical hard-limiters

The optical hard limiters used in [39]are defined as

$$g(x)=\begin{cases} v_f, x > T_h \\ 0, 0 \le x \le T_h \end{cases} \quad (4.6.1)$$

where v_f is the fixed value dependent on the signal intensity and T_h is the threshold level of optical hard-limiters. The first optical hard limiter would clip the intensity back to v_f, and thus exclude or reduce the channel interference by other undesired interferers' pulses. The second optical hard-limiter is used to exclude some interference patterns which are not completely removed with the first optical hard-limiter when the desired user sends '0'. The second optical hard limiter would clip the output intensity from the optical correlator, that is, after the correlation back to zero if the optical light intensity (x) is smaller than T_h. At the receiver, the matched optical correlator is used to recognize the arrival of the desired sequence. The optical correlator is a set of optical delay lines inversely matched to the pulse spaces. When the desired optical sequence passes through the correlator, the output light intensity traces out the correlation function of the sequence. At the last chip position, the sum of received optical intensity located in the same positions as the positions of '1' of the optical orthogonal sequence code used for the desired channel is obtained. The output of the second optical hard-limiter is converted into electrical signal by the photodetector and then is passed to OOK decoder. The OOK decoder compares the correlator output voltage over the last chip position with the threshold level θ, then decides that '1' is sent if the output voltage is larger than the threshold level θ, and '0' is sent otherwise.

Performance analysis is done under the assumption that chips are synchronous among users (because the effect of interference is largest in the chip synchronous case and thus the performance in the chip synchronous case results in the upper bounds on the performance of the optical CDMA systems) and Poisson shot-noise model for the receiver photodetector is used where the noise due to detector dark current exists. The background light is not included in the analysis. Each user is assumed to be assigned a unique optical orthogonal sequence code of length F and weight ν: the kth user is assigned the code sequence $(a_0^k, ..., a_{F-1}^k)$ where $a_i^k \in \{0,1\}$ and the number of i's with $a_i^k=1$ equals ν. Under the assumption of

Poisson shot noise model for the receiver photodetector, the photocount over the last chip of the first user modeled as a conditional Poisson random variable Y^1 is

$$Y^1 = Z^1 + W^1 + X^1 \tag{4.6.2}$$

where W^1 is a Poisson photocount due to the detector dark current noise, and Z^1 and X^1 are conditionally independent Poisson photocounts due to the desired signal and the multiple-user interference, respectively. The optical signals and the optical noise are additive in intensity because the direct detection system is assumed. No noise is assumed to added at the transmitter and through the transmission in optical fiber networks; without the external noise, bit error rate(BER) are only floor values . Denoting the noise photon rate by λ_0, the mean of W^1 is

$$E[W^1] = \lambda_0 T_C \tag{4.6.3}$$

where T_c is the chip time. The Poisson random variable Z^1 for the first user depends only on the data $b_j^1 \in \{0,1\}$and its conditional mean is given by

$$E\left[Z^1 \middle| b_j^1 = 1\right] = \nu\lambda_s T_C \tag{4.6.4}$$

$$E\left[Z^1 \middle| b_j^1 = 0\right] = 0 \tag{4.6.5}$$

where $\nu\lambda_s$ is the signal photon rate after the sequence encoder. For the optical CDMA systems with double optical hard-limiters, the effect of the channel interference is reduced.

When the optical amplification is present, optimum values of limiters are no longer obvious. The number of hits on the ith mark of the desired user signal $a^1(t)$, i=1, 2, .., ν by N-1 undesired interferers' marks is denoted by κ_i. Let

$$\kappa \equiv (\kappa_1, \kappa_2, ..., \kappa_\nu) \tag{4.6.6}$$

be the interference state pattern, $|\kappa|$ the number of nonzero elements in κ, and I^1 the total summation of κ_i. Let also

$$\epsilon \equiv (\epsilon_1, \epsilon_2, ..., \epsilon_\nu) \tag{4.6.7}$$

be the normalized interference state pattern where

$$\epsilon_i = \begin{cases} 1, \kappa_i \neq 0 \\ 0, otherwise \end{cases} \tag{4.6.8}$$

Notice the following equation:

$$\sum_{i=1}^{\nu} \epsilon_i = |\kappa| \tag{4.6.9}$$

The performance of the system with double optical hard-limiters depends on $|\kappa|$ as well as I^1, while the system performance without hard-limiter depends on only I^1, and that with the single optical hard-limiter depends on $|\kappa|$ and I^1.

Acccrding to the development given in [39], the bit error probability of the optical CDMA system with double optical hard-limiters can be derived as

$$P_b = \frac{1}{2}\left[\Pr\left(Y^1 > \theta \middle| b_j^1 = 0\right) + \Pr\left(Y^1 \le \theta \middle| b_j^1 = 1\right)\right] \tag{4.6.10}$$

where

$$\Pr\left(Y^1 > \theta \middle| b_j^1 = 0\right) = \Pr\left(Y^1 > \theta \middle| I_1 = 0, b_j^1 = 0\right) p_{I^1}(0) + \sum_{j=1}^{N-1} \Pr\left(Y^1 > \theta \middle| I_1 = j, b_j^1 = 0\right) p_{I^1}(j)$$

$$= \Pr\left(Y^1 > \theta \middle| I^1 = 0, b_j^1 = 0\right) p_{I^1}(0) + \sum_{j=1}^{N-1} \sum_{\alpha=1}^{\min(\nu, I^1 = j)} \Pr\left(Y^1 > \theta \middle| I^1 = j, |\kappa| = \alpha, b_j^1 = 0\right)$$

$$\cdot p_{I^1}(j) \Pr\left(|\kappa| = \alpha, \middle| I^1 = j\right)$$

$$= \sum_{k=\lfloor\theta\rfloor+1}^{\infty} Pos(k, m_0) p_{I^1}(0) + \sum_{j=1}^{N-1} \sum_{\alpha=1}^{\min(\nu, I^1 = j)} \sum_{k=\lfloor\theta\rfloor+1}^{\infty} Pos(k, m_0) p_{I^1}(j) \Pr\left(|\kappa| = \alpha, \middle| I^1 = j\right)$$

$$= \sum_{k=\lfloor\theta\rfloor+1}^{\infty} Pos(k, K_b) p_{I^1}(0) + \sum_{j=1}^{N-1} \sum_{\alpha=1}^{\min(\nu, I^1 = J)} \sum_{k=\lfloor\theta\rfloor+1}^{\infty} Pos(k, m_0) p_I(j) \Pr\left(|\kappa| = \alpha \middle| I^1 = j\right)$$

and

$$\Pr\left(Y^1 \le \theta \middle| b_j^1 = 1\right) = \sum_{j=0}^{N-1} \Pr\left(Y^1 \le \theta \middle| I^1 = j, b_j^1 = 1\right) p_{I^1}(j)$$

$$= \sum_{j=0}^{N-1} \sum_{k=0}^{\lfloor\theta\rfloor} Pos(k, m_1) p_{I^1}(j)$$

$$= \sum_{j=0}^{N-1} \sum_{k=0}^{\lfloor\theta\rfloor} Pos(k, K_s + K_b) p_{I^1}(j)$$

Here $\lfloor\theta\rfloor$ denotes the integer portion of the real value θ and

$$Pos(x, \lambda) \equiv \frac{e^{-\lambda} \lambda^x}{x!} \tag{4.6.11}$$

Under the light of equations 4.10 and 4.11, bit error probability performances of different parameters for the optical CDMA system is obtained.

Figure 4.28 [39] shows the bit error probability versus K_s for the optical CDMA systems without the optical hard-limiter, with the single optical hard-limiter, with double optical hard-limiters where the parameters are set as follows: F=1000, ν=10, N=10 and λ_0/R_0=100.0. From figure 4.28 it can be seen that when each user accesses to the network asynchronously, the system with double optical hard-limiters has much better performance than the systems with and without the optical hard-limiter.

This is because the system with double optical hard-limiters can exclude combinations of interference patterns that the system with the single optical hard-limiter can not exclude: all the mark positions of the desired user are not hit by undesired interference marks when the desired user sends '0'. When the number of simultaneous users is smaller than or equal to the weight of OOC's, N≤ν, the system with double optical hard-limiters can exclude all the combinations of interference patterns, and thus no floor exists for the system with double optical hard limiters.

Figure 4.29 [39] shows the bit error probability versus the number of simultaneous users N for the optical CDMA systems without the optical hard-limiter, with the single optical hard-limiter and with double optical hard-limiters when F=500, ν=5, K_s=50 λ_0/R_0=100.0 for the chip synchronous case; the performance thus results in the upper bounds on the performance of the optical CDMA systems. The maximum number of users N_{max} is 24 when F=500 and ν=5, and 99 when F=2000 and ν=5. It can be seen that the systems with double optical hard-limiters have the constant low bit error probability when N is smaller than or equal to ν: N≤5. This is because the optical hard-limiters can exclude all the combinations of interference patterns when N≤ ν.

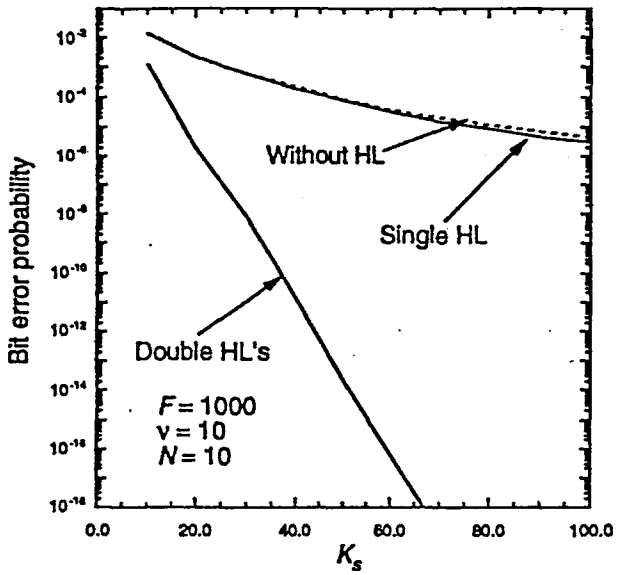

Figure 4.28. Bit error probability versus K_s for the optical CDMA system without the optical hard-limiter, with the single optical hard-limiter, and with double optical hard-limiters: F=1000, ν=10, N=10 and λ_0/R_0=100.0.

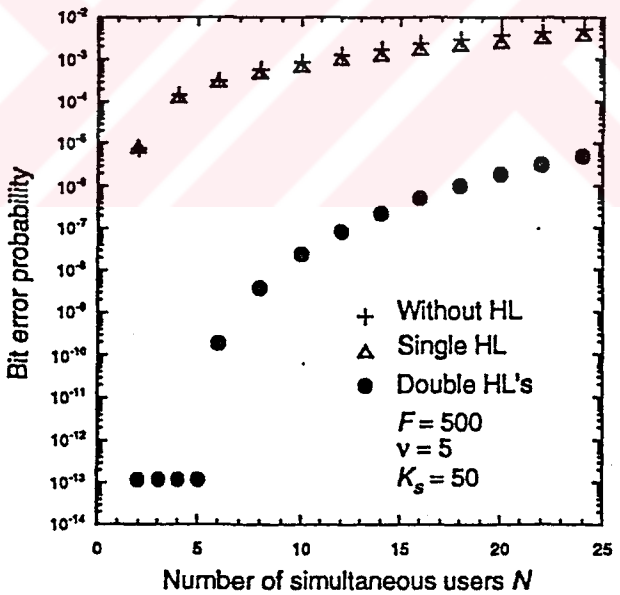

Figure 4.29. Bit error probability versus the number of simultaneous users N for the optical CDMA system without the optical hard-limiter, with the single optical hard-limiter, and with double optical hard-limiters F=1000, ν=5, K_s=50 and λ_0/R_0=100.0.

Therefore , the optical CDMA systems with double optical hard-limiters are effective to improve the bit error probability performance and to accommodate more simultaneous users in the practical optical fiber networks.

Figures 4.30-4.43 illustrate the operation of the FOMD using the decoder in figure 4.27. Three data sequences are written into the loop memory and the signals in the decoder designed according to C_1 are shown.

In the simulation of the memory using double optical hard-limiters, 3 successive write operations are performed using codewords C_1 , C_2 and C_3 for 3 blocks of data . Input data sequences are (0,1) sequences as in the previous case of single hard-limiter simulation. In figures 4.32-4.45 , the input data sequences, output of the common hard-limiter, outputs of the correlators separately, outputs of the second optical hard-limiters following the correlators and outputs of the OOK decoders will be seen. Note that when the desired optical sequence passes through a correlator, the output light intensity traces out the correlation function of the sequence. At the last chip position, the sum of received optical intensity located in the same positions as the positions of '1' of the optical orthogonal sequence code used for the desired channel is obtained. Also note that the OOK decoder compares the correlator output voltage over the last chip position of with the threshold level θ, then decides that '1' is sent if the output voltage is larger than the threshold level θ, and '0' is sent otherwise.

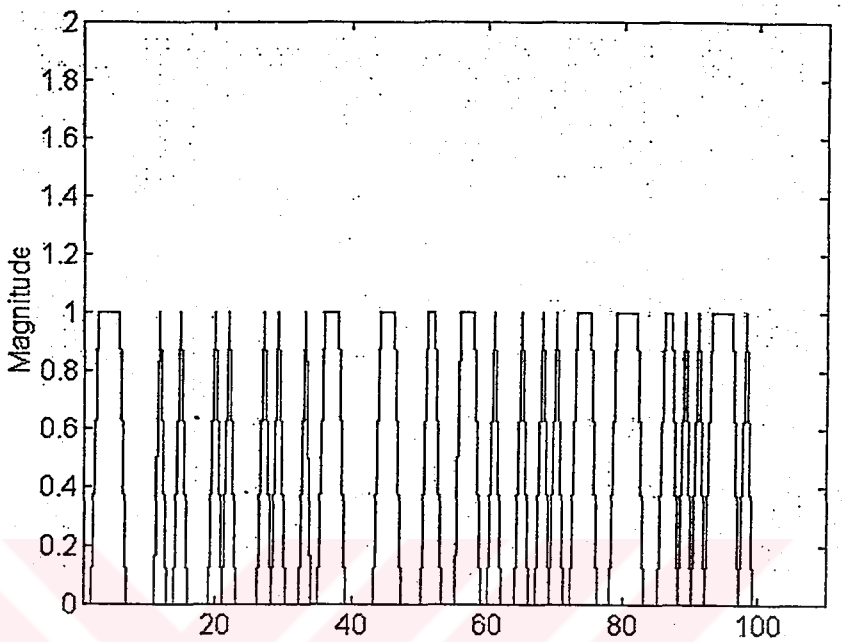

Time(normalized wrt chip duration)

Figure 4.30. First input data sequence

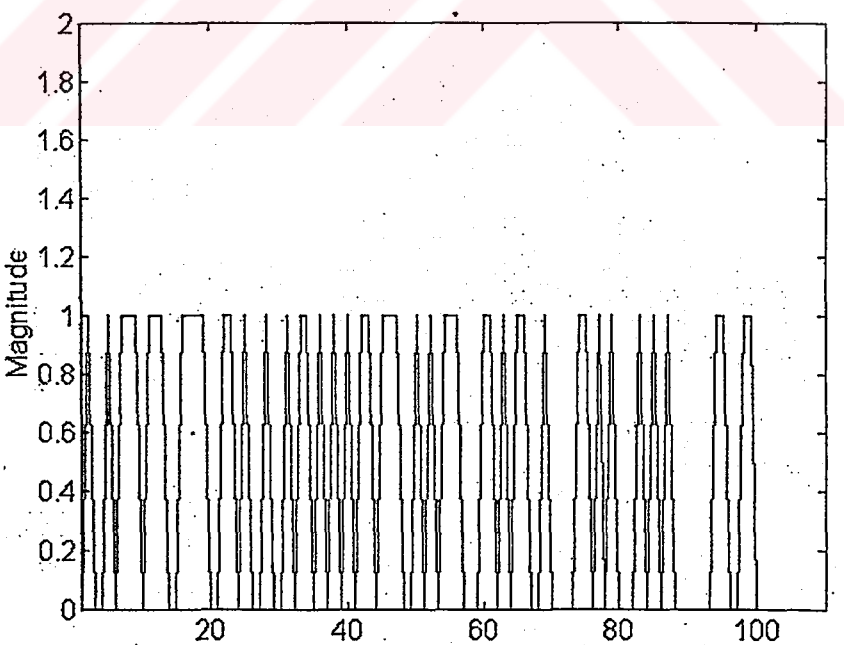

Time(normalized wrt chip duration)

Figure 4.31. Second input data sequence

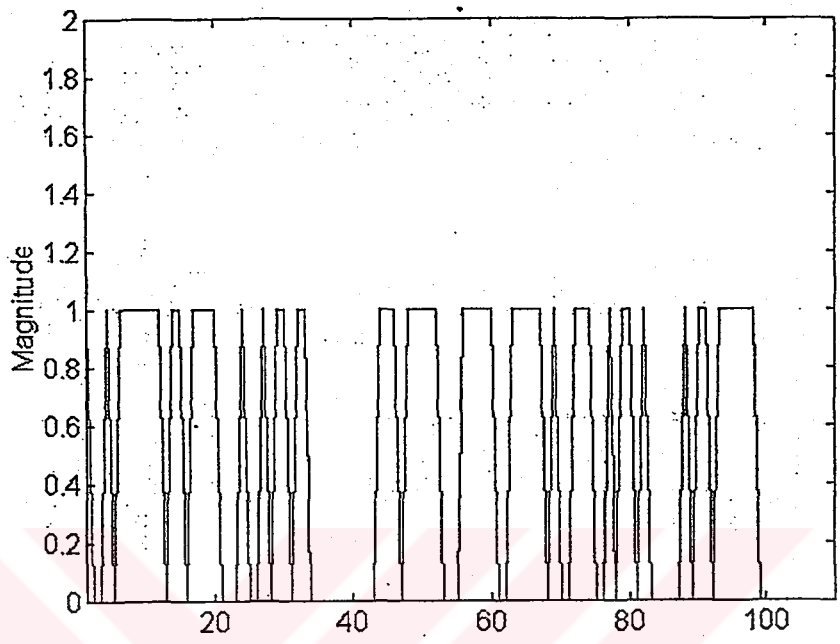

Figure 4.32. Third input data sequence

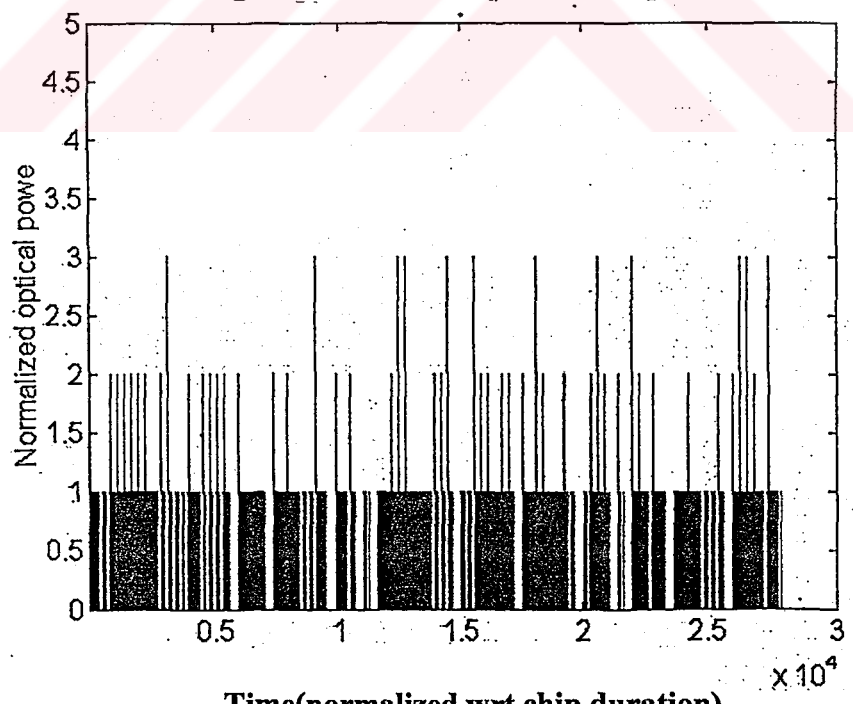

Figure 4.33. Sum of the encoder outputs

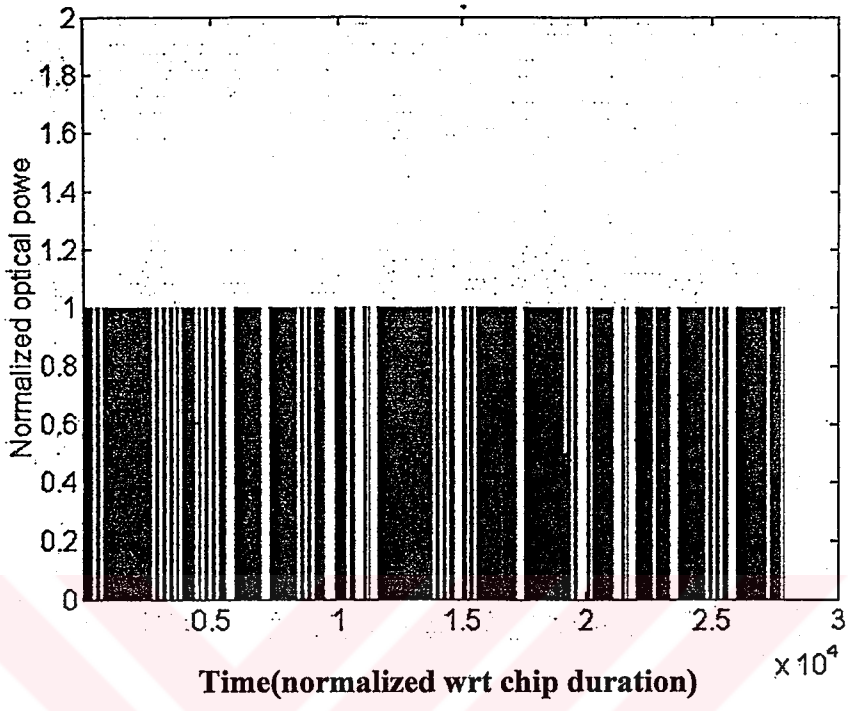

Figure 4.34. Output of the optical hard-limiter placed before the correlators

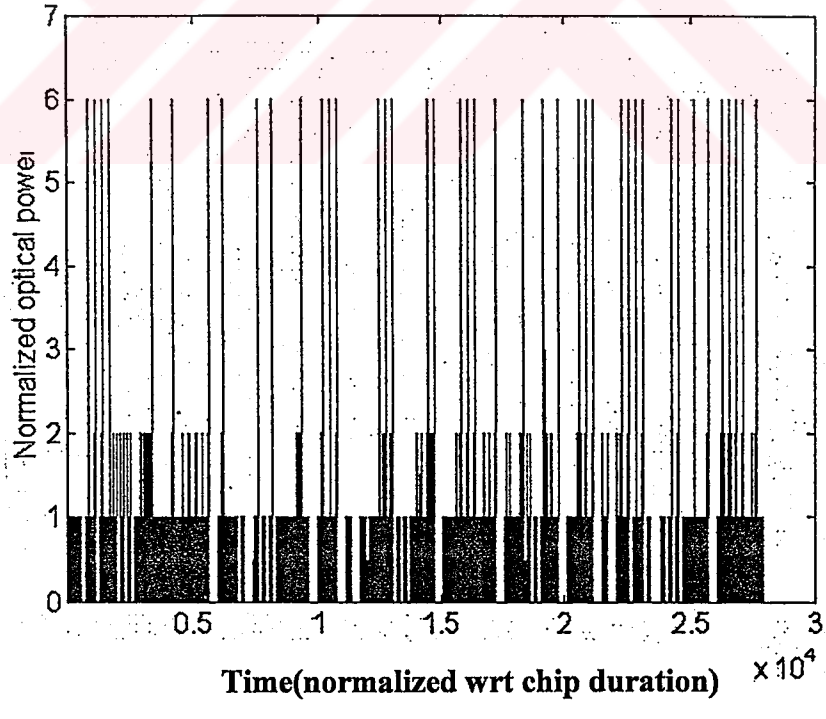

Figure 4.35. Output of the correlator based on C_1

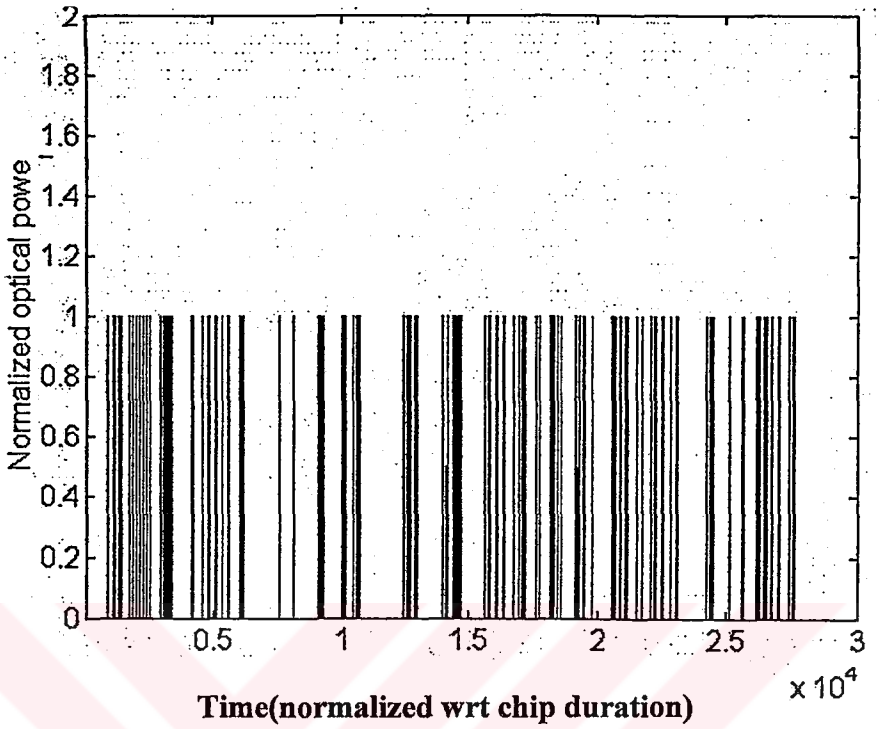

Figure 4.36. Output of the second optical hard-limiter following the correlator based on C_1

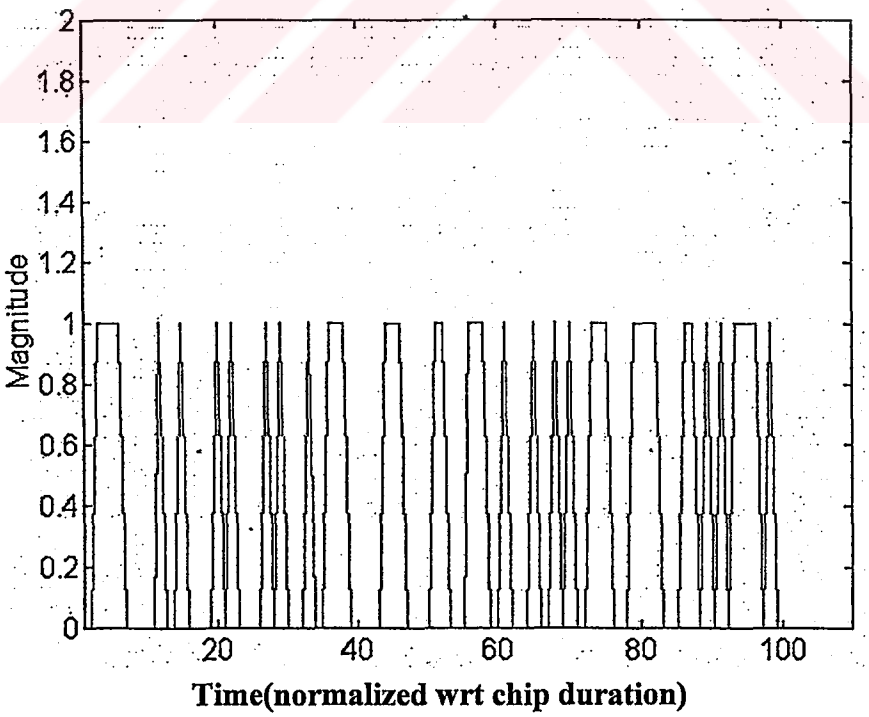

Figure 4.37. OOK decoder output for the structure based on C_1

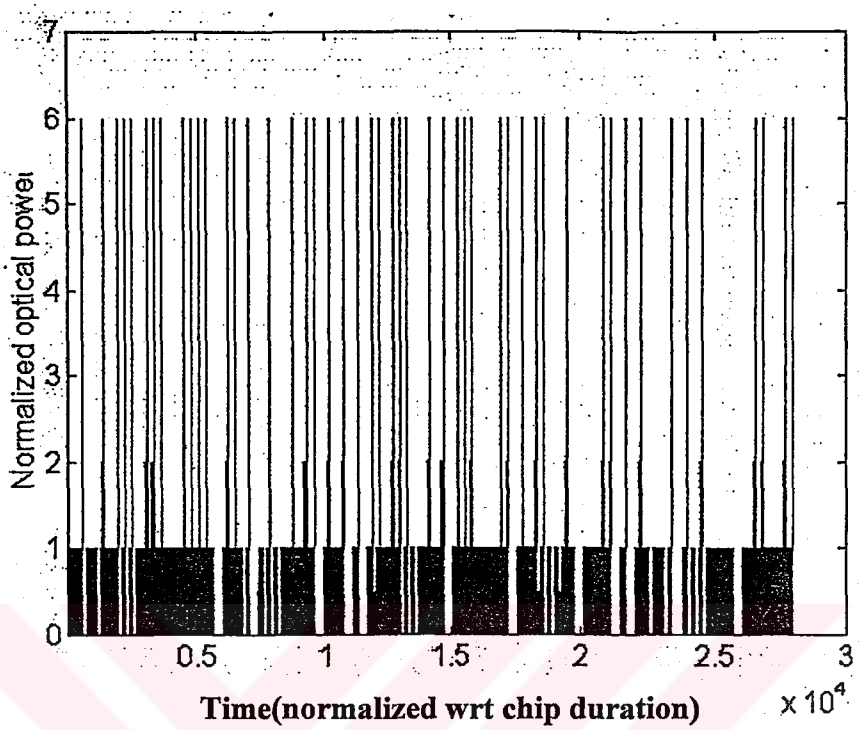

Figure 4.38. Output of the correlator based on C_2

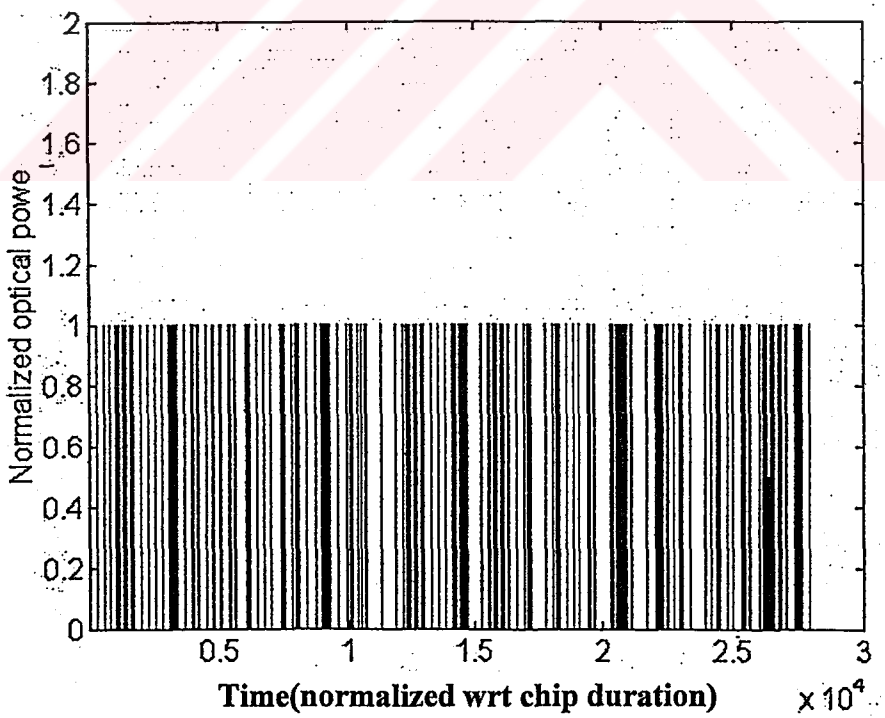

Figure 4.39. Output of the second optical hard-limiter following the correlator based on C_2

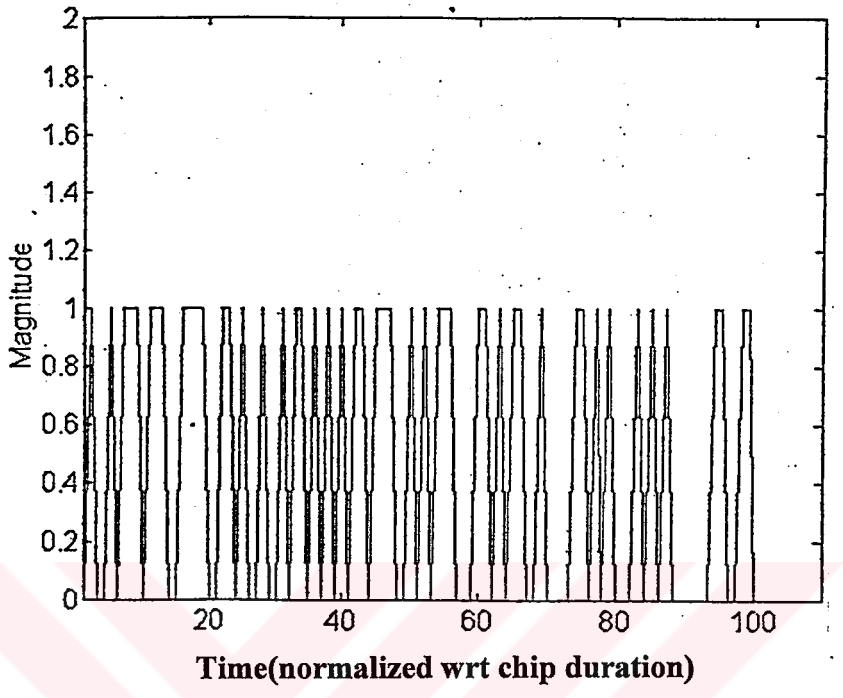

Figure 4.40. OOK decoder output for the structure based on C_2

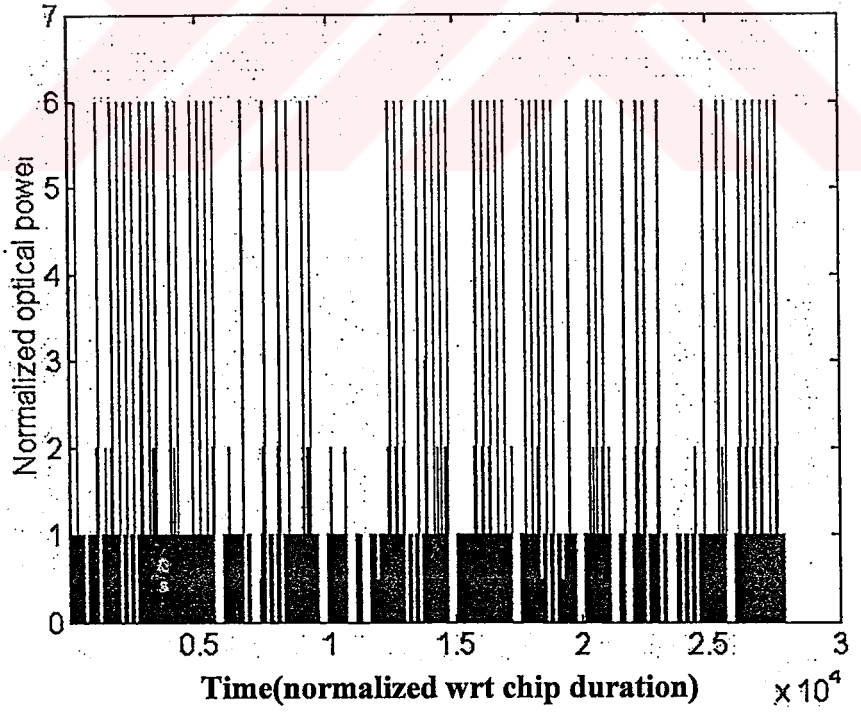

Figure 4.41. Output of the correlator based on C_3

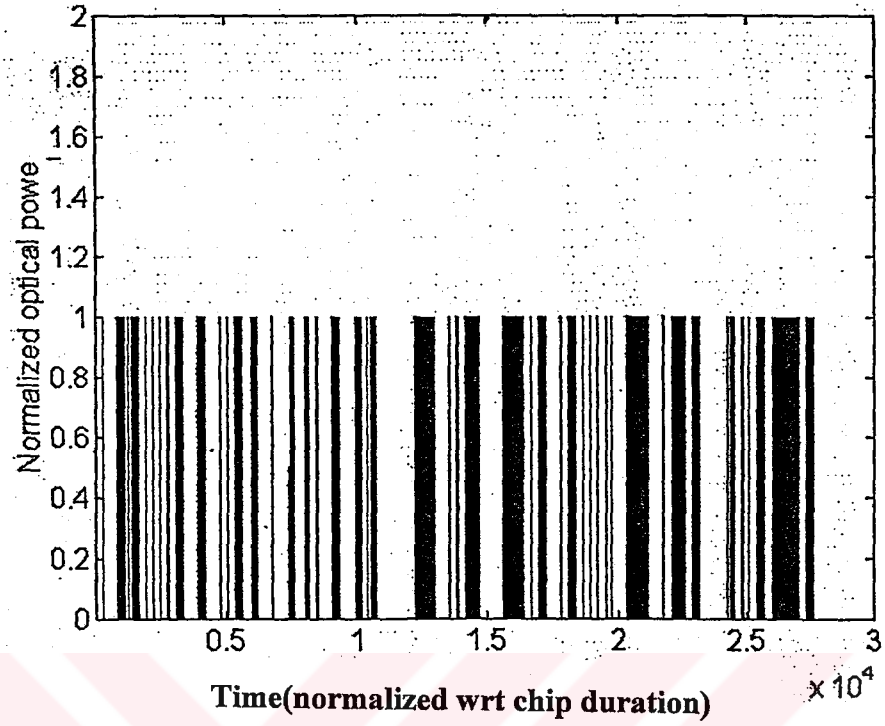

Figure 4.42. Output of the second optical hard-limiter following the correlator based on C_3

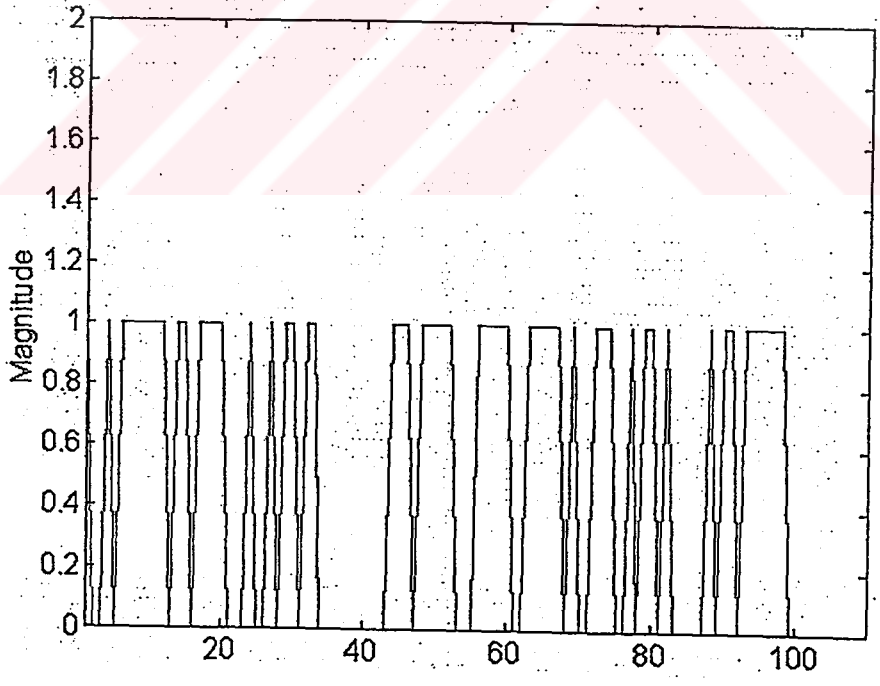

Figure 4.43. OOK decoder output for the structure based on C_3

These plots illustrate the operation principles of the memory structure with double optical hard-limiter. The required error level in the system that use ATM error ratio should be equal to or better than 10^{-9}. Therefore it is difficult to develop a computer program that will simulate the hardware of the FOMD. It may be more adavantageous to implement the system in laboratory to investigate its performance.

CHAPTER 5

CONCLUSIONS

In this thesis, the aim was to investigate the application of code division multiple access technique to the fiber-optic loop memory structure. The properties and advantages of using CDMA as the method of encoding is explained.

Optical orthogonal codes to be assigned to the virtual channels of the FOMD were presented. The fundamental properties and upper bounds on the size of this type of codes were given. The optical orthogonal codes are true (0,1) sequences and the construction methods are completely different from known binary code constructions. The (500,6,1,1) optical orthogonal code based on extended sets and which achieves the best autocorrelation and cross-correlation properties in intensity modulation-direct detection optical systems was introduced.

Various fiber-optic loop memory structures using different configurations and methods to store information were presented. Optical data storage using multistable oscillations was investigated and the experimental results were shown. Fiber-optic loop memory for optoelectronic computer was discussed and the usage of contrary-directed circulation of signals were explained. A fiber-optic loop memory device with an all-optical regeneration and the experimental results obtained by implementing the structure were introduced. Fiber-optic loop memory used in ATM

packet buffering was investigated. Bit-error ratio (BER) measurements in random access fiber loop optical memory were given.

Furthermore, fiber-optic loop memory structure based on optical code division multiple access was presented. Basic properties of storage capacity and advantage of using OOC's is explained. Loss mechanism in the loop memory was introduced. Plots for the amount of loss versus the number of turns in the loop and the maximum number of round trips that can be traveled by a pulse versus the length of the fiber loop were given. Working principles of the FOMD based on optical CDMA was explained. Examples of memory allocation and usage of codewords were illustrated. And the time plots for the input data, and loop content for 6 random write operations as an example. Using double optical hard-limiters increases the performance of the FOMD since some interference patterns caused by other users can also be excluded by means of a second optical hard-limiter replaced after the optical correlation in each decoding branch. Analysis of bit error probability was made under the assumption that the effects of the quantum noise and thermal noise are neglected. Bit error probability curves for different parameters were plotted. It was explained that using double optical hard-limiters enables the designer to use more than 10 codewords which results a huge increase in the storage capacity. If the bit rate greater than 10 Gbps is increased in addition to using more than 10 codewords, capacity will be much much greater than that of our design. Increasing the bit rate is mostly dependent on the improvements in the laser technology but using new codes designed for efficient memory usage will contribute to the technology a lot.

Wavelength division multiplexing can also be used to increase the memory storage capacity together with CDMA technique. It requires laser sources producing light at different wavelengths and it makes the structure more complex.

It is expected that optical memories using optical CDMA will be a very powerful tool for the optical networks. Trying new configurations like the double optical hard-limiter structure presented in this work will improve the system performance. Nevertheless, system complexity will increase. The implementation of

optical CDMA networks seems very attractive and as a future work, a FOMD should be fully implemented using both WDM and CDMA.

REFERENCES

[1] J. A. Salehi, 'Emerging optical code division multiple access communication systems', IEEE Network Magazine, 3,31(1989).

[2] P. R. Prucnal, et al., ' Spread spectrum fiber-optic local area network using optical processing', IEEE J. Lightwave Technol., LT-4(5), 547(1986).

[3] J. A. Salehi, 'Code division multiple access techniques in optical fiber networks-part I: fundamental principles', IEEE Trans. Commun., 37(8), 824(1989).

[4] P. A. Davies, A. A. Shaar, ' Asynchronous multiplexing for an optical fiber local area network', Electronics Letters, 19(10), 390(1983).

[5] G. J. Foschini, G. Vaccuni, 'Usins spread spectrum in a high-capacity fiber-optic local area network', J. Lightwave Technol., 6(3), 370(1988).

[6] M. E. Marhic, 'Coherent optical CDMA networks', IEEE J. Lightwave Technol., 11(5/6), 854(1993).

[7] A. S. Holmes, R. R. A. Syms, 'All-optical CDMA using quasi-prime codes', IEEE J. Lightwave Technol., 10(2), 279(1992).

[8] D. Zaccarin, M. Kavehrad, 'An optical CDMA system based on spectral encoding of LED', IEEE Photonics Technol. Lett., 4(4), 479(1993).

[9] W. B. Jones, Introduction to Optical Fiber Communication Sytesms, HRW, New York (1988).

[10] B. E. A. Saleh, M. C. Teich, Fundamentals of Photonics, John Wiley & Sons, New York (1991).

[11] J. M. Senior, Optical Fiber Communications, Principles and Practice, 2nd Ed., Prentice-Hall, New York (1992).

[12] J. G. Proakis, Digital Communications, 2nd Ed., McGraw Hill, New York(1992).

[13] D. V. Sarvate, M. B. Pursley, 'Crosscorrelation properties of pseudorandom and related sequences', Proc. IEEE, 68(5), 593(1980).

[14] R. Gold, 'Optimal binary sequences for spread spectrum multiplexing', IEEE Trans. Information Theory, IT-13, 619(1967).

[15] T. J. Healy, 'Coding and decoding for code division multiple user communication systems', IEEE Trans. Commun. , COM-33(4), 310(1985).

[16] S. Tamura, et al., 'Optical code-multiplex transmission by Gold sequences', IEEE J. Lightwave Technol., LT-3(1),121(1985).

[17] F. R. R. Chung, et al., 'Optical orthogonal codes: design, analysis, and applications', IEEE Trans. Information Theory, 35(3), 595(1989).

[18] C. Weber, et al., 'Performance considerations of code division multiple access systems', IEEE Trans. Vehicular Technol., VT-30(1), 2(1981).

[19] J. S. Lehnert, M. B. Pursley, ' Error probabilities for binary direct-sequence spread spectrum communications with random signature sequences', IEEE Trans. Commun., COM-35(1),87(1987).

[20] J. M. Holtzmann, 'A single accurate method to calculate sprad spectrum mutliple access error probabilities', IEEE Trans. Commun., 40(3), 461(1992).

[21] J. A. Salehi, C. A. Brackett, 'Code division multiple access techniques in optical fiber networks-part II: systems performance analysis', IEEE Trans. Commun., 37(8), 834(1989).

[22] A. W. Lam, A. M. Hussain, 'Performance analysis of direct-detection optical CDMA communications systems with avalanche photodiodes', IEEE Trans. Commun., 40(4), 810(1992).

[23] D. Brady, S. Verdu, 'A semiclasssical analysis of optical code division multiple access', IEEE Trans. Commun., 39(1), 85(1991).

[24] M. Azizoglu et al., 'Optical CDMA via temporal codes', IEEE Trans. Commun., 40(7), 1162(1992).

[25] C. Argon, Application of code division multiple access in fiber-optic communication systems, M.S. Thesis, Metu, Ankara, 1994.

[26] T. Aida, P. Davis, 'Experimental demonstration of novel dynamical memory function in a nonlinear electro-optical ring resonator', Japanese J. of Applied Physics, L1241-L1243,29(1990).

[27] K. Ikeda, K. Matsumoko, ' High-dimensional chaotic behavior in systems with time delayed feedback', Physica, 1987, 29D, pp. 223-235.

[28] V. A. Pilipovic, et al.,' Fiber-optic loop memory structure for optoelectronic computer', Inst. Phys. Conf. Ser. No 139: Part VI,pp.645, 1995.

[29] Y. Aoki, J. Lightwave Technology 6, 1225-1239, 1988

[30] V. A. Pilipovic, et al., Soviet Lightwave Communications 3, 169-175, 1993

[31] P. Cinato et al., 'Electrooptical switcing node based on fast packet and frequency switching techniques', ISS, Stockholm, May 27 to June 1, 1990.

[32] B. Bostica et al., in Proc. Photonics in Switching, OSA Proceedings Series, Vol. 16. (Optical Society of America, Washington, D.C., 1993), paper PMA2.

[33] B. Glance, et al., Electronics Letters 28, 1714(1992).

[34] A. Cavaciuti et al, in Conference on Optical Fiber Communications / International Conference on integrated optics and Optical Fiber Communication, 1993 Technical Digest Series, Vol. 4 (Optical Society of America, Washington, D.C., 1993), paper WD4.

[35] M. Calzavara et al., in Conference on Optical Fiber Communication / International Conference on integrated optics and Optical Fiber Communication, 1993 Technical Digest Series, Vol. 4 (Optical Society of America, Washington, D.C., 1993), paper TuE3.

[36] R. Langerhorst, W. Pieper, M. Eiselt, H.G. Weber, 'Balanced phase and polarization diversity coherent optical receiver', IEEE Photonics Technol. Lett., 1991, 3, pp.80-82

[37] A. A. Sawchuk and T. C. Strand, 'Digital optical computing', Proc. IEEE, Special Issue on Optical Computing, pp. 758-779, July 1984

[38] H. M. Kwon, 'Optical orthogonal code-division multiple access system-part I: APD noise and thermal noise', IEEE Trans. Commun., vol. 42, pp. 2470-2479, July 1994

[39] Tomoaki Ohtsuki, 'Performance analysis of direct-detection optical asynchronous CDMA systems with double optical hard-limiters', IEEE Journal of Lightwave Technology, vol.15, no.3, pp.452-457, March 1997.

[40] T. Aida, P. Davis, 'Storage of optical pulse data sequences in loop memory using multistable oscillations', Electronics Letters, vol.27, no.17, pp. 1544-1546, August 1991.

[41] E. Dietrich, G. Grobkopf, et.al., 'Ber measurements in random access fiber loop optical memory', Electronics Letters, vol.27, no.17, pp.1585-1586, August 1991.

[42] M. Calzavara , P. Gambini, et.al., 'Simultaneous buffering of ATM packets in a multiwavelength optical-fiber-loop memory', OFC '94 Technical Digest, pp.195-196.

[43] V. I. Belotitski, E. A. Kuzin, et.al., 'Demonstration of over 100 million round-trips in recirculating fiber-loop with all optical regeneration', Electronics Letters, vol. 29, no.1, January 1993.

APPENDIX

MATLAB SOURCE PROGRAMS FOR THE SIMULATION OF FOMD BASED ON OPTICAL CDMA

Simulation for the structure with single optical hard-limiter

```
clear
% Assign the chip positions of (500,1,1) Optical Orthogonal Codes
cw=zeros(10,282);
cw(1,1)=1;cw(1,3)=1;cw(1,15)=1;cw(1,43)=1;cw(1,93)=1;cw(1,178)=1;
cw(2,1)=1;cw(2,4)=1;cw(2,17)=1;cw(2,47)=1;cw(2,100)=1;cw(2,189)=1;
cw(3,1)=1;cw(3,5)=1;cw(3,20)=1;cw(3,53)=1;cw(3,108)=1;cw(3,201)=1;
cw(4,1)=1;cw(4,6)=1;cw(4,23)=1;cw(4,57)=1;cw(4,114)=1;cw(4,209)=1;
cw(5,1)=1;cw(5,7)=1;cw(5,25)=1;cw(5,61)=1;cw(5,122)=1;cw(5,223)=1;
cw(6,1)=1;cw(6,8)=1;cw(6,28)=1;cw(6,66)=1;cw(6,130)=1;cw(6,234)=1;
cw(7,1)=1;cw(7,9)=1;cw(7,30)=1;cw(7,71)=1;cw(7,139)=1;cw(7,244)=1;
cw(8,1)=1;cw(8,10)=1;cw(8,33)=1;cw(8,77)=1;cw(8,150)=1;cw(8,256)=1;
cw(9,1)=1;cw(9,11)=1;cw(9,36)=1;cw(9,83)=1;cw(9,162)=1;cw(9,272)=1;
cw(10,1)=1;cw(10,12)=1;cw(10,38)=1;cw(10,87)=1;cw(10,171)=1;cw(10,282)=1;
chip(1,1:6)=[1 3 15 43 93 178];
chip(2,1:6)=[1 4 17 47 100 189];
chip(3,1:6)=[1 5 20 53 108 201];
chip(4,1:6)=[1 6 23 57 114 209];
chip(5,1:6)=[1 7 25 61 122 223];
chip(6,1:6)=[1 8 28 66 130 234];
chip(7,1:6)=[1 9 30 71 139 244];
chip(8,1:6)=[1 10 33 77 150 256];
chip(9,1:6)=[1 11 36 83 162 272];
chip(10,1:6)=[1 12 38 87 171 282];
% Data length
L=100;
```

```
% Chiplength of the optical orthogonal codes
cwl=282;
% Maximum value of n (nT gives the refresment instances)
N=15;
% Constructing the data sequences to be written to the memory
init_inf=round(rand(1,L));
init_inf(1)=1;
inf=round(rand(N,L));
inf(1:15,1)=ones(15,1);
% Display the first data written into the memory
plot(init_inf)
title('First Data')
xlabel('Time')
ylabel('Signal Magnitude')
axis([1 100 0 1.5])
pause
axis('normal')
clc
look_up=zeros(1,10);
disp('Encoding First Data ')
m_loop=encode(init_inf,cw(1,1:282));
plot(m_loop)
axis([1 3e4 0 2])
title('Initial Content of the Fiber-optic Loop')
xlabel('Time')
ylabel('Normalized Optical Power')
pause
pointer=1;
look_up(pointer)=1;
w_order=1;
AC=0.0479;
C=9;
for time=1:N
    clc
    m_loop=m_loop*AC;
    output=m_loop/C;
    plot(output)
        title('Output of the Fiber Coupler at t=nT (n=1,2,3..)')
        xlabel('Time')
```

```
ylabel('Normalized Optical Power')
l=length(output);
Th=0.0053;
for i=1:l
  if ((output(i)>Th) | (output(i)=Th)),
        output(i)=Th;
  else
      output(i)=0;
  end;
```

% Decode the loop content using optical decoders

```
output=output/10;
dec_seq1=recover(output,chip(10,1:6));
dec_seq2=recover(output,chip(1,1:6));
dec_seq3=recover(output,chip(2,1:6));
dec_seq4=recover(output,chip(3,1:6));
dec_seq5=recover(output,chip(4,1:6));
dec_seq6=recover(output,chip(5,1:6));
dec_seq7=recover(output,chip(6,1:6));
dec_seq8=recover(output,chip(7,1:6));
dec_seq9=recover(output,chip(8,1:6));
dec_seq10=recover(output,chip(9,1:6));
channel=ones(1,10);
ldec=length(dec_seq1);
if dec_seq1==zeros(1,ldec),
 channel(1)=0;
end
if dec_seq2==zeros(1,ldec),
 channel(2)=0;
end
if dec_seq3==zeros(1,ldec),
 channel(3)=0;
end
if dec_seq4==zeros(1,ldec),
 channel(4)=0;
end
if dec_seq5==zeros(1,ldec),
 channel(5)=0;
end
if dec_seq6==zeros(1,ldec),
```

```
            channel(6)=0;
           end
           if dec_seq7==zeros(1,ldec),
            channel(7)=0;
           end
           if dec_seq8==zeros(1,ldec),
            channel(8)=0;
           end
           if dec_seq9==zeros(1,ldec),
            channel(9)=0;
           end
           if dec_seq10==zeros(1,ldec),
            channel(10)=0;
           end
```

% Clear information

```
esignal=input('Clear data group (0/1) :');
           if esignal==1,
             address=input('Write order:');
         clear place
for i=1:10
 if look_up(i)==address;
    place=i
 end
end
if place==1,
  dec_seq2=zeros(1,ldec)
end
if place==2,
  dec_seq3=zeros(1,ldec)
end
if place==3,
  dec_seq4=zeros(1,ldec)
end
if place==4,
  dec_seq5=zeros(1,ldec)
end
if place==5,
  dec_seq6=zeros(1,ldec)
end
```

```
if place==6,
  dec_seq7=zeros(1,ldec)
end
if place==7,
  dec_seq8=zeros(1,ldec)
end
if place==8,
  dec_seq9=zeros(1,ldec)
end
if place==9,
  dec_seq10=zeros(1,ldec)
end
if place==10,
  dec_seq1=zeros(1,ldec)
end
look_up(place)=0;
end
% Refresh the codes
disp('REFRESHING THE CODES ')
        rfr_code=encode(dec_seq1,cw(1,1:282));
        rfr_code=rfr_code+encode(dec_seq2,cw(2,1:282));
        rfr_code=rfr_code+encode(dec_seq3,cw(3,1:282));
        rfr_code=rfr_code+encode(dec_seq4,cw(4,1:282));
        rfr_code=rfr_code+encode(dec_seq5,cw(5,1:282));
        rfr_code=rfr_code+encode(dec_seq6,cw(6,1:282));
        rfr_code=rfr_code+encode(dec_seq7,cw(7,1:282));
        rfr_code=rfr_code+encode(dec_seq8,cw(8,1:282));
        rfr_code=rfr_code+encode(dec_seq9,cw(9,1:282));
        rfr_code=rfr_code+encode(dec_seq10,cw(10,1:282));
    l=length(m_loop);
    pos=round(rand*l);
    m_loop(l+1:(ldec*cwl)+(pos-1))=zeros(1,(ldec*cwl)-(l-pos+1));
    m_loop(pos:pos+(ldec*cwl)-1)=m_loop(pos:pos+(ldec*cwl)-1)+rfr_code;
    temp=look_up(10);
        look_up(2:10)=look_up(1:9);
    look_up(1)=temp;
    plot(m_loop)
        title('Fiberoptic Loop Content After Refreshment')
        xlabel('Time')
```

```
        ylabel('Normalized Optical Power')
        pause
% Read information
rsignal=input('Read data group (0/1) :');
        if rsignal==1,
          address=input('Write order:');
      clear place
for i=1:10
 if look_up(i)==address;
    place=i;
 end
end
if place==1,
  readout=dec_seq1;
end
if place==2,
  readout=dec_seq2;
end
if place==3,
  readout=dec_seq3;
end
if place==4,
  readout=dec_seq4;
end
if place==5,
  readout=dec_seq5;
end
if place==6,
  readout=dec_seq6;
end
if place==7,
  readout=dec_seq7;
end
if place==8,
  readout=dec_seq8;
end
if place==9,
  readout=dec_seq9;
end
```

```
if place==10,
  readout=dec_seq10;
end
plot(readout)
title('Desired  Data  Group')
xlabel('Time')
ylabel('Magnitude')
pause
end
if channel==ones(1,10),
   disp('Writing more data is not possible!')
else
   wsignal=input('Write data (0/1) :');
   if wsignal==1,
     w_order=w_order+1;
     disp('Encoding New Data ')
     if w_order<11,
      l=length(m_loop);
      pos=round(rand*l);
           plot(inf(time,1:L))
           title('Data Sequence')
           xlabel('Time')
           ylabel('Signal Magnitude')
           axis([1 100 0 1.5])
      pause
      m_loop(l+1:(L*cwl)+(pos-1))=zeros(1,(L*cwl)-(l-pos+1));
      new_code=encode(inf(time,1:L),cw(pointer,1:282));
      m_loop(pos:pos+(L*cwl)-1)=m_loop(pos:pos+(L*cwl)-1)+new_code;
      look_up(pointer)=w_order;
     else
       i=1;
       flag=0;
     while ((channel(i)==1)&(i<11)),
        i=i+1;
     end
     x=i;
      l=length(m_loop);
      pos=round(rand*l);
      m_loop(l+1:(L*cwl)+(pos-1))=zeros(1,(L*cwl)-(l-pos+1));
```

```
      new_code=encode(inf(time,1:L),cw(pointer,1:282));
      m_loop(pos:pos+(L*cwl)-1)=m_loop(pos:pos+(L*cwl)-1)+new_code;
      look_up(x)=w_order;
     end
   end
     if wsignal==0,
       pointer=pointer+1;
            pointer=pointer-floor(pointer/10)*10;
     end
end
end
```

FUNCTION USED FOR ENCODING

```
function cd=encode(data,c);
l=length(c);
ld=length(data);
cd=zeros(1,l*ld);
k=1;
for p=1:ld
  if data(p)==1,
      cd(k:k+281)=c;
          k=k+282;
  else
      k=k+282;
  end
end
```

FUNCTION USED FOR DECODING

```
function d=recover(code,cpos);
lsum=length(code);
lc=282;
ptr=1;
result=0;
t1=cpos(1);
t2=cpos(2);
```

```
t3=cpos(3);
t4=cpos(4);
t5=cpos(5);
t6=cpos(6);
while ((result==0)&(ptr<=(lsum-lc+1))),
 dec_out=code(ptr+t1-1)+code(ptr+t2-1)+code(ptr+t3-1)+code(ptr+t4-1)+code(ptr+t5-
1)+code(ptr+t6-1);
 if dec_out>0.0027,
   result=1;
   d(1)=1;
 end
 ptr=ptr+1;
end
if result==0,
  count=1;
  ptr=1;
 else
  count=2;
  ptr=ptr+lc-1;
end
while ptr<=(lsum-lc+1),
 dec_out=code(ptr+t1-1)+code(ptr+t2-1)+code(ptr+t3-1)+code(ptr+t4-1)+code(ptr+t5-
1)+code(ptr+t6-1);;
 if dec_out>0.0027,
    d(count)=1;
  else
    d(count)=0;
 end
 ptr=ptr+lc;
 count=count+1;
end
temp=d;
clear d
d=temp(1:100);
clear temp
```

Simulation for the structure with double optical hard-limiter

```
clear
cw=zeros(10,282);
cw(1,1)=1;cw(1,3)=1;cw(1,15)=1;cw(1,43)=1;cw(1,93)=1;cw(1,178)=1;
cw(2,1)=1;cw(2,4)=1;cw(2,17)=1;cw(2,47)=1;cw(2,100)=1;cw(2,189)=1;
cw(3,1)=1;cw(3,5)=1;cw(3,20)=1;cw(3,53)=1;cw(3,108)=1;cw(3,201)=1;
inf=round(rand(3,100));
plot(inf(1,1:100))
axis([1 110 0 2])
title('First Data Sequence');
xlabel('Time')
ylabel('Magnitude')
pause
axis('normal')
plot(inf(2,1:100))
axis([1 110 0 2])
title('Second Data Sequence');
xlabel('Time')
ylabel('Magnitude')
pause
axis('normal')
plot(inf(3,1:100))
axis([1 110 0 2])
title('Third Data Sequence');
xlabel('Time')
ylabel('Magnitude')
pause
axis('normal')
code1=encode(inf(1,1:100),cw(1,1:282));
code2=encode(inf(2,1:100),cw(2,1:282));
code3=encode(inf(3,1:100),cw(3,1:282));
m_loop=code1+code2+code3;
%AC=0.0053;
%GAIN=100;
```

```
%m_loop=m_loop*AC;
%m_loop=m_loop*GAIN;
plot(m_loop)
axis([1 3e4 0 5])
title('Sum of the Encoder Outputs');
xlabel('Time')
ylabel('Normalized optical power')
pause
axis('normal')
Th=1;
l=length(m_loop);
for i=1:l
 if ((m_loop(i)>Th)|(m_loop(i)==Th)),
    m_loop(i)=Th;
 else
    m_loop(i)=0;
 end;
end;
plot(m_loop)
axis([1 3e4 0 2])
title('Output of the optical Hard Limiter Placed Before The Correlators');
xlabel('Time')
ylabel('Normalized optical power')
pause
axis('normal')
count=0;
for i=1:282:l-281
  count=count+1;
  temp1=m_loop(i:i+281);
  a=xcorr(temp1,cw(1,1:282));
  temp2=a(1:282);
  oco1(i:i+281)=temp2;
end;
count=0;
for i=1:282:l-281
  count=count+1;
  temp1=m_loop(i:i+281);
  a=xcorr(temp1,cw(2,1:282));
  temp2=a(1:282);
```

```
  oco2(i:i+281)=temp2;
end;
count=0;
for i=1:282:l-281
  count=count+1;
  temp1=m_loop(i:i+281);
  a=xcorr(temp1,cw(3,1:282));
  temp2=a(1:282);
  oco3(i:i+281)=temp2;
end;
plot(oco1)
axis([1 3e4 0 7])
title('Output of the correlator based on C1');
xlabel('Time')
ylabel('Normalized optical power')
pause
axis('normal')
for i=1:l
 if oco1(i)>Th,
    oco1(i)=Th;
 else
    oco1(i)=0;
 end;
end;
% First Receiver
plot(oco1)
axis([1 3e4 0 2])
title('Output of The Second Optical Hard Limiter Following the Correlator Based on C1');
xlabel('Time')
ylabel('Normalized optical power')
pause
axis('normal')
t=0;
for i=1:282:l-281
  t=t+1;
  temp1=oco1(i:i+281);
  if temp1(282)==Th,
        dec1(t)=1;
  else
```

```
        dec1(t)=0;
  end;
end;
plot(dec1)
axis([1 110 0 2])
title('OOK Decoder Output (C1)');
xlabel('Time')
ylabel('Magnitude')
pause
axis('normal')
% Second Receiver
plot(oco2)
axis([1 3e4 0 7])
title('Output of the correlator based on C2');
xlabel('Time')
ylabel('Normalized optical power')
pause
axis('normal')
for i=1:l
 if oco2(i)>Th,
    oco2(i)=Th;
 else
    oco2(i)=0;
 end;
end;
plot(oco2)
axis([1 3e4 0 2])
title('Output of The Second Optical Hard Limiter Following the Correlator Based on C2');
xlabel('Time')
ylabel('Normalized optical power')
pause
axis('normal')
t=0;
for i=1:282:l-281
  t=t+1;
  temp1=oco2(i:i+281);
  if temp1(282)==Th,
        dec2(t)=1;
  else
```

```
        dec2(t)=0;
  end;
end;
plot(dec2)
axis([1 110 0 2])
title('OOK Decoder Output (C2)');
xlabel('Time')
ylabel('Magnitude')
pause
axis('normal')
% Third Receiver
plot(oco3)
axis([1 3e4 0 7])
title('Output of the correlator based on C3');
xlabel('Time')
ylabel('Normalized optical power')
pause
axis('normal')
for i=1:l
  if oco3(i)>Th,
     oco3(i)=Th;
  else
     oco3(i)=0;
  end;
end;
plot(oco3)
axis([1 3e4 0 2])
title('Output of The Second Optical Hard Limiter Following the Correlator Based on C3');
xlabel('Time')
ylabel('Normalized optical power')
pause
axis('normal')
t=0;
for i=1:282:l-281
  t=t+1;
  temp1=oco3(i:i+281);
  if temp1(282)==Th,
        dec3(t)=1;
  else
```

```
            dec3(t)=0;
    end;
end;
plot(dec3)
axis([1 110 0 2])
title('OOK Decoder Output (C3)');
xlabel('Time')
ylabel('Magnitude')
pause
axis('normal')
```